Green Chemistry

CRITICAL REVIEW

View Article Online
View Journal | View Issue

Cite this: *Green Chem.*, 2023, **25**, 9603

Recent developments in polysaccharide and lignin-based (nano)materials for CO_2 capture

Zahra Nezafat,[a] Mahmoud Nasrollahzadeh, *[b] Shahrzad Javanshir, [a] Talat Baran[c] and Yahao Dong[d]

Received 2nd July 2023,
Accepted 12th October 2023

DOI: 10.1039/d3gc02373g

rsc.li/greenchem

Global warming in 2023 shows no signs of slowing down. The situation alarms scientists, including the Intergovernmental Panel on Climate Change, the international body responsible for regularly developing knowledge on climate change. Indeed, some impacts are already threatening the environment. Today, the average global temperature has increased by about 1 °C compared to the pre-industrial era (1850–1900). At the current rate, the increase in global average temperature will reach 1.5 °C between 2030 and 2052. The greenhouse effect is unbalanced by human activities, in particular the use of fossil fuels (oil, gas, and coal), which lead to the release of greenhouse gases. CO_2 represents nearly 2/3 of global greenhouse gas emissions caused by human activities and has the tendency to linger in the atmosphere for a long time. This is why the effect of other greenhouse gases is usually measured in CO_2 equivalent. Current CO_2 emissions will impact atmospheric concentrations and global temperatures for decades. To date, some solutions have been proposed to deal with this (energy transition, regulation of emissions, *etc.*). However, most of these solutions have not yet been sufficiently developed and/or do not offset the effects of ever-increasing industrialization on anthropogenic CO_2 emissions. As a result, carbon capture and sequestration processes appear to be attractive solutions. CO_2 capture can take place by absorption (chemical and/or physical) and/or adsorption (chemisorption and/or physisorption). Various compounds can act as sorbents, among which polysaccharides and lignin have special importance due to their many advantages, the most important of which are biodegradability, availability, relatively cheapness, environmental friendliness, *etc*. In this review, we report recent studies regarding polysaccharides and lignin-based materials for CO_2 capture. Such materials can be in different forms such as composites, aerogels, hydrogels, pellets, heteroatom-doped materials, membranes, metal–organic frameworks (MOFs), porous carbons, *etc*. These materials are used for CO_2 capture through the adsorption or absorption processes.

1. Introduction

Since the end of the industrial revolution (19^{th} century), global warming has been described as being mainly due to human activities leading to the continuous increase in the emission of greenhouse gases including carbon dioxide.[1] This translates to a rise in temperatures, which impacts our ecosystem and jeopardizes the living conditions for future generations. In spite of recent awareness regarding global warming, it still remains a major current problem. With the increase in human population, the need for energy also increases. A large part of the world's energy still comes from the combustion of fossil fuels, which leads to the emission of greenhouse gases.[2–4] It is commonly accepted that global warming is closely linked to the emission of anthropogenic greenhouse gases, mainly CO_2. Increasing the amount of CO_2 from 280 to 410 ppm increases the global temperature between 0.6 and 1 °C. There are several sources of CO_2 emission, both natural and human, the most important of which are represented in Fig. 1.[5–7]

The increase in the CO_2 concentration in the world causes the irregularity of the weather and the rise of the average level of seas and oceans. These factors can endanger life under the seas and the survival of living organisms.[2,8] The Intergovernmental Panel on Climate Change has estimated that the concentrations of CO_2 in the world will reach 570 ppmv by 2100, which will lead to an increase of 1.9 °C in air temperature and a rise of 3.8 m in average sea and ocean

---

[a] Pharmaceutical and Heterocyclic Compounds Research Laboratory, Chemistry Department, Iran University of Science and Technology, Tehran, 16846-13114, Iran
[b] Department of Chemistry, Faculty of Science, University of Qom, Qom 37185-359, Iran. E-mail: mahmoudnasr81@gmail.com
[c] Department of Chemistry, Faculty of Science and Letters, Aksaray University, 68100 Aksaray, Turkey
[d] Henan Key Laboratory of Green Chemistry, Collaborative Innovation Center of Henan Province for Green Manufacturing of Fine Chemicals, Henan Engineering Laboratory of Chemical Pharmaceutical and Biomedical Materials, Key Laboratory of Green Chemical Media and Reactions, Ministry of Education, School of Chemistry and Chemical Engineering, Henan Normal University, Xinxiang 453007, PR China

levels.[9] To reduce these environmental risks, researchers around the world are studying ways to reduce the amount of CO_2. To deal with global warming, in parallel with the efforts undertaken to develop renewable energies and reduce emissions, the capture of anthropogenic CO_2 appears to be an essential solution given the still predominant use of fossil fuels. To achieve this, many solutions are being studied, including the use of solid adsorbents.[10–16] There are several CO_2 capture processes (post-combustion capture, precombustion capture, or oxy-fuel combustion) the main ones being pre-combustion and post-combustion. Although post-combustion is the most restrictive solution in terms of separation due to the low concentration of CO_2, it nevertheless remains the most applicable from an industrial point of view since it does not require any modification of the equipment.[17] There may be other methods, but they have limitations including expensiveness and excessive energy usage, long processing time, production of side products, *etc.*[18–23] There are some review papers pertaining to the removal of CO_2 using different methods.[24–30]

CO_2 capture can take place by absorption (chemical and/or physical) and/or by adsorption (chemisorption and/or physisorption).[31–35] Promising materials for CO_2 capture include amines as well as porous materials such as MOFs,[36,37] metal oxides,[38] graphene,[39] zeolites,[40] synthetic and natural polymers, *etc.*[41–44] Among these, natural polymers or biopolymers are very efficient materials for CO_2 capture and polysaccharides have attracted much attention.[45–51]

Polysaccharides and lignin are important and large groups of biopolymers with many properties such as biodegradability, environmental friendliness, accessibility, low price, *etc.*[52–56] In addition, polysaccharides and lignin have many useful functional groups such as hydroxyl, carboxyl, carbonyl, aldehyde, *etc.*, making them very applicable.[57–61] Polysaccharides and lignin-based materials can be obtained in different forms for various purposes such as food-packaging, catalysis, environmental applications, *etc.*[62–68] The properties of polysaccharides and lignin make them very efficient for CO_2 capture. Cellulose, alginate, starch, gum, chitosan, and pectin are diverse kinds of polysaccharides, which can be applied for the capture of CO_2.[69–71] In addition, lignin-based materials can be used for CO_2 capture applications.[72–76] In fact, the mentioned polysaccharides and lignin have a special chemical structure, which enables them to be used in different forms such as aerogels, composites, N-doped materials, MOFs, membranes, hydrogels, *etc.* In addition, they can be functionalized with various materials.[77–86] These features make polysaccharides and lignin very suitable and effective options for CO_2 capture. In this review paper, we report recent studies using alginate, starch, cellulose, chitosan, gum, pectin, and lignin-based materials for CO_2 capture. These materials are in different forms such as composites, hydrogels, aerogels, pellets, MOFs, membranes, *etc.*

2. CO_2 capture processes

There are several CO_2 capture processes including oxy-combustion, pre-combustion, and post-combustion capture (Fig. 2a). In oxy-combustion process, the combustion is carried out with pure oxygen instead of air, resulting in the production of a CO_2/H_2O mixture. CO_2 is therefore easily captured since it is then sufficient to condense the water to recover CO_2. However, the most studied and main processes are pre-combustion and post-combustion. In the pre-combustion, adapted for example to power stations, the coal is first gasified, leading to a high-

Zahra Nezafat

Zahra Nezafat was born in Iran. She received her MSc in organic chemistry in 2021 from the University of Qom. She is currently pursuing her PhD in organic chemistry at the Iran University of Science and Technology under the supervision of Dr Shahrzad Javanshir and Dr Mahmoud Nasrollahzadeh. Her research interests are mainly focused on the design and the fabrication of biopolymer-based (nano)catalysts and green synthesis of metal nanoparticles applied for the synthesis of organic compounds as well as electrocatalytic applications.

Mahmoud Nasrollahzadeh

Mahmoud Nasrollahzadeh is an Associate Professor at the University of Qom, Iran, and the Director of the Nanobiotechnology Laboratory. Since July 2023, he has been working as a Guest Researcher at TU Dresden, Dresden, Germany. His research program focuses on the application of biowaste and nature-inspired (nano)materials in catalysis, energy conversion, biomass conversion, and the development of novel functional materials; especially chitosan and lignin-based materials. He is the recipient of several research awards including the 2021 Abu Rayhan Prize given by the Iranian Academy of Sciences for the Top Young Chemist of Iran, and the 2020 Distinguished Researcher Award by the Iran Science Elites Federation. He has received research funding from different institutions and corporate entities.

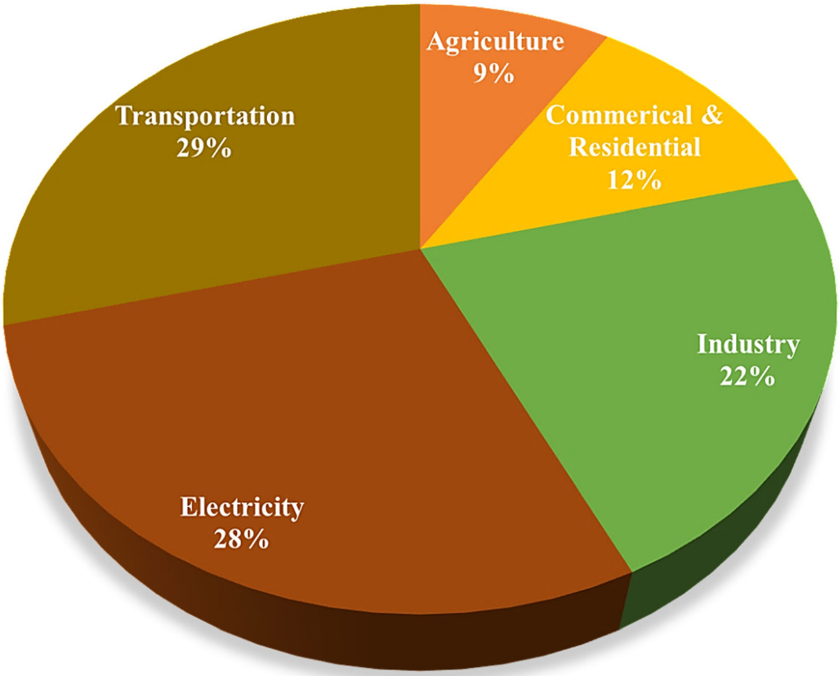

Fig. 1 Schematic representation of different sources and amounts of CO_2 emission.[5]

pressure gas (at a pressure and temperature of about 10 bar and close to 150 °C) composed of H_2 (55%), CO_2 (38%), N_2 (4%), CO (2%), and traces of other species. The hydrogen can then be used to obtain electricity. Afterward, the generated CO_2 is separated through chemical and physical absorption processes. The hydrogen-rich fuel can be applied in furnaces, gas turbines, and boilers.[13,87] In the post-combustion capture process, the CO_2 is captured after combustion in the exhaust

Shahrzad Javanshir

Shahrzad Javanshir (born October 19, 1960) is an Associate Professor in the Department of Chemistry at Iran University of Science and Technology. She received his BS in Chemistry in 1983, and her Master's and M. Phil. in Organic Chemistry in 1984 and 1985, respectively, from Claude Bernard University Lyon I. She received her PhD from Alzahra University in 2007. She has authored over 100 published scientific articles. Her work is focused on synthesizing organic compounds, the development of new bio-based materials, and heterogeneous catalysts.

Talat Baran

Talat Baran received his doctoral degree from Aksaray University in 2015. He currently serves as an Associate Professor in the Department of Chemistry at Aksaray University. In his research, he focuses on the synthesis and characterization of various environmentally friendly materials, such as carbohydrate polymers, clay, zeolite, carbon-based materials, etc. *He also works on the production of metal and metal oxide nanoparticles supported on these materials, which can function as homogeneous or heterogeneous catalysts. He examines the catalytic activities and reaction mechanisms of these catalysts in various applications, including the treatment of hazardous substances in water/wastewater, different organic transformations, hydrogen production, and microbial fuel cells. Currently, he has 118 publications in international ISI journals and 3 book chapters published by Elsevier. His work has received over 5100 citations, and his h-index is 48.*

gases. The concentration of CO_2 in these gases fluctuates between 10 and 30%. CO_2 post-combustion capture methods include absorption (amines, ethylene glycol, *etc.*), adsorption and membranes. Adsorption is a promising technique for CO_2 capture owing to its advantages such as simplicity of handling, absence of corrosion difficulties, reduced energy necessity, and cost-effectiveness.[9,88] Different adsorbents such as zeolites and carbon-based materials can be used for capturing CO_2.[89–91] In the absorption process, the capturing of CO_2 flue gas occurs by reaction with a chemical solvent, which is usually an amine-based solvent.[9] The use of amine-based solvents has some disadvantages such as a low capacity for CO_2 capture, high energy price for the recycling of the absorbent owing to the presence of H_2O in the solution of amine, thermal degradation, and losses of amines by evaporation.[92] Solid amine-based absorbents can be used to overcome the problem caused by soluble amines. The advantage of solid amine-based absorbents over soluble amines is lower energy consumption because the water evaporation step is eliminated. In addition, solid amine-based absorbents have high-capacity performance compared to soluble amines. Nevertheless, these solid sorbents have not been applied on an industrial scale since this knowledge is not yet fully developed.[12,93] Another post-combustion capturing technique is membrane separation. A membrane is defined as a permeable and selective barrier, active or passive, separating two media. Under the effect of a driving force, it allows the selective passage of certain compounds in a gaseous and/or liquid mixture. Membrane separation is the ability of materials to control the penetration of different species. One of the advantages of CO_2 membrane separation is its continuous mode of operation, unlike absorption and adsorption processes where, once the storage capacity has been reached, the solvent (or solid) must be regenerated. Owing to the exceptional structural properties of CO_2, it can reversibly react with Brønsted and Lewis bases such as KOH and amines, respectively.[94,95] Fig. 2b shows the properties, opportunities, and challenges associated with these techniques.[13]

Yahao Dong

Yahao Dong received his Ph.D. from Huazhong University of Science and Technology in 2020. He is currently working at the School of Chemistry and Chemical Engineering, Henan Normal University. His research interest is the synthesis of heterogeneous catalysts for organic reactions and CO_2 conversion.

3. Mechanism for CO_2 capture

The elimination of acid gases depends on their ability to react with alkanolamines. CO_2 reacts with alkanolamines as a Lewis acid at a finite rate, but with variable reaction mechanisms depending on the degree of substitution or steric hindrance of the amine nitrogen. Two main mechanisms have been proposed to explain the reaction between CO_2 with primary (R^1NH_2) and secondary (R^1R^2NH) alkanolamines; namely, the zwitterion and the Crooks and Donnellan mechanisms.[96] In this mechanism, first, the amine reacts with CO_2 to form a zwitterion (eqn (1)) intermediate, which then reacts with the base (such as OH^-, H_2O, or amine) to yield neutral carbamate (eqn (2)).[97–102]

Unlike the zwitterion mechanism,[103] a one-step mechanism has been proposed for the reaction between CO_2 with primary or secondary amines simultaneously and the formation of carbamate in a one-step (eqn (3)). In such mechanism, monoethanolamine (MEA) does not function as a proton acceptor.[104]

Carbamic acid is generated in the other mechanism. In this mechanism, in the first step, MEA reacts with CO_2 (eqn (4)). In the second step, the fabricated carbamic acid reacts with another MEA to form the carbamate (eqn (5)).[105]

$$CO_2 + RNH_2 \rightleftharpoons RNH_2{}^+COO^- \tag{1}$$

$$RNH_2{}^+COO^- + RNH_2 \rightleftharpoons RNHCOO^- + RNH_3{}^+ \tag{2}$$

$$CO_2 + RNH_2 \cdots B \rightleftharpoons RNHCOO^- \cdots BH^+ \tag{3}$$

$$CO_2 + RNH_2 \rightleftharpoons RNHCOOH \tag{4}$$

$$RNCOOH + RNH_2 \rightleftharpoons RNHCOO^- + RNH_3{}^+ \tag{5}$$

Among these mechanisms, the zwitterion mechanism is more considered. In the meantime, it is moreover broadly applied to describe the reaction of CO_2 absorption into other solvents, including mixed amines and functionalized ionic liquids.[106–108] In a study, Jing and co-workers described the mechanism of CO_2 adsorption onto MEA.[109] In the first step, the reversible reaction occurs between CO_2 (at low loading) and MEA to form the carbamate. Following high CO_2 loading, $HCO_3{}^-/CO_3{}^{2-}$ is formed through the hydration of CO_2. In this step, the carbamate is hydrolyzed (Fig. 3a). In addition, the absorption of CO_2 can occur in diethanolamine (DEA) and triethanolamine (TEA). CO_2 absorption by DEA is similar to that by MEA. However, in the case of TEA, the mechanism is different.[110] Tertiary amines do not have the necessary (N–H) bond to form the carbamate ion, and therefore do not react directly with CO_2. Thus, Donaldson and Nguyen proposed the mechanism presented in Fig. 3b in 1980, which describes the reaction of CO_2 with tertiary amines, followed by the hydrolysis of CO_2 to form bicarbonate.[111] In a study, Zheng and colleagues investigated the synthesis of SiO_2 nanoparticles (NPs) and organic hybrid materials (NOHMs).[112] For this purpose, they used SiO_2 NPs as core and 3-glycidoxypropyl trime thoxysilane (KH-560) (NOHM-C) or 3-(trihydroxysilyl)-1-propane sulfonic acid (SIT) (NOHM-I) as the corona. Additionally, they used

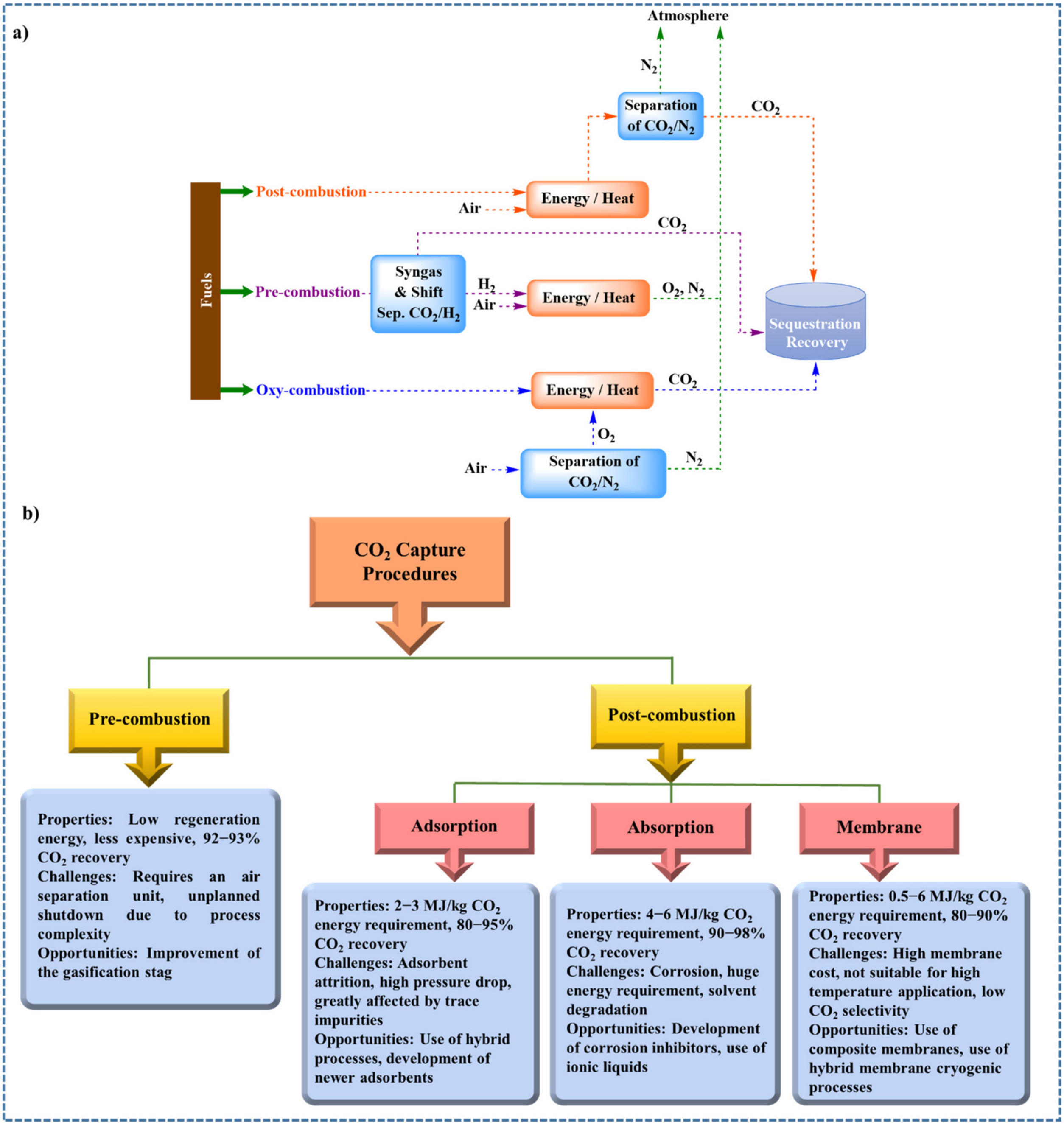

Properties: Low regeneration energy, less expensive, 92–93% CO_2 recovery
Challenges: Requires an air separation unit, unplanned shutdown due to process complexity
Opportunities: Improvement of the gasification stag

Properties: 2–3 MJ/kg CO_2 energy requirement, 80–95% CO_2 recovery
Challenges: Adsorbent attrition, high pressure drop, greatly affected by trace impurities
Opportunities: Use of hybrid processes, development of newer adsorbents

Properties: 4–6 MJ/kg CO_2 energy requirement, 90–98% CO_2 recovery
Challenges: Corrosion, huge energy requirement, solvent degradation
Opportunities: Development of corrosion inhibitors, use of ionic liquids

Properties: 0.5–6 MJ/kg CO_2 energy requirement, 80–90% CO_2 recovery
Challenges: High membrane cost, not suitable for high temperature application, low CO_2 selectivity
Opportunities: Use of composite membranes, use of hybrid membrane cryogenic processes

Fig. 2 Schematic representation of (a) CO_2 capture processes by post-, pre-, and oxy-combustion and (b) different properties of the two methods for CO_2 capture.[13]

polyetheramine M-1000 (M-1000) as the canopy. The NOHMs applied for CO_2 capture and the mechanism are displayed in Fig. 3c. There are three types of active sites for the CO_2 capture and storage. In the active site 1, secondary amine groups can react with CO_2. In the active site 2, there are other groups, which can react with CO_2 *via* Lewis acid–base interactions. In addition, active site 3, which is a potential space between the long organic chains and facilitates the physical adsorption of CO_2, can be removed by applying vacuum.

4. Current CO_2 capture polysaccharides and lignin-based materials

4.1. Polysaccharides-based materials for CO_2 capture

4.1.1. Alginate-based materials. Alginate (another name is alginic acid or align) is a polysaccharide of anionic nature present in the cell walls of brown algae. The two main functional groups are $-COO^-$ and –OH. In the acid form, this poly-

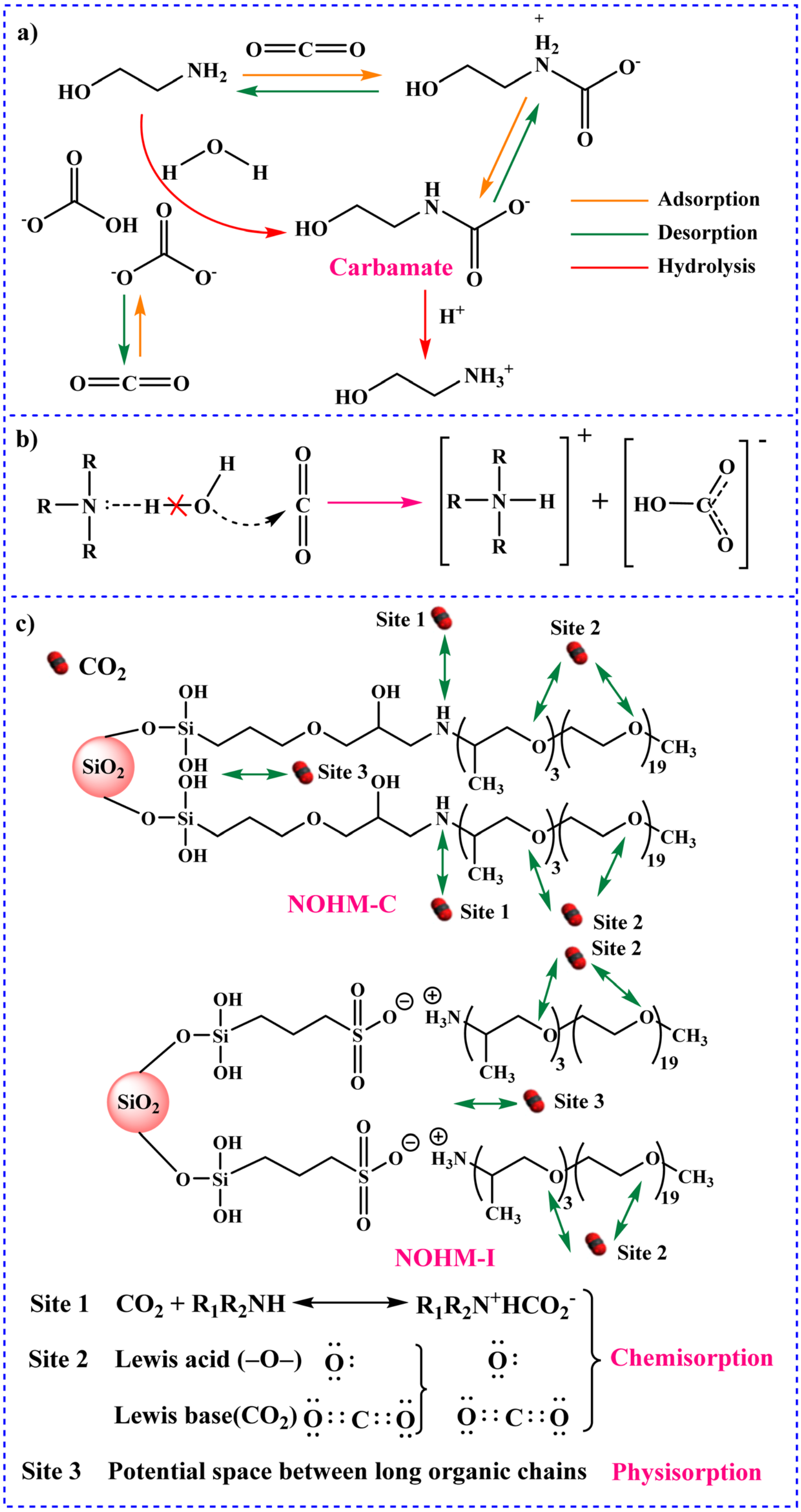

Fig. 3 Schematic representation of the mechanism for CO_2 capture using (a) MEA,[109] (b) TEA[111] and (c) SiO_2 NPs functionalized amine.[112]

saccharide can be found in different types of salts such as sodium and calcium Alginate. Other properties of alginate include linearity and solubility in water.[57,113–115] β-D-Mannuronic and α-L-guluronic acid are two units forming the structure of the alginate. The structure and functional groups of the alginate make this polysaccharide a suitable option for all kinds of applications including drug delivery, tissue engineering, food industry, catalysis, and environmental purposes.[116–120] Alginate has advantages such as biodegradability, environmental friendliness, non-toxicity, *etc*. However, it has disadvantages, including low chemical and thermal stability as well as low mechanical strength.[121,122] To overcome these disadvantages and increase its absorption properties, alginate can be modified by different methods and different structures such as composites, hydrogels, aerogels, *etc.*[113,123–125] In this section, we review the CO_2 adsorption properties of the different structures of alginate-based materials.

4.1.1.1. *Alginate-based composite materials.* One of the most interesting materials for the removal of CO_2 is composites. Composites can be synthesized using different materials. For example, Rasoulzadeh and colleagues reported the synthesis of one composite by the functionalization of alginate with amine materials.[126] As mentioned earlier, alginate alone has low stability. Therefore, they used biosilica to enhance the thermal stability and mechanical strength of alginate. In addition, for enhancing the adsorption property, they used (3-aminopropyl)triethoxysilane (APTES) to prepare amine-functionalized bio silica/alginate (NH_2-SiO_2/ALG). The NH_2-SiO_2/ALG composite was applied for CO_2 capture in a fixed-bed reactor. They optimized different parameters such as moisture content (MC), gas flow rate (FR), and temperature. The results displayed that the removal efficiency (RE) of CO_2 was 93.08% at optimum conditions including 5%, 40 mL min^{-1}, and 40 °C for MC, FR, and temperature, respectively. In this example, the adsorption capacity and stability of alginate were increased by adding an amine-containing compound. Hosseini and co-workers investigated the preparation of calcined eggshell/sodium alginate (CES/SA) composite.[127] They synthesized a gel bead by modification of CES/SA with ammonia and applied it for CO_2 adsorption. In the experimental work, they optimized FR, the concentration of CO_2, temperature, and pressure. The highest CO_2 capture (0.2380 mmol g^{-1}) happened when the temperature, pressure, and concentration of CO_2 were 30 °C, 1 bar, and 45%, respectively. In fact, they synthesized eggshell materials using alginate for CO_2 capture for the first time.

4.1.1.2 *Alginate-based nitrogen-doped materials.* Today, nitrogen-doped materials are one of the most efficient materials for CO_2 adsorption. As a result, in a study in 2021, Huang *et al.* developed a technique for the preparation of N-doped hierarchically porous carbon spheres.[128] They synthesized the mentioned materials through co-pyrolyzation of poly(vinylidene chloride) and melamine in an alginate gel bead (Fig. 4a). In this structure, melamine played two roles including a template for the macropore structures and a nitrogen source. The prepared N-doped material was applied for CO_2 capture. The innovation of this work is the application of melamine to make gel beads, which also helps adsorb CO_2.

The preparation of N-doped activated carbon (AC) using microalgae-sodium alginate (NaAlg) was performed by Liu and colleagues in 2018.[129] NaAlg has a high nitrogen content and can be applied as an efficient precursor. The N-doped materials showed a high activity for CO_2 adsorption owing to high N content and suitable pore size distributions. The adsorption capacity was 3.75 mmol g^{-1} at the temperature and pressure of 25 °C and 1 bar, respectively. Fig. 4b shows the effect of composition in microalgae-NaAlg. As mentioned, one of the important features of this adsorbent is the large number of nitrogen groups and the proper size of the holes, which helps increase the adsorption of CO_2.

Cao and co-workers studied the preparation of N-doped carbon monolith (SA-*x*N-*y*P) using binary H_3PO_4–HNO_3 and Na-alginate (SA) as co-activating agents and carbon precursor, respectively (Fig. 4c).[130] The *x* and *y* in the sample name correspond to the volumes of HNO_3 and H_3PO_4, respectively. The prepared SA-2N-P sample had HSSA (1740 m^2 g^{-1}) and CO_2 adsorption (8.99 mmol g^{-1}) at 273 K. In addition, at 298 K, the amount of CO_2 adsorption was 4.57 mmol g^{-1}. These results indicated that the SA-2N-P sample had high adsorption capacity and selectivity for CO_2.

4.1.1.3 *Alginate-based MOF materials.* Today, one of the most promising porous materials is MOFs. These materials consist of hybrid materials from organic and inorganic compounds including organic linkers and metals. MOFs have some properties including high specific surface area (HSSA), ease of modification, and suitable pore sizes. Thus, they are widely used today for absorbing and removal of gases. Nevertheless, these compounds may be less effective for CO_2 adsorption because the organic rings in the structure of MOF may have a weak affinity with CO_2. Therefore, these compounds have been functionalized using nitrogen groups.[131–135] For example, in 2021, Xiao and co-workers investigated the synthesis of zirconium-based MOF beads for CO_2 capture applications.[136] For this purpose, they prepared Zr-based DUT-68 into alginate beads. Gas capture performance was then assessed through CO_2 and volatile iodine adsorption. They synthesized DUT-68 beads by cross-linked polymerization of Na-alginate using Ca^{2+} ions. The prepared composites had HSSA as well as high porosity. The DUT-68@Alginate bead (60% MOF) exhibited a 1.25 mmol g^{-1} CO_2 adsorption capacity at 273 K. In this work, the alginate stability and the adsorption performance were enhanced. In the same year, Salehi and Hosseinifard reported the synthesis of MIL-101-derived nano porous carbon (MDC)/polysaccharides nanocomposite[137] using the impregnation of alginate, chitosan, and cellulose on the MDC. They used waste Cr for the synthesis of MIL-101. The prepared nanocomposite was applied for the uptake of CO_2 and CH_4. In another study, Mondino *et al.* successfully developed the preparation of MOF and alginate-based sphere, referred to as CPO-27-Ni/alginate spheres, through spray-granulation technique.[138] The CPO-27-Ni/alginate spheres were very suitable materials for the moving-bed temp-swing adsorption (MBTSA) process in the post-combustion capture of CO_2.

4.1.1.4 *Miscellaneous alginate-based materials.* Nanofiber (NF) is one of the types of nano materials, which have HSSA and are broadly applied for the removal of CO_2. NF materials can be synthesized through different methods, electrospinning being the most widely applied. Electrospun NFs are used for CO_2 adsorption owing to their properties including HSSA, high

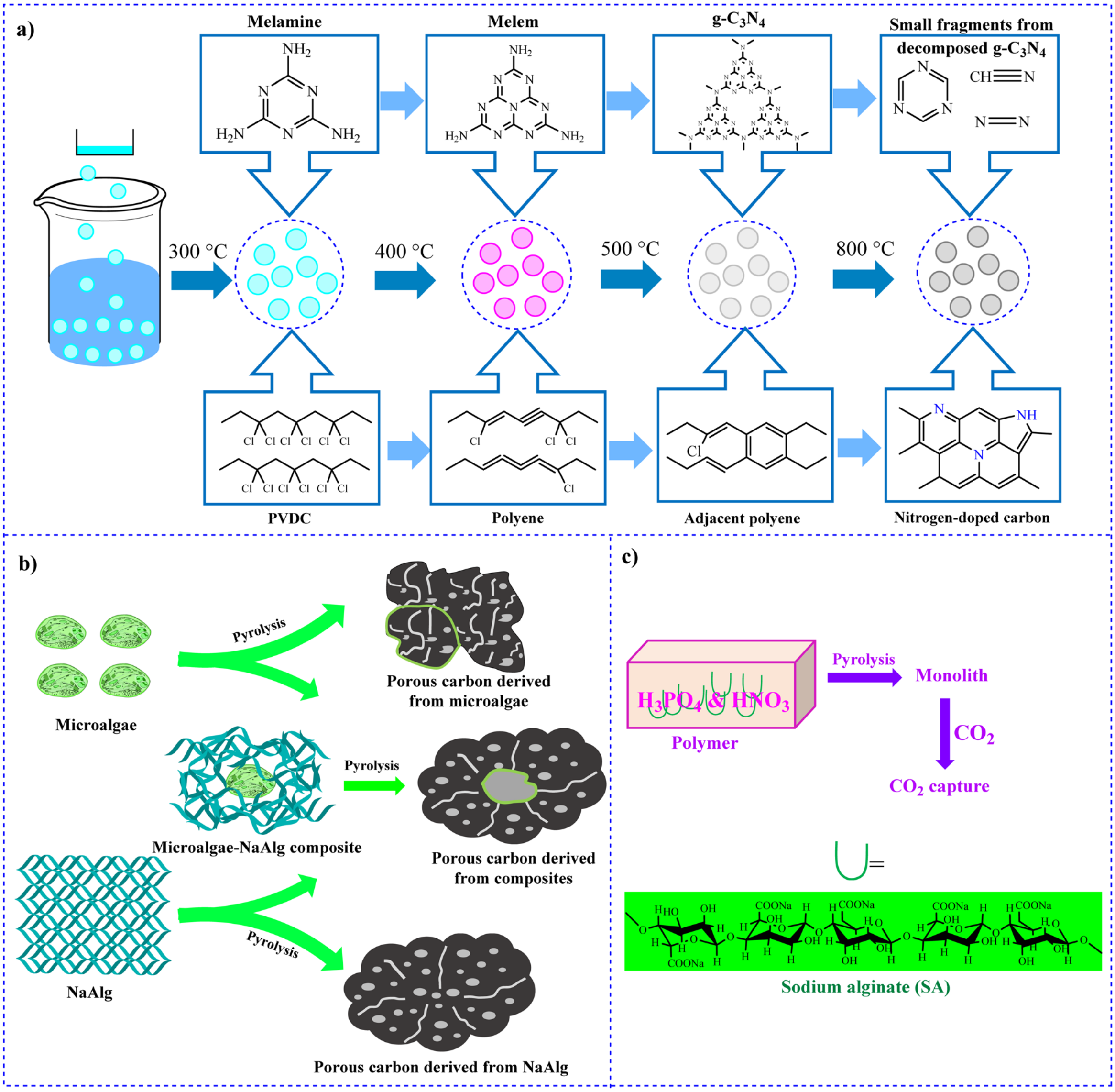

Fig. 4 Experimental procedure for (a) preparation of N-doped materials,[128] (b) N-doped-based alginate porous carbon[129] and (c) the preparation of the highly porous carbons.[130]

porosity, suitable pore size, excellent interconnectivity, and mechanical properties.[139] In 2022, Suratman and colleagues reported the synthesis of alginate NF using the incorporation of poly(vinyl alcohol) (PVA) in alginate (Alg/PVA NFs) by electrospinning method (Fig. 5a).[140] To improve the performance of the alginate NF, they used the impregnation of zeolite (Z) into the solution of polymer (Alg/PVA/Z NFs) (Fig. 5b). The CO_2 adsorption capacities of the prepared Alg/PVA NFs and Alg/PVA/Z NFs were 3.286 and 10.710 mmol g^{-1}, respectively. In this example, a combination of zeolite and alginate was used to synthesize a novel composition. In addition, in 2020, Koly and colleagues prepared another type of NF; named alginate/polyethylene oxide/Triton X-100 NFs (Alg/PEO/TX NFs) by electrospinning method.[141] They evaluated the CO_2 capture capacity of the synthesized NFs. Their results displayed that the optimum adsorption capacity of 12.398 mmol g^{-1} was achieved using FR and contact time of 10 mL min^{-1} and 25 min, respectively. The electrospinning method is a novel technique for the preparation of adsorbents.

One of the most efficient biocompounds for CO_2 capture is carbonic anhydrase. In fact, using carbonic anhydrase for CO_2 capture, the cost and size of the reactor were reduced. A specific form of carbonic anhydrase is the immobilization of it on the reactor, which maintains the suitability of separation and controls the process.[142–145] In 2016, Zhu *et al.* reported the decoration of carbonic anhydrase on the alginate and investigated its effect on the acceleration of CO_2 capture in post-combustion.[146] The immobilization of carbonic anhydrase on the alginate was carried out using glutaraldehyde cross-linking technique. The batch-scale results exhibited that CO_2 adsorp-

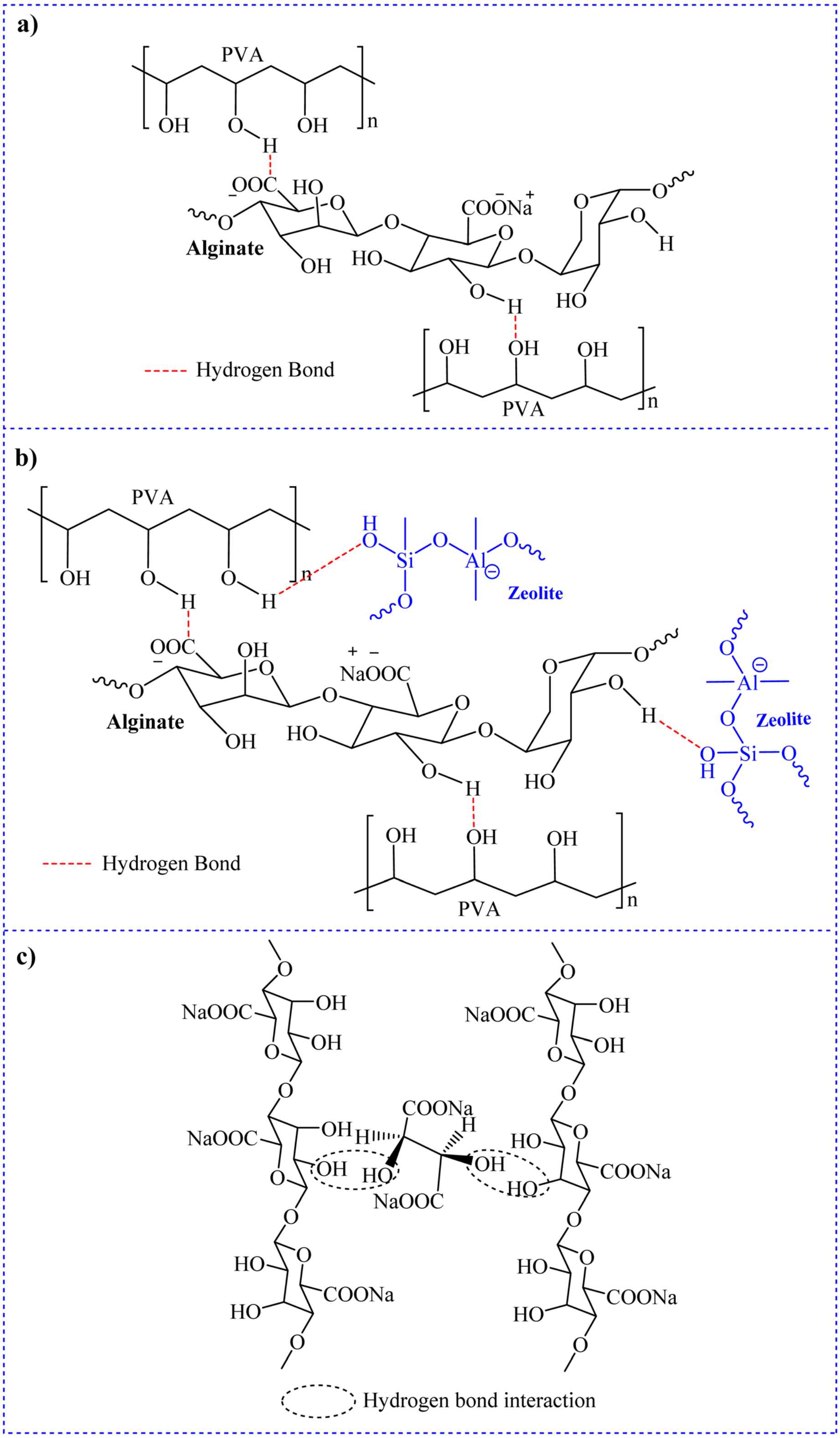

Fig. 5 Schematic representation of intermolecular interactions of (a) Alg/PVA NFs, (b) Alg/PVA/Z NFs[140] and (c) hydrogen bond between NaAlg and Na-tartrate.[149]

tion was improved by the addition of immobilized carbonic anhydrase. By immobilization of carbonic anhydrase on the alginate, the operational stability and porosity were increased.

Membranes provide an excellent potential for the capture of CO_2 owing to their advantages such as low cost, easy industrialization, small energy necessity, and eco-friendly nature.[147,148] In a study, Zhi and colleagues reported a membrane-based CO_2 separation procedure.[149] For this aim, they used NaAlg and Na-tartrate, which were connected through hydrogen bonds (Fig. 5c). The prepared membranes were applied for the separation of CO_2 and N_2. In this study, the presence of nitrogen-containing compounds may have increased the efficiency of the adsorbent.

4.1.1.5 Summary of this section. Alginate has low stability, which necessitates the preparation of alginate-based materials. Regarding the capture of CO_2 by alginate, relatively few studies have been carried out and most of them were based on N-doped materials. However, given the capability of alginate to form all kinds of gels; especially hydrogels, novel alginate-based hydrogels can be made for CO_2 absorption. Considering that the removal efficiency of composites is higher than that of other structures (93.08% in one case), novel structures can be prepared since alginate has hydroxyl and acid functional groups, which can form composites with various materials. In general, most materials and structures used with alginate for CO_2 capture are N-doped and MOF-based materials. In the case of N-doped materials, since there are no amine functional groups in the alginate, which is very important for CO_2 capture, these materials are very noteworthy. Furthermore, MOFs are good for CO_2 capture owing to their porous structure and the results indicate the considerable effect of the application of alginate on the enhancement of their structure and performance.

4.1.2. Starch-based materials. One of the most plentiful and low-cost polysaccharides is starch. Starch is fabricated from some plants for the storage of carbohydrates. The natural sources of starch include potato, cassava, rice, maize, wheat, *etc*. Two types of polysaccharides form the structure of starch including (1,6) α-D-glucan amylopectin and (1,4)-linked α-D-glucan amylose, which are linear and branched, respectively. Starch has different features such as biodegradability, accessibility, and low-price. In the structure of starch, there are many –OH functional groups, making it very useful. Therefore, starch can be applied as a support, stabilizer, template, *etc*. for different applications.[150–153] In this section, we report different studies regarding starch-based materials for CO_2 capture.

4.1.2.1 Starch-based nitrogen-doped materials. In 2022, Lin *et al.* reported the fabrication of a series of N-doped microporous carbon materials.[154] In this research, they used starch as a carbon source, melamine and formaldehyde (MF) as a polymer resin, and KOH as an activator (MF@Cs). The presence of MFs enhances the active site of carbon materials owing to their rich N and O groups. In addition, MFs form 3D networks. At the temperature and pressure of 273 K and 100 kPa, respectively, MF@Cs show great performance for CO_2 adsorption with the adsorption capacity of 6.54 mmol g^{-1}. Interestingly enough, they also used resin to make the adsorbent.

In 2021, Park and co-workers prepared two sequences of novel materials including corn starch-derived microporous carbons modified with/without thiourea (Fig. 6).[155] For this aim, they used different types of activation materials such as K_2CO_3, KOH, and $K_2C_2O_4$. The sample doped with thiourea was more porous than the undoped carbon sample. Thiourea-doped $K_2C_2O_4$ AC (STO) displayed well-defined micropores. The porous structure of STO considerably improved the performance of STO for CO_2 adsorption. The results displayed that the adsorption performance was 269.61 mg g^{-1} at 0 °C and 1 bar. The innovation of this work was the effect of thiourea on the efficiency of the CO_2 adsorbent.

Isahak *et al.* reported the fabrication of an N-doped porous carbon hybrid from starch (SH800).[156] In this study, they investigated the CO_2 capture capacity of SH800. The results displayed that SH800 had an excellent CO_2 capture capacity of 29.8 wt% for biohydrogen gas adsorption.

4.1.2.2 Starch-based pellets materials. Preparation of sorbent pellets using Ca-based sorbents with a starch pore *via* the extrusion–spheronization method was performed by Han and colleagues.[157] For this aim, they used starch and cement as template and stabilizers, respectively. Their results exhibited that the optimum uptake of CO_2 was achieved using 10 and 20% of starch and cement, respectively. The 0.15 g g^{-1} CO_2 capture was achieved after 20 cycles.

In 2021, the synthesis of monolithic porous nanostructures of CaO–MgO composites using a self-sustained combustion reaction of molded pellets was performed by Nethravathi and colleagues.[158] For this purpose, they used a mixture of starch, nitrate salts of calcium and magnesium, and urea. The starch was applied as a binder and template and urea was used as fuel. Porous monoliths had high CO_2 capture at 650 °C in a 20% CO_2 gas stream. However, the adsorption capacity of the CaO–MgO porous nanostructures was 67–51 mass% of the sorbent.

4.1.2.3 Other starch-based materials. Tan *et al.* reported the fabrication of AC from carbonized gelatin and starch biomass using the dry chemical activation approach.[159] The synthesized samples had gelatin (G) and starch (S), activated by KOH (K), G and S being mixed with different amounts (*y*) at 700 °C and were referred to as GSK*y*-700. The results displayed considerably excellent CO_2 adsorption (7.49 mmol g^{-1} at 0 °C and 1 bar) by GSK1-700. In another study, Fuertes and Sevilla prepared porous carbons using the chemical activation of hydrothermally carbonized starch and cellulose as well as sawdust biomass.[160] The samples prepared were used as sorbents for the capture of CO_2. The samples produced under mild activation conditions (KOH/HC = 2) performed well, showing a high capacity for CO_2 uptake. In addition, the samples synthesized at 600 °C had a high capacity (4.8 mmol g^{-1} at 25 °C and 1 atm) for storage of CO_2 at ambient temperature.

4.1.2.4 Summary of this section. Starch has been mainly used as a carbon source and in most cases, carbonized and used as a source of AC. Starch has been used as a template,

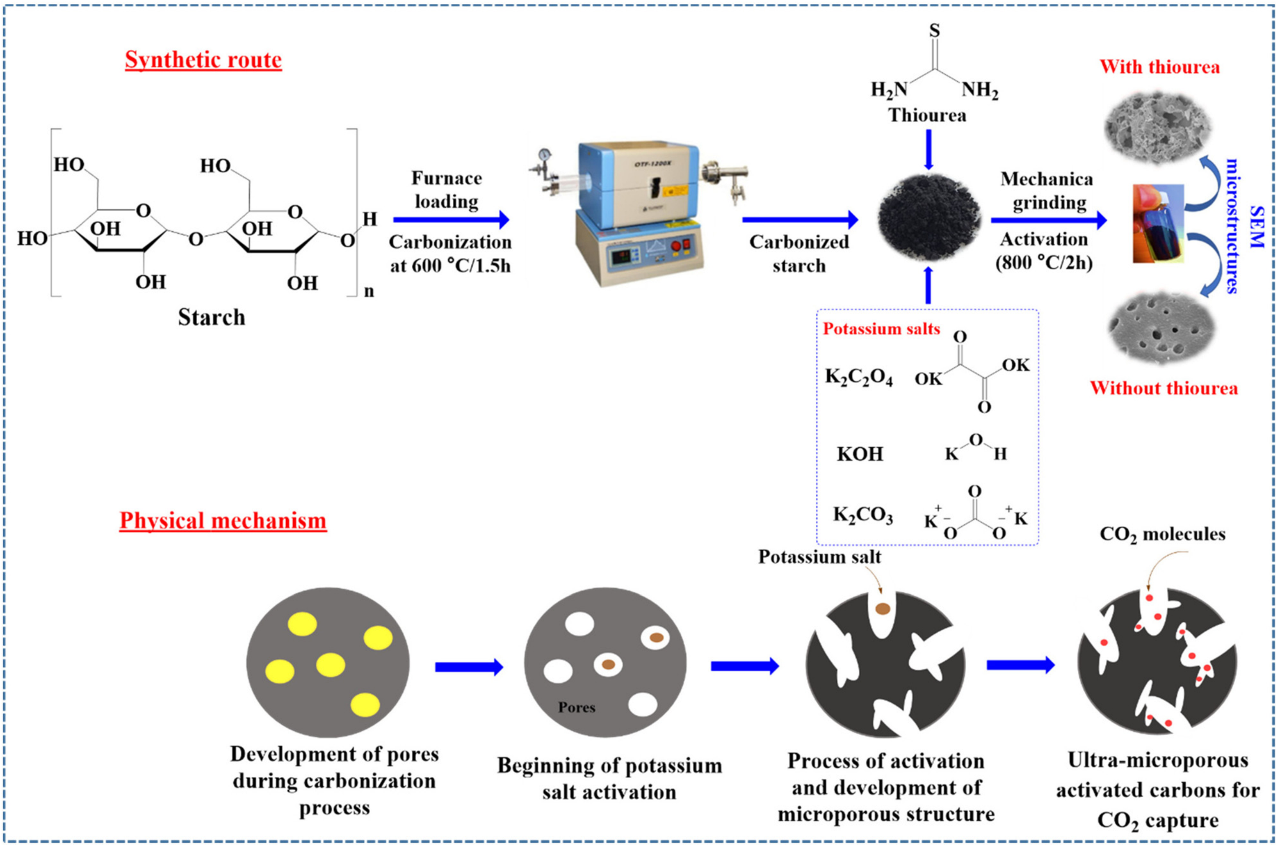

Fig. 6 Schematic representation of the preparation of the undoped/N,S co-doped with different activation salts of potassium starch-derived micro porous carbons and probable activation mechanism. Reproduced from ref. 155 with permission from Elsevier, copyright 2021.

but not widely used to make CO_2 capture materials. Thus, studies in this area are scarce and there is much to be done including starch-based, N-doped, and pellet materials. As a suggestion for future studies, starch can be used to fabricate composites using the combination of starch and MOF to increase the adsorption capacity of fabricated materials for CO_2 capture.

4.1.3 Gum-based materials. Gum is made up of many hydroxyl groups and is found in a variety of sources such as seeds, trees, and aquatic weeds. Gums are made from trees including Arabic, Kondabolu, karaya, tragacanth, Gum Ghatti, *etc.*[58] Gums are well-known natural polysaccharides made of sugar and are frequently utilized in the industry owing to their biocompatibility, odorlessness, non-toxicity, solubility in water, renewability, cost-effectiveness, and accessibility.[81,161] In this part, we review recent studies on gum-based materials for CO_2 capture application.

4.1.3.1 Gum-based pellet materials. In a study, Hussin and co-workers utilized to synthesize high-quality carbon pellets. AC was combined with organic binders such as tapioca starch (TS) and xanthan gum (XG) to produce pellets.[162] Both kinds of carbon pellets (TS-AC and XG-AC) continued to yield a high carbon content after the addition of water and the binder. Given their many functional groups, a longer breakthrough time, and a higher CO_2 adsorption capacity compared with xanthan gum, carbon pellets made with tapioca starch performed better than those prepared using xanthan gum. In comparison to XG-AC pellets (16.86 mg g^{-1}), TS-AC carbon pellets had remarkably high breakthrough time and CO_2 adsorption capacity of 16.2 min and 21.84 mg g^{-1}, respectively, at 25 °C. The innovation of this work is that two types of biopolymers have been used for the synthesis of adsorbents.

4.1.3.2 Other gum-based materials. In another study, Tasmanian Blue Gum (TBG) tree bark was chosen by Prasankumar *et al.* as the starting material for producing activated porous carbon utilizing an easy KOH activation and carbonization procedure.[163] For CO_2 collection from concentrated sources and diluted 4% CO_2 simulated flue streams, AC-TBG was used. With a 1.6 mmol g^{-1} working capacity at 40 °C and 4% of CO_2, AC-TBG demonstrated exceptional CO_2 absorption (4.5 mmol g^{-1}) at 0 °C and 1 bar for pure CO_2.

4.1.3.3 Summary of this section. There are very few examples of gums-based materials for CO_2 capture (only 2 studies are available). In these examples, gum has been used as a source for making AC. In general, the application of gums to make materials capable of capturing CO_2 is not very efficient. However, the structure of gum is similar to that of alginate such that it can easily form a gel and hence it can be very effective in making hydrogels. Thus, one of the issues, which should be addressed in the future is the preparation of hydrogels based on different types of suitable and effective gums for CO_2 capture. The structure of these hydrogels must be such that amine groups are located on the top so that they can have a high efficiency for CO_2 capture.

4.1.4 Pectin-based materials. Pectin is a complex polysaccharide made up of linear -(1,4) galacturonic acid residues connected throughout the chain by -(1–4) glycosidic links with hydroxyl and carboxyl groups.[164,165] Fruit peels and many plant cell walls contain pectin. Considering its capacity to form aqueous gels, it is employed as a stabilizer in the food industry. The biocompatibility, biodegradability, non-toxicity, hydrophilicity, and flexibility of pectin make it suitable for biomedical and cosmetic uses.[166]

4.1.4.1 Pectin-based other materials. In 2022, to prepare micro–mesoporous carbon powders, which are both oxygen and nitrogen-loaded, Vafaeinia *et al.* used pectin and melamine as the corresponding organic precursors.[167] Given its unique micro–mesoporous structure and abundance of basic nitrogen-containing functionalities, at 273 K at 1 bar, the ideal porous carbon had CO_2 adsorption capacities of up to 3.1 mmol g^{-1}.

Jovellana and Pajarito demonstrated the viability of pectin as the foundation for amine functionalization by coating it on zeolites for CO_2 absorption.[168] Pectin has been successfully modified using NH_3 and triethylenetetramine (TETA) as alternative amine-functionalized coating agents and coated on substrates such as zeolites for CO_2 uptake. Adsorbents coated with NH_3 and TETA-modified pectins had adsorption capacities of 2.24 and 2.28 mmol g^{-1} at 5% breakthrough, respectively. In this study, zeolite was used along with pectin for better efficiency. Moreover, in 2016, pectin was used as the primary starting material to synthesize nanoporous AC in a two-step method through hydrothermal carbonization of a pectin water dispersion at 230 °C, followed by chemical activation with KOH at 700 °C. At 1 atm and room temperature, this material had a considerable CO_2 capture capability of 13–7 mmol g^{-1}.[169]

4.1.4.2 Summary of this section. In the field of CO_2 capture, pectin is often used as a functional biopolymer to make porous activated carbon. Nitrogen-enriched pectin, prepared by functionalization with various amine materials, exhibits high efficiency for CO_2 capture since the obtained porous sorbent is enriched in both oxygen and nitrogen.

4.1.5 Chitosan-based materials. The only naturally occurring polysaccharide with an amino group, chitosan (CS), is prepared by deacetylating chitin, which is found in abundance in nature. Over 10 billion tons of chitin are produced by biosynthesis each year, and after cellulose, it is the most frequently occurring biopolymer in nature, which is found in the shells of crabs and shrimp, fungi, and insects.[170,171] As a natural biopolymer, CS has several inherent benefits, including affordability, biodegradability, biocompatibility, non-toxicity, and effective sorption capabilities. In particular, the free amino-hydroxyl groups give CS features including antibacterial activity, chelating with heavy metals, protein affinity, solubility in water, and most significantly, the simplicity of processing and modification.[166,172,173] CS has a strong adsorption capacity. However, given its low reusability, weak mechanical properties, and ease of solubilization in acids, its applicability is limited.[170] Nevertheless, these limitations can be resolved by chemical or physical modifications. In addition to enhancing mechanical strength and adsorption capabilities, physical and chemical modifications can prevent the dissolution of CS in strong acids. Physical modification often involves combining (derivatives) CS with other materials or transforming it into distinct forms, including membranes, microspheres, fibers, gels, and porous particles without altering the inherent features of CS.[174] Given the capability of CO_2 molecules to hop between the matrix's arbitrary openings, CS is anticipated to allow selective CO_2 permeation due to the basic amino groups present in the polymeric chain (Fig. 7).[175,176] In this section, we have reviewed the CO_2 adsorption features of different CS-based materials such as composites, membranes, hydrogel, *etc.*

4.1.5.1 Chitosan-based aerogel materials. To prepare aerogels with high CO_2 absorption, much research has been carried out. For example, in 2021, using a phase inversion technique followed by freeze-drying, Luzzi *et al.* were able to successfully embed zeolite 13X (ZX) powder in the CS framework to prepare composite aerogel beads (Fig. 8).[177] This method completely utilized the potential of the constituents, resulting in a sample with 561 m^2 g^{-1} HSSA and 4.23 mmol g of CO_2 uptake capacity for the sample containing 90% zeolite. The beads were coherent, mechanically stable, and reusable after regeneration using a gentle pressure swing technique, and had an exceptional ability to adsorb CO_2. In this study, the presence of zeolite has increased the efficiency of the adsorbent due to its porous structure.

Furthermore, in 2021, Liu and colleagues developed a model high-strength hydrogel and aerogel using CS and lithium sulfonate double networks using an electron beam.[178] The aerogels had a double network structure with CO_2-philic properties, which gave them a porous structure and 67.9 mg g^{-1} CO_2 capture capacity at 0.1 MPa and 298 K, indicating that they had a HSSA of 114.18 m^2 g^{-1}. Applications for harvesting CO_2 in real-world settings are feasible because of the physical and chemical strength of the aerogel. The innovation of this is the shape of the adsorbent structure, which is in the form of a double network structure.

A unique GO/Laponite® RD/CS was prepared by Du and co-workers.[179] Ternary composite produced using the freeze-drying and sol–gel methods was then employed as a CO_2 adsorbent. Aerogel-type solid amine adsorbent had a CO_2 adsorption capacity of 78.9 mg g^{-1} and was capable of both physical and chemical adsorptions. This adsorbent had several advantages, including inexpensive starting materials, environmental friendliness, and a comparatively high adsorption capacity.

According to the research by Hsan and co-workers in 2019, CS-grafted GO aerogels have a wide surface area, high porosity, and a significant number of amine groups, which allow CO_2 adsorption gas. At 1 bar, CS-grafted GO aerogels had an

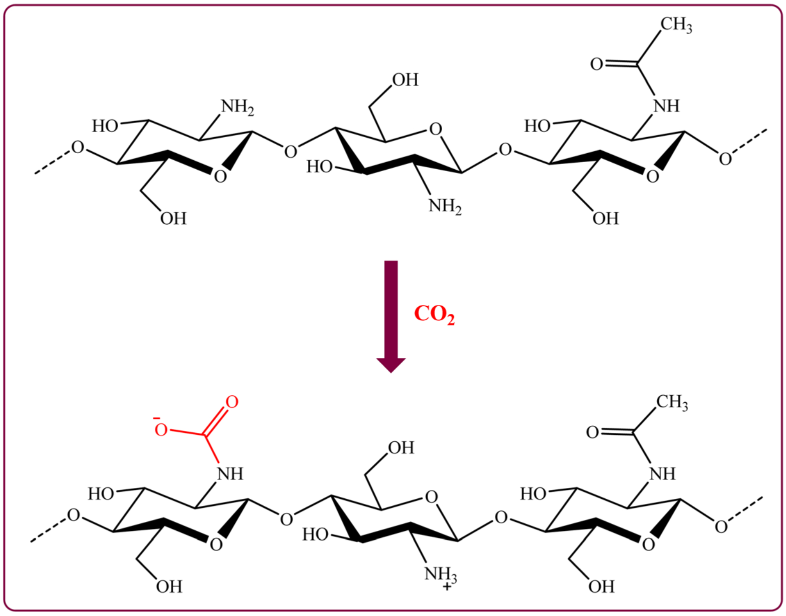

Fig. 7 Adsorption of CO_2 molecules by CS.

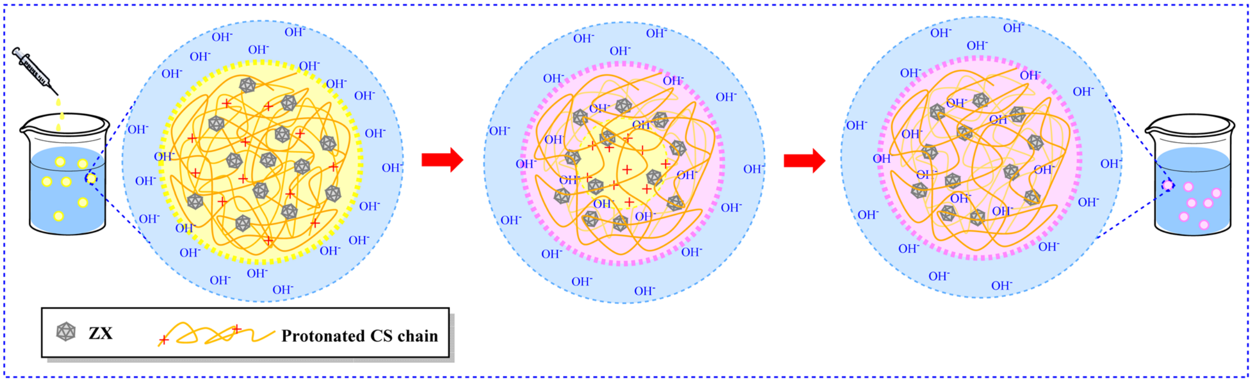

Fig. 8 Production of the hydrogel beads by the phase inversion method.[177]

approximate adsorption capacity of 0.257 mmol g^{-1}.[180] To reversibly capture CO_2 from the environment through humidity swing, Song *et al.* employed cost-effective quaternized CS (QCS)/PVA hybrid aerogels containing quaternary ammonium groups and hydroxide ions (Fig. 9a). The capability of QCS/PVA hybrid aerogel to extract CO_2 was predicted to be 0.18 mmol g^{-1} in the temperature range of 10–30 °C (Fig. 9b).[181]

Alhwaige *et al.* synthesized MMT-CTS-PBZ nanocomposite aerogels using biobased CS-poly benzoxazine (CTSPBZ) as a precursor for high CO_2 adsorbing carbon aerogels and montmorillonite (MMT) to reinforce the CTS-PBZ aerogel.[182] MMT-CTS-PBZ aerogels were prepared using the freeze-drying method and subsequently cross-linked by the ring-opening polymerization of benzoxazine and carbonization at 800 °C. Even at high pressure, polybenzoxazine enhanced the structural stability for CO_2 removal from the environment. The carbon aerogels had strong reversible CO_2 adsorption–desorption activity by a maximum of 5.72 mmol g^{-1} and mesoporous materials with pore sizes in the 2–7 nm range, high BET surface area, and mesoporous materials. The innovation of this work was the application of MMT along with chitosan to make the absorbent. In another study in 2013, CS, an environmentally safe biopolymer was combined with varying concentrations of GO by Alhwaige *et al.* to develop hybrid monolith aerogels. The adsorption capacities of the aerogels for CO_2 collection were investigated. Upon the addition of 20 wt% GO, the quantity of CO_2 adsorbed at 25 °C increased from 1.92 to 4.15 mol kg^{-1}.[183] In fact, the addition of GO significantly improved the adsorption capacity.

4.1.5.2 Chitosan-based composite materials. In the conversion of CO_2 to valuable products, in 2018, Kumar *et al.* studied CO_2 adsorption and its conversion to cyclic carbonates in the absence of any solvent using an environmentally friendly method based on CS/GO nanocomposite film. At 4.6 bar, a

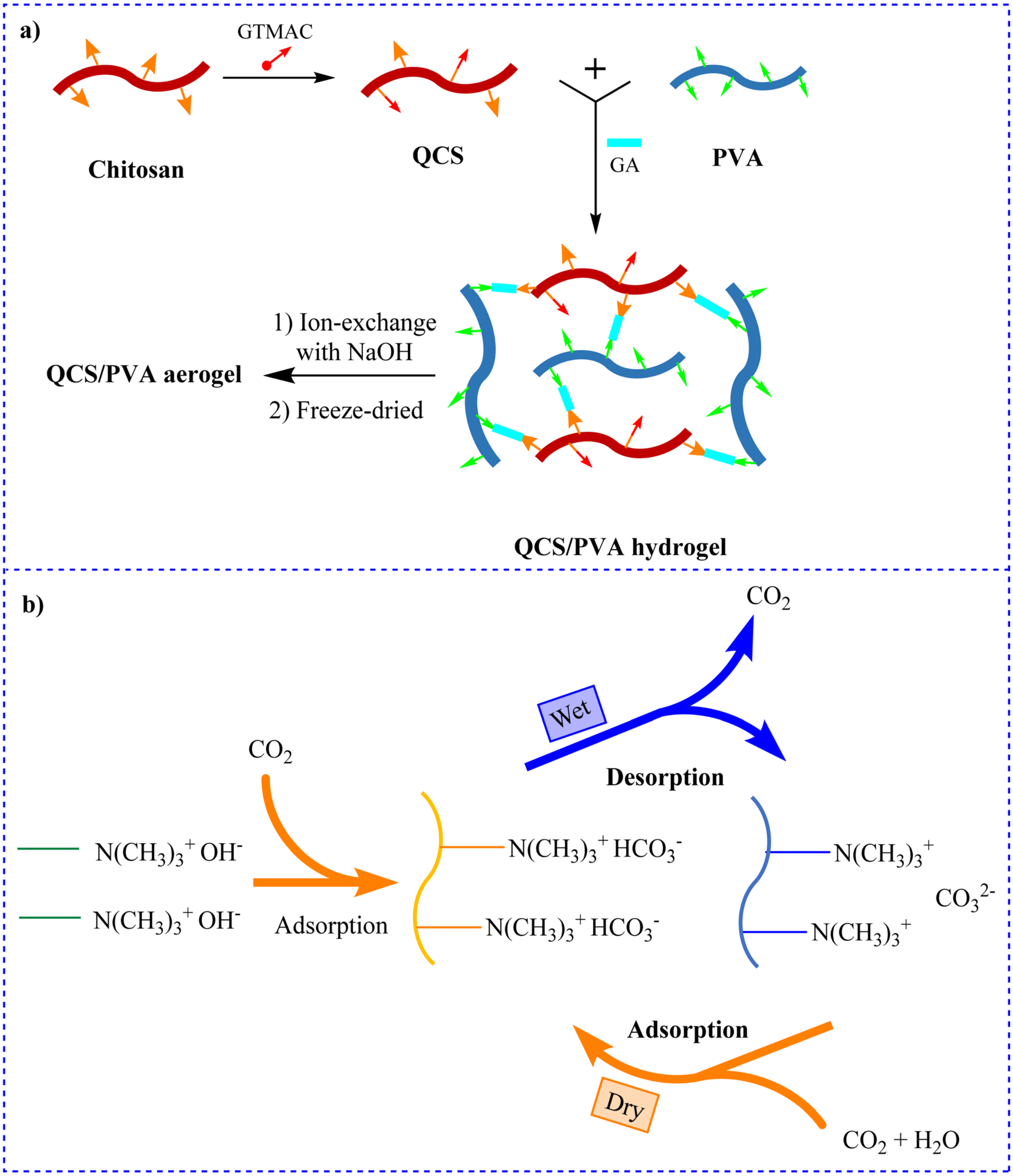

Fig. 9 (a) Preparation of QCS/PVA hydrogel and QCS/PVA aerogel[181] and (b) adsorption of CO_2 by humidity swing.[181]

CSGO nanocomposite with an adsorption capacity of 1.0152 mmol g^{-1} was reported.[184] In this study, after adsorbing CO_2, it was converted into carbonate products, which is an interesting innovation.

4.1.5.3 Chitosan-based hydrogel materials. One method for CO_2 capture is the use of hydrogels, which are made of a polymeric network. In 2021, Kunalan *et al.* examined the gas transport properties of hydrogel CS and CS-polyethylene glycol (CS + PEG) polymer mix surface-modified poly-vinyl trimethyl silane (PVTMS) composite membranes for pure CO_2, N_2, and CH_4 gases.[185] The transmembrane pressure of 76 cmHg and the reaction temperature of 30 °C, which were the optimal conditions, allowed the CS + PEG-modified PVTMS membranes to achieve an acceptable CO_2 permeability of 153 barrer. The innovation of this work is the application of a mixed polymer matrix to make membranes. In another study, Wen and colleagues prepared a unique bimetal-based inorganic–carbonic anhydrase hybrid nanoflower (CANF), which immobilized carbonic anhydrase using bimetal ions (Cu^{2+} and Zn^{2+}) rather than individual metal ions. These CANF composites were then embedded into PVA/CS hydrogel membranes (PVA/CS@CANF) to produce a new decorated carbonic anhydrase for CO_2 capture.[186] Exceptional mechanical strength, great catalytic performance, and ease of flow were all characteristics of the PVA/CS@CANF hydrogel membranes. PVA/CS@CANF, in particular, might effectively absorb CO_2. $CaCO_3$ production by PVA/CS@CANF was 9 and 2-fold more than those of free carbonic anhydrase and CANF, respectively. Consequently, there may be a lot of potential applications for bimetallic-based protein hybrid hydrogel membranes in CO_2 capture.

4.1.5.4 Chitosan-based membrane materials. Technologies employing membranes to capture CO_2 have the following advantages: they use less energy, are easier to design and operate, and have superior thermal and mechanical stability. In 2022, Li *et al.* fabricated thin-film composite (TFC) membranes with piperazine (PIP) solution and carboxymethyl chitosan (CMC) chains, which have water-swelling properties, using interfacial polymerization (IP) to enhance the performance of CO_2 separation (Fig. 10a)[187] This research proposed a quick and efficient way to adjust the membrane shape and improve assisted transport. The application of CO_2/N_2 mixed gas, PIP/TMC, CMC/TMC, and PIP-CMC/TMC membranes was also investigated. For CO_2 capture from flue gas, PIP-CMC/TMC membranes with octopus-branched nanostructures exhibited good CO_2 permselectivity and offered a wide range of potential applications.

Shen *et al.* fabricated a transport mixed matrix membranes *via* the surface coating process by dispersing GO grafted with hyperbranched polyethylenimine (HPEI-GO) nanosheets in CS cross-linked with polyvinyl amine (PVAm) polymer matrix solution for CO_2/N_2 separation (Fig. 10b).[188] The maximum CO_2 performance was 36 GPU in a 2 wt% HPEI-GO membrane, while the best CO_2/N_2 selectivity was 107 in a 3 wt% HPEI-GO membrane.

4.1.5.5 Chitosan-based MOF materials. Due to their advantages, MOFs, a type of hybrid nanoparticle material, have attracted a lot of attention. Using a packed bed column and a gas mixture containing 15% CO_2 and 85% N_2, Singo and coworkers impregnated a sodalite zeolite-like MOF (sod-ZMOF) with CS in 2017 and studied its capability of absorbing CO_2.[189] At a temperature of 25, an FR of 25 ml min^{-1}, and a pressure of 1 bar, Sod-ZMOF-CS showed maximum adsorption capacity of 978 mg g^{-1}. In this study, sodalite, which is a scarce mineral, was used in the preparation of the absorbent.

Using mathematical modeling, Yoro *et al.* studied the behavior of Sod-MOFs/CSs as an adsorbent for post-combustion CO_2 absorption.[190] Sod-ZMOF/CS demonstrated a two-stage adsorption process with an initial quick CO_2 absorption and a later sluggish CO_2 adsorption process under various adsorption temperatures. The tests performed to validate these models were carried out at temperatures of 30, 45, and 60 °C, an operating pressure of 200 kPa, a gas FR of 2.5 mL s^{-1}, and a mass of adsorbent of 0.1 g.

4.1.5.6 Chitosan-based heteroatom-doped materials. Malini and co-workers prepared N-doped porous AC using CS and hexamethylenetetramine (HMT) (in ratios of 1 : 1 and 1 : 3 wt/wt) as the carbon precursor and an additional nitrogen source, respectively.[191] The CS/HMT-derived AC had a larger N-content and enhanced thermal stability, but as the HMT content increased, the surface characteristics decreased. At 25 °C, the CO_2 adsorption of AC produced from CS was determined to be 97.98 mg g^{-1}, compared to 72.95 and 55.11 mg g^{-1} for AC/HMT (1 : 1) and AC/HMT (1 : 3), respectively.

In another study, CS and $NaNH_2$ were used by Yang *et al.* to synthesize N-doped under solvent-free conditions.[192] At 273.15 K and 100 kPa, the adsorption capacity of CO_2 reached 6.33 mmol g^{-1}. Using N-doped porous carbon as a promoter, CO_2 could be converted into various formamides with good yields in the absence of metals. These CS-based N-doped porous carbons are therefore possible candidates for CO_2 capture and conversion due to their good uptake of CO_2, great reactivity, the cost-effectiveness of the precursor, and simple production method. The novelty of this work was the preparation of the absorbent in the absence of solvents.

Li *et al.* prepared N-doped carbon nanosheets using various activators such as KOH, KAc, K_2CO_3, $KHCO_3$, and CS derived from biomass as a carbon precursor.[193] The materials produced by KOH activation (CN6-750-KOH) demonstrated a remarkable CO_2 adsorption capacity of 3.91 mmol g^{-1} at 298 K and 1 bar. Surprisingly, a carbon activated *via* KAc (CN6-750-Kac), performed comparably to CN6-750-KOH, attaining a CO_2 capture capacity of 3.54 mmol g^{-1}. In this study, different types of activators were used.

Preparation of the N,P co-doped porous carbon materials (NPPCs) with phytic acid (PA)-induced self-assembled CS materials was performed by Xiao and colleagues through pyrolysis and activation processes.[194] PA works as a P source, an acid regulator, and a structure-directing agent to form more pores with enhanced activation efficiency. A small amount of $NaNO_3$ is concurrently utilized as a template and an activator. The as-prepared NPPCs, which are bifunctional carbon materials, performed well at adsorbing CO_2 and storing electrochemical energy. NPPC-0.75-600 showed CO_2 adsorption capacities of 5.31 and 3.02 mmol g^{-1} at pressures of 500 and 100 kPa, respectively.

He and colleagues synthesized AC by carbonizing rice husk, followed by activation with KOH. KOH activation was carried out concurrently with surface modification using CS as a nitrogen source.[195] At 273 K and 1 bar, with a CO_2 adsorption activity of 5.83 mmol g^{-1}, CAC-5 (modified AC) outperformed AC-5 (generic AC) due to the formation of CO_2-philic active sites on the surface of the modified AC by N-species.

To fabricate N,S co-doped carbons (NSCDCs), Shi *et al.* developed a unique and simple strategy through the chemical blowing process.[196] Carbon and nitrogen were provided by CS while sulfur was supplied by hydroquinonesulfonic acid potassium salt (HAPS), which was also utilized as the blowing agent (Fig. 11a). By carbonizing, a combination of CS and HAPS in one step, NSCDC with a hierarchically porous structure was produced. At pressures of 20 and 1 bar and temperature of 25 °C, the best CO_2 uptakes were 12.9 and 2.4 mmol g^{-1}, respectively.

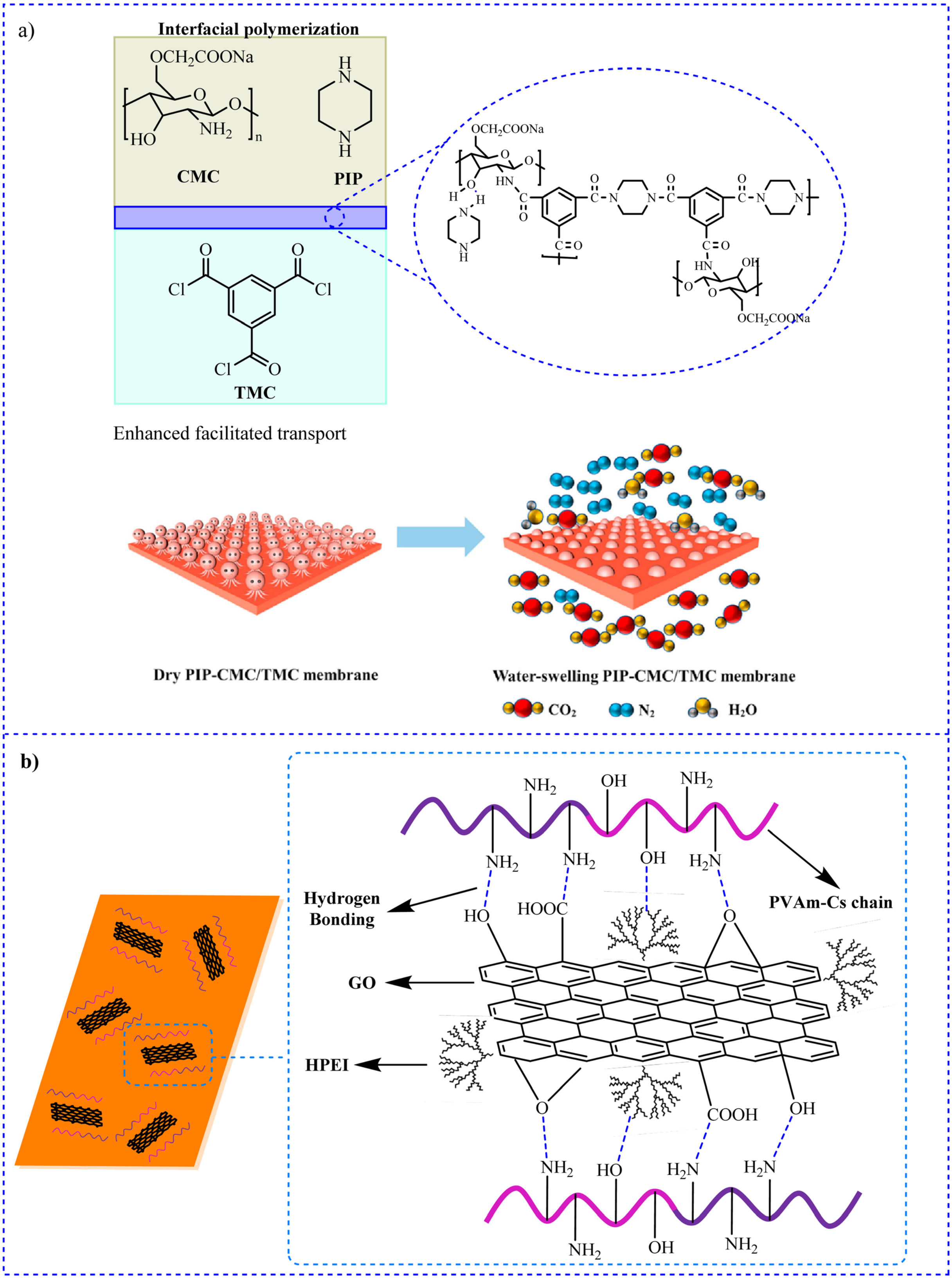

Fig. 10 Preparation of (a) PIP-CMC/TMC membranes. Reproduced from ref. 187 with permission from Elsevier, copyright 2022 and (b) HPEI-GO/CS-PVAm/PS membranes.[188]

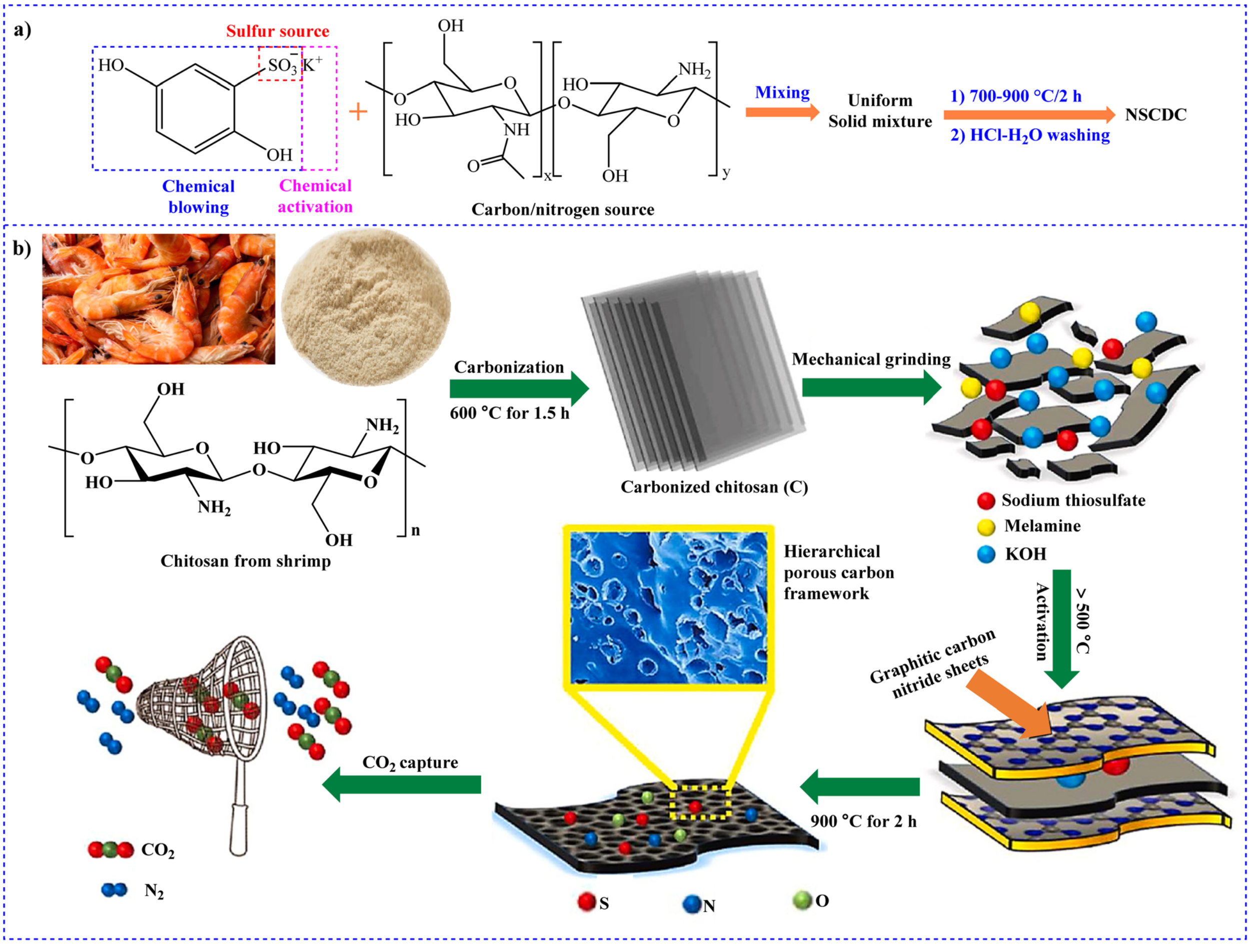

Fig. 11 Synthesis of (a) NSCDC[196] and (b) N,S,O doped hierarchical micro porous carbons from CS. Reproduced from ref. 197 with permission from Elsevier, copyright 2021.

Nazir *et al.* designed a sequence of non-doped/heteroatom (N,S,O)-doped porous carbons by a two-step pyrolysis-KOH chemical activation after extracting CS from used shrimp shells by deproteination and deacetylation methods (Fig. 11b).[197] At 273 K and 1 bar, the as-prepared material exhibited outstanding CO_2 adsorption capacity (236.8 mg g^{-1}).

In 2019, using CS (NCS-T) and glucose (NCS_{NH3}-T) as the starting materials, Wu *et al.* synthesized two kinds of carbon microspheres with abundant porous N-containing groups utilizing practical and affordable methods.[198] Due to the micropores and ultramicro pores formed, the CO_2 adsorption capacities of NCS-T and NCS_{NH3}-T were 51–141 and 180–243 mg g^{-1}, respectively. In this study, two types of starting materials were used to synthesize N-containing materials.

Fujiki and Yogo prepared extremely porous N-doped AC (NACs) *via* chemical CS activation using alkali carbonates.[199] 1.6 and 4.9 mmol g^{-1} CO_2 capacities were displayed by the NACs at temperatures and pressure of 25, 15 °C and 100 kPa, respectively. At low partial pressures, the addition of N-doped improved CO_2 adsorption. Furthermore, Fan and co-workers used CS and K_2CO_3 as a precursor and activator, respectively, to prepare N-doped porous carbons for CO_2 capture.[200] These porous carbons exhibited high CO_2 adsorption capacity. In particular, the sample prepared using K_2CO_3/CS = 2 at 635 °C showed a considerably high CO_2 capture capacity of 3.86 mmol g^{-1} at temperature and pressure of 25 °C and 1 atm., respectively. In another study, Thote *et al.* used CS as the biopolymer template to produce N-doped mesoporous alumina. At 55 °C, the adsorption capacity was 29.4 mg g^{-1}.[201] At 55 °C, this value was 4 times higher than that of commercial mesoporous alumina. This increased CO_2 adsorption is caused by the basicity of the alumina surface in combination with the nitrogen in the template in the synthesized sample.

Table 1 shows further examples of CO_2 capture technologies based on chitosan-based polymers.

4.1.5.7 Summary of this section. Chitosan is a natural polymer containing an amine functional group. On the other hand, it can form various types of gels. As a result, many studies have been conducted in the field of CO_2 capture using chitosan-based materials. In the field of chitosan-based gels for CO_2 capture, two studies have been performed using hydrogels and aerogels. Moreover, chitosan is capable of forming Com with other materials. However, there is still much work to be done in the future. Membranes are also effective materials

Table 1 Chitosan-based materials for CO_2 capture

Entry	CS-based sorbent	Operating conditions (temperature and pressure (bar))	Capacity (mmol g^{-1})	Ref.
1	NaOH@CS-Fe_3O_4	25 °C and 9	3.21	202
2	CM-Cs in BMI·OAc	r.t. and 1 atm	2.32	203
3	Biochar derived CS	0 °C and 1	4.11	204
4	HTC of CS[a]	25 °C and 1	4-Fold	205
5	N-ACs from CS[b]	0 °C/25 °C and 1	7.9/5.6	206
6	CSMWCNT[c]	298 K and 1	1.92 ccg^{-1}	207
7	TiO_2-grafted CS film	—	—	208
8	CNFs/Cu/BTC-3[d]	298 K and 100 kPa	9.5 cm^3 g^{-1}	209
9	Micro porous carbons from CS	273 K and 1	280 mg g^{-1}	210
10	Micro porous carbons from CS	0 °C and 0.15	17.3–22	211
11	Furfuryl-imine-CS fibers	295 K and 0.610	0.978	212
12	CS-derived mesoporous carbon	100 °C under atmospheric pressure	3.72	213
13	Chi-BE[e]	38.13 °C	344.98 mg g^{-1}	214
14	CS/MWCNT	45 °C and 1.1	3 mg g^{-1}	215
15	CS-TPPS[f]	—	0.9	216
16	Triphenyl amine CS derivative	5	0.85 mmol/mmol	217
17	CS/mesoporous silica	25 °C and 1 atm	0.98	218
18	PEI-CS bead[g]	313 K and 15 kPa	2.3	219
19	AC-CS[h]	298 K and 40	13.65	220
20	CGAC[i]	—	0.25 mol kg^{-1}	221
21	CS modified CMK-3s	—	—	222
22	Graphitic carbons derived from CS	0 °C and atmospheric pressure	5	45
23	Zeolite ZY-chitosan composite	4.6	1.7	223
24	CS/ZIF-8 composite	275.15 K and 500 kPa	3.6	224

[a] Hydrothermal carbonization of CS. [b] Hierarchical porous nitrogen-containing AC derived from CS. [c] CS grafted multi-walled carbon nanotube. [d] Cu-BTC-integrated CS/PVA nanofibrous membranes. [e] CS-bleaching earth clay composite. [f] CS based *meso*-tetrakis(4-sulfonatophenyl)porphyrin. [g] Polyethylenimine-functionalized porous CS. [h] Amine-functionalized AC with CS. [i] AC impregnated CS.

for CO_2 capture and chitosan has been used to make membranes. Of course, membranes are mostly used when there is a mixture of several gases. The combination of chitosan and MOFs has also been reported to have a relatively high adsorption capacity. As pointed out at the beginning, chitosan possesses an amino functional group. However, there are relatively many studies on the application of chitosan-based N-doped materials for CO_2 capture. This shows that the presence of amine groups is useful and necessary for the capture of CO_2. In addition, and the studies in this field show the high adsorption capacity of CO_2 in these materials.

4.1.6 Cellulose-based materials. The most common polymer on earth is cellulose, a linear polysaccharide. Natural cellulose fibers may be found in materials such as cotton, linen, and wood. These materials are reasonably priced, biodegradable, and biocompatible.[225–228] Linear homopolysaccharide cellulose, with the chemical formula $(C_6H_{10}O_5)_n$, is built of β-D-anhydroglucopyranose units and possesses a hydrogen bond because of the electrostatic interactions between hydrogen and oxygen atoms. This hydrogen bond reduces the solubility of cellulose in polar liquids.[229,230]

As shown in Fig. 12, some examples of nanocelluloses are cellulose nanofibril (CNF), cellulose nanocrystal (CNC), cellulose nanocomposite, and bacterial cellulose (BC).[231,232] Low mechanical properties, poor microbiological resistance, and limited porosity are only a few of the challenges associated with the practical application of cellulose. Several conventional methods, including physical adsorption and surface chemical alterations, have been developed over time to provide various functions on cellulose materials.[233–236] The CO_2 adsorption characteristics of several cellulose-based materials, including hydrogel, composites, membranes, *etc.*, have been reviewed in this part.

4.1.6.1 Cellulose-based composite materials. To investigate the impact of packing materials on the efficiency of cryogenic CO_2 removal from natural gas, in 2019, Babar and colleagues used three different types of packing materials; namely, spherical glass beads, cellulose acetate (CA) monofilament and hollow fibers, and composite CA/NH_2-MIL-101(Al) hollow fibers.[237] In addition, it was found that the composite CA/NH_2-MIL-101(Al) hollow fibers collected CO_2 more effectively than glass beads and pure CA fibers. Additionally, it was found that the CO_2 removal efficiencies of composite hollow fibers were 141.9 and 9.5% higher than those of spherical glass beads and pure CA hollow fibers, respectively. In another study in 2016, Gunathilake *et al.* developed amidoxime-functionalized microcrystalline cellulose (MCC)-mesoporous silica composites using a two-step procedure. At first, in the presence of Pluronic P123 triblock copolymer under acidic conditions, solvent evaporation-induced self-assembly of MCC, tetraethylorthosilicate, and (3-cyanopropyl)triethoxysilane produced MCC-mesoporous silica containing cyanopropyl groups (MCC-CP).[238] The material was then treated with hydroxylamine hydrochloride in a further step to convert the cyanopropyl groups into amidoxime functionalities and generate a mesoporous MCC-AO composite. At a high temperature of 120 °C, they achieved the remarkable CO_2 adsorption capacities of 2.15–2.41 mmol g^{-1} (MCC-CP) and 2.84–3.85 mmol g^{-1} (MCC-AO).

4.1.6.2 Cellulose-based MOF materials. MOFs have been broadly employed as adsorbents for CO_2 adsorption and separ-

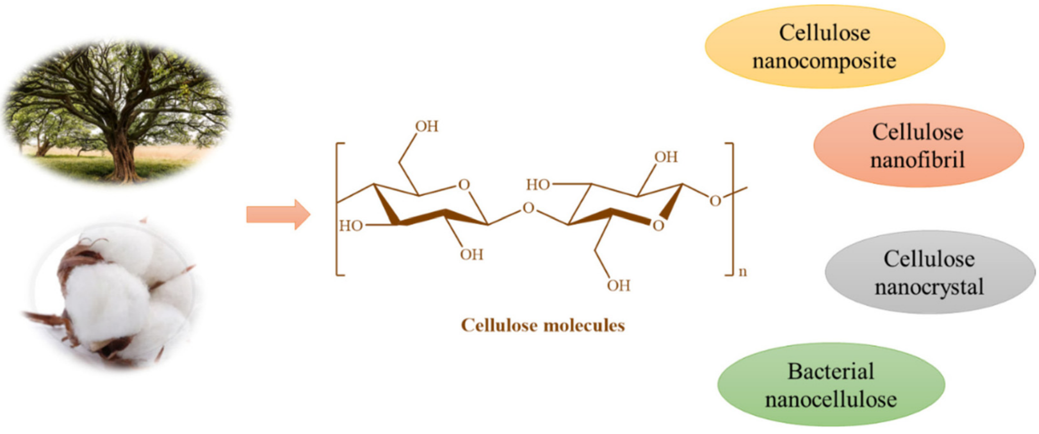

Fig. 12 Types and structure of cellulose.

ation. For example, Jabbar *et al.* prepared micro and nanocomposites of cellulose@MOF-199 using cotton fabrics and nanobacterial cellulose (NBC) (Fig. 13).[239] Under standard conditions of temperature and pressure, NBC@MOF-199 and Cotton@MOF-199 both displayed high adsorption capacities of 2.9 and 1.2 mmol g^{-1}, respectively.

In 2021, by synthesizing Cu Luzzi *et al.* were able to successfully embed zeolite-1,3,5-tricarboxylate [$Cu_3(BTC)_2$], Zn 2-methylimidazolate [$Zn(MeIm)_2$], and AlBTC *in situ* in a mesoporous cellulose template made of balsa wood, Wang *et al.* successfully prepared foam-like TO-wood/MOF composites (Fig. 14).[240] TO-wood/$Cu_3(BTC)_2$ composite had a greater CO_2 adsorption

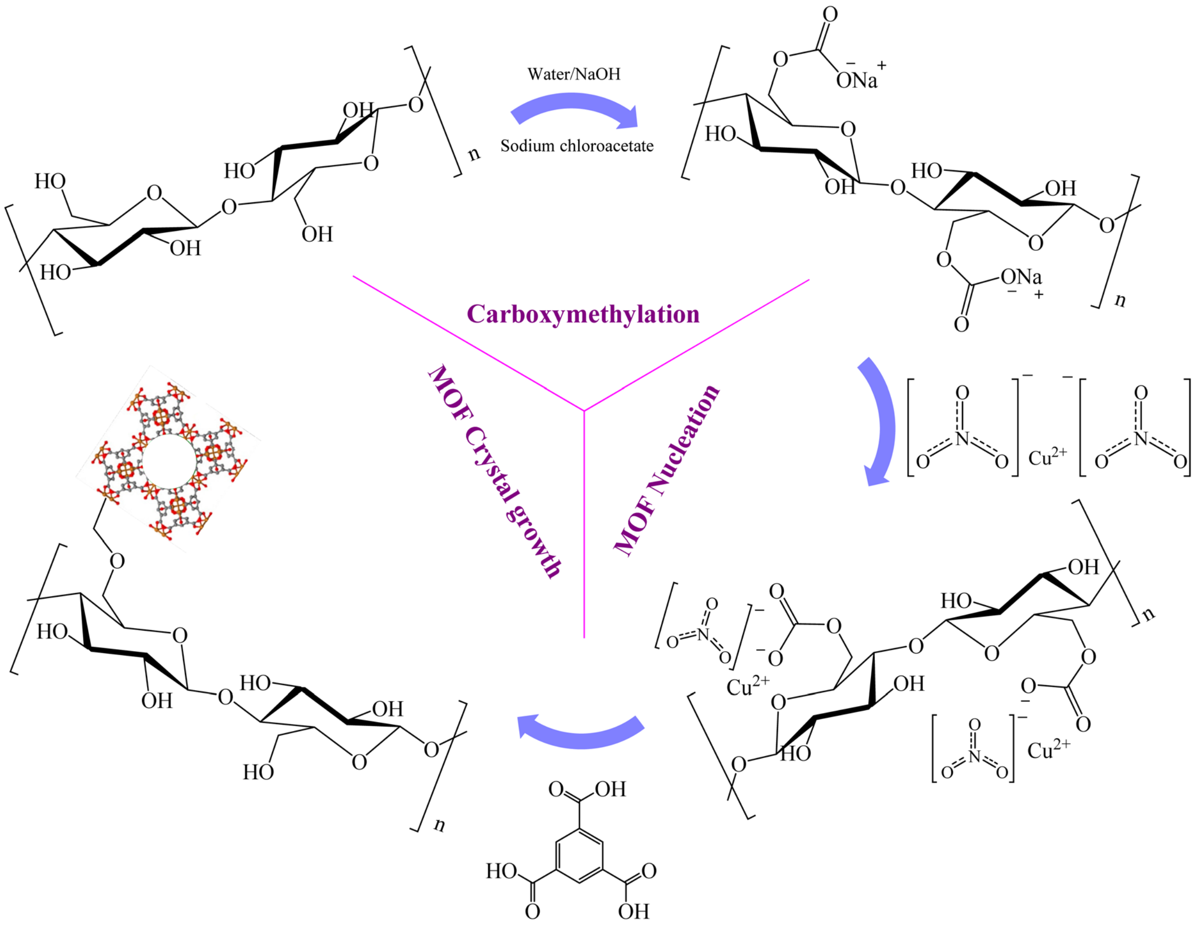

Fig. 13 Schematic representation of carboxymethylation and MOF-199 growth processes on the surface of nanobacterial cellulose.[239]

capacity than TO-wood/Zn(MeIm)$_2$ and TO-wood/AlBTC composites, at 1.46 mmol g^{-1} at 25 °C and atmospheric pressure.

To capture CO_2, Policicchio and colleagues developed a novel composite containing 2% CNC with a range of surface functional groups (such as carboxylic acids, sulfonic acids, and amines) incorporated into UiO-66.[241]

Yang *et al.* used cellulose paper packed with precipitated calcium carbonate (PCC) to produce cellulose paper@MOF-5 composite (Fig. 15).[242] According to gas adsorption experiments, the as-prepared paper@MOF-5 composite showed a superior capacity to adsorb nitrogen gas and may have a lot of potentials to adsorb or store other gaseous products such as H_2, CO_2, CH_4, *etc.*

4.1.6.3 Cellulose-based membrane. In 2022, Brunetti *et al.* continuously exposed cellulose-based carbon hollow fiber membranes to a gas stream, which also contained H_2S and/or water vapor for 183 days while observing the separation performances of the membranes.[243] At 298 K and 10 bar, CO_2 and CH_4 showed adsorption capacities of 2.98 and 2 mmol g^{-1}, respectively. Moreover, in 2022, mixed matrix membranes (MMMs) with better CO_2 adsorption capability were prepared by Rehman and colleagues.[244] Cu-MOF-GO composite was added to CA polymer matrix as filler at a rate of 1 to 5 wt% to form MMMs (Fig. 16a). At a pressure of 15 bar, the maximal CO_2 absorption rate was 1.79 mmol g^{-1} and 7.98 wt%. According to the adsorption data, Cu-MOF-GO composite and CA-based MMM can both effectively collect CO_2.

To produce a novel class of MMMs for selective biogas upgrading, Regmi and co-workers combined TiO_2 nanotube (TNT) amalgamated GO matrix with cellulose triacetate (CTA) (TNT@GO/CTA).[245] The resulting MMMs had a higher affinity for CO_2 adsorption. Almost 7 times more CO_2 was permeable, reaching 22.54 Barrer. Using materials such as TNT, GO, and CTA, the adsorption performance was considerably enhanced. In a cellulose-based polymer matrix, Ali *et al.* assessed the possible intercalated effects of metal-induced microporous polymer (MMP) dots.[246] Under both dry and humid conditions, the CO_2 separation efficiency and plasticization pressure of MMP-intercalated smart membranes were assessed. According to the gas permeation measurements, adding MMP nanodots to cellulose polymer increased CO_2 permeability from 14.1 to 108.9 Barrer. HSSA, hydrolytic stability, and effective performance for natural gas-type effluents under humid conditions are only a few of the promising characteristics of ultrathin intercalated membranes developed employing MMP nano-dots.

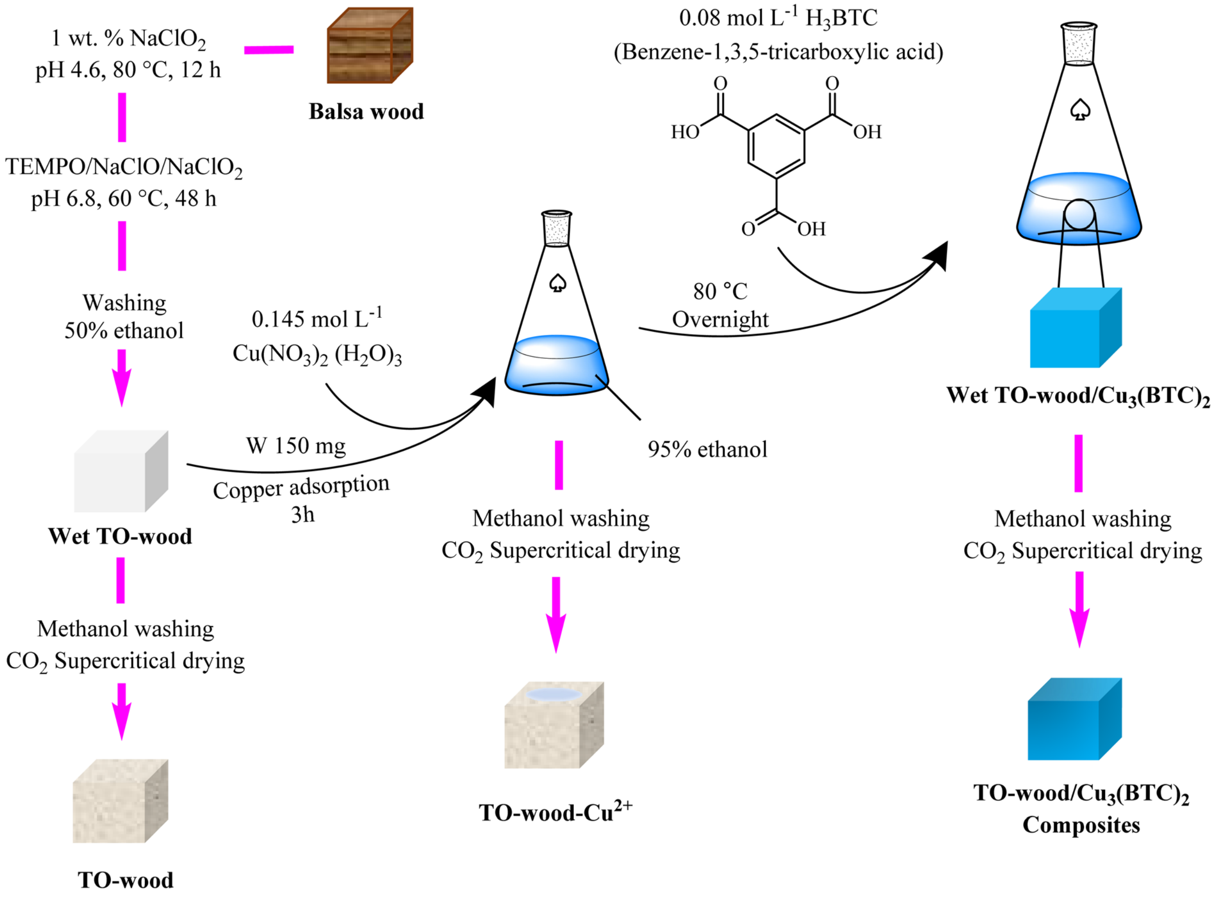

Fig. 14 Synthesis of the TO-wood/MOF composite using $Cu_3(BTC)_2$. Reproduced from ref. 240 with permission from American Chemical Society, copyright 2021.

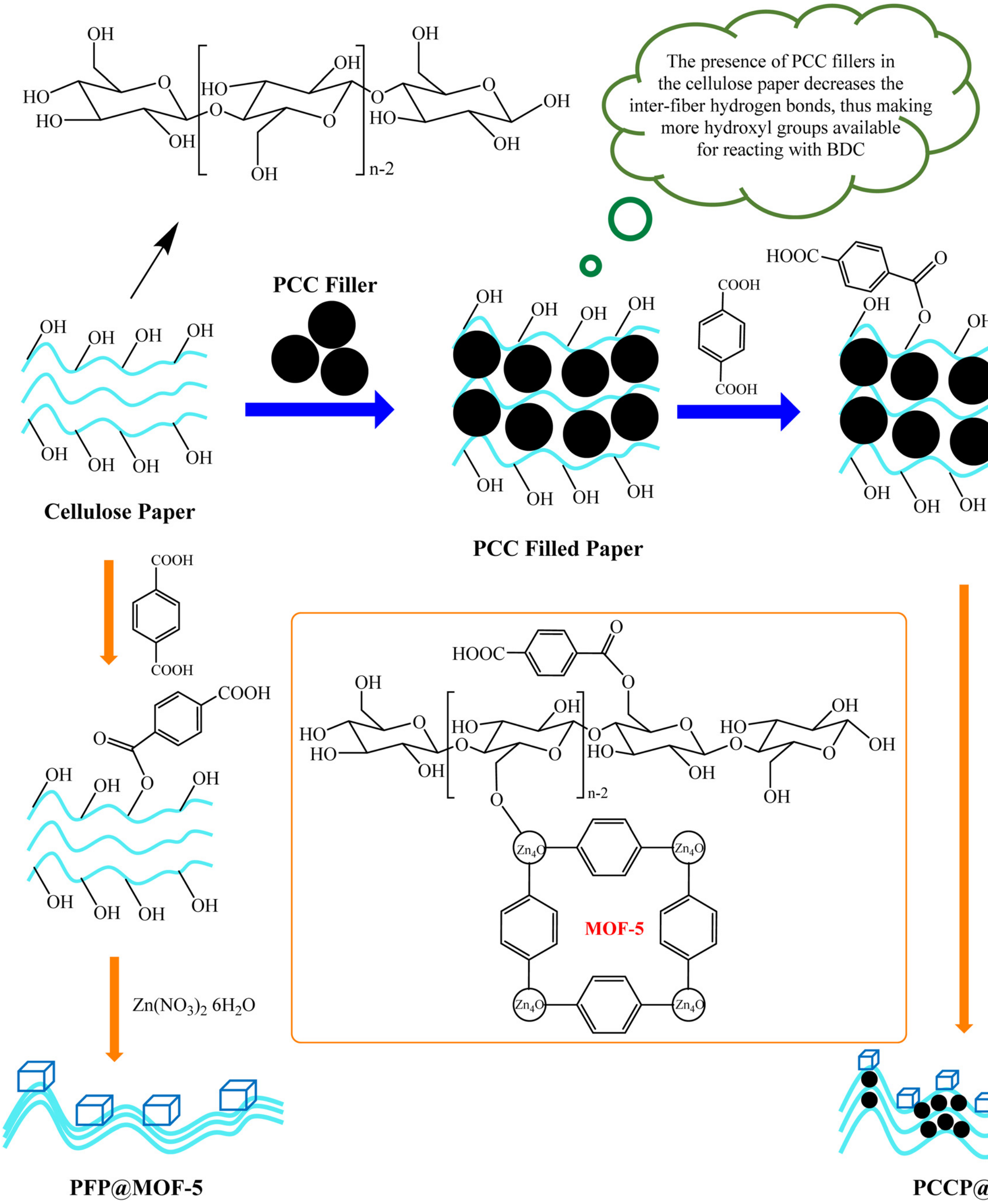

Fig. 15 Preparation of cellulose paper@MOF-5 composite.[242]

Green blend membranes were developed by Akbarzadeh *et al.* using glassy CA combined with *ortho*-linked thiazole-based polyimine (PM-4) and thioether linkage (Fig. 16b).[247] The materials had great resistance to thermal properties. 3.72 mmol g^{-1} of this polymer may absorb a lot of CO$_2$ at 1 bar and 298 K.

For CO$_2$ separations, Raza and colleagues produced novel blended membranes made of CTA and cellulose diacetate (CDA).[248] CTA and CDA blends were selected due to their similar chemical structures, strong separation performance, availability, and environmental friendliness. With a CO$_2$ permeability of 17.32 barrer and a CO$_2$/CH$_4$ selectivity of 18.55, CTA : CDA (80 : 20) has moved higher in Robeson's upper bound curve. In 2020, to separate CO$_2$/CH$_4$ and CO$_2$/N$_2$, Jamil *et al.* prepared MMMs using CA and various bentonite (Bt) clay loadings.[249] At a pressure of 2 bar pressure and 1 wt% Bt loading, the highest value of optimum selectivity for CO$_2$/CH$_4$ was attained, which is 79% greater than that of pure CA membranes. The optimal selectivity for CO$_2$/N$_2$ at a pressure of 4 bar was 123% greater than that of the clean membranes.

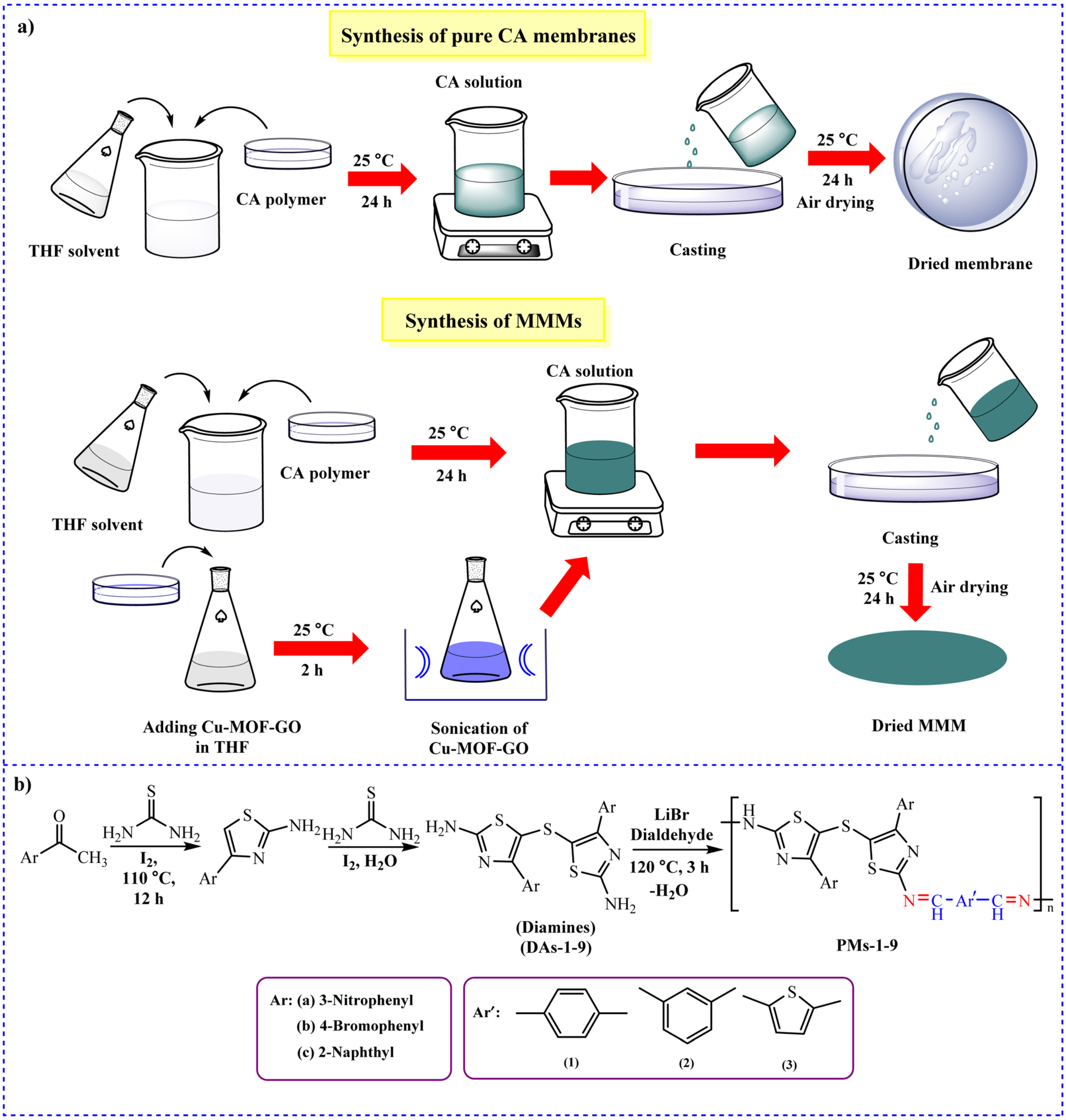

Fig. 16 Synthesis of (a) pristine CA membranes (blank) and MMMs of Cu-MOF-GO loading in CA-matrix[244] and (b) thiazole-based PMs-1-9.[247]

Nanocellulose fibril surfaces may be effectively modified for improved performance in CO_2 separation membranes, as shown by Janakiram and colleagues.[250] Using humid gas permeation experiments, thin composite membranes with the modified nanofibers in water-swelling PVA and a combination of sterically hindered polyallylamine (SHPAA) and PVA were formed and evaluated (Fig. 17). Compared to pure PVA membranes, the addition of nanocellulose showed improved CO_2 permeance and CO_2/N_2 selectivity. Using a combination of SHPAA and PVA, CO_2 permeance up to 652 GPU and a CO_2/N_2 selectivity of 41.3 was achieved.

In 2015, pure CA and CA-TiO_2 composite membranes were produced by Hafeez and co-workers to study the CO_2 adsorption behavior.[251] The high CO_2 adsorption capacity may improve CO_2 solubility and diffusion in the CA-TiO_2 composite membrane, improving CO_2 separation. Nevertheless, compared to pure CA membrane, CO_2 adsorption is higher in the CA-TiO_2 mixed membranes from 2.5 bars.

4.1.6.4 Cellulose-based aerogel materials. In 2023, Chen *et al.* developed an epoxy-functionalized PEI-modified epichlorohydrin-cross-linked cellulose aerogel as an adsorbent for CO_2 collection during the freezing-thawing processes

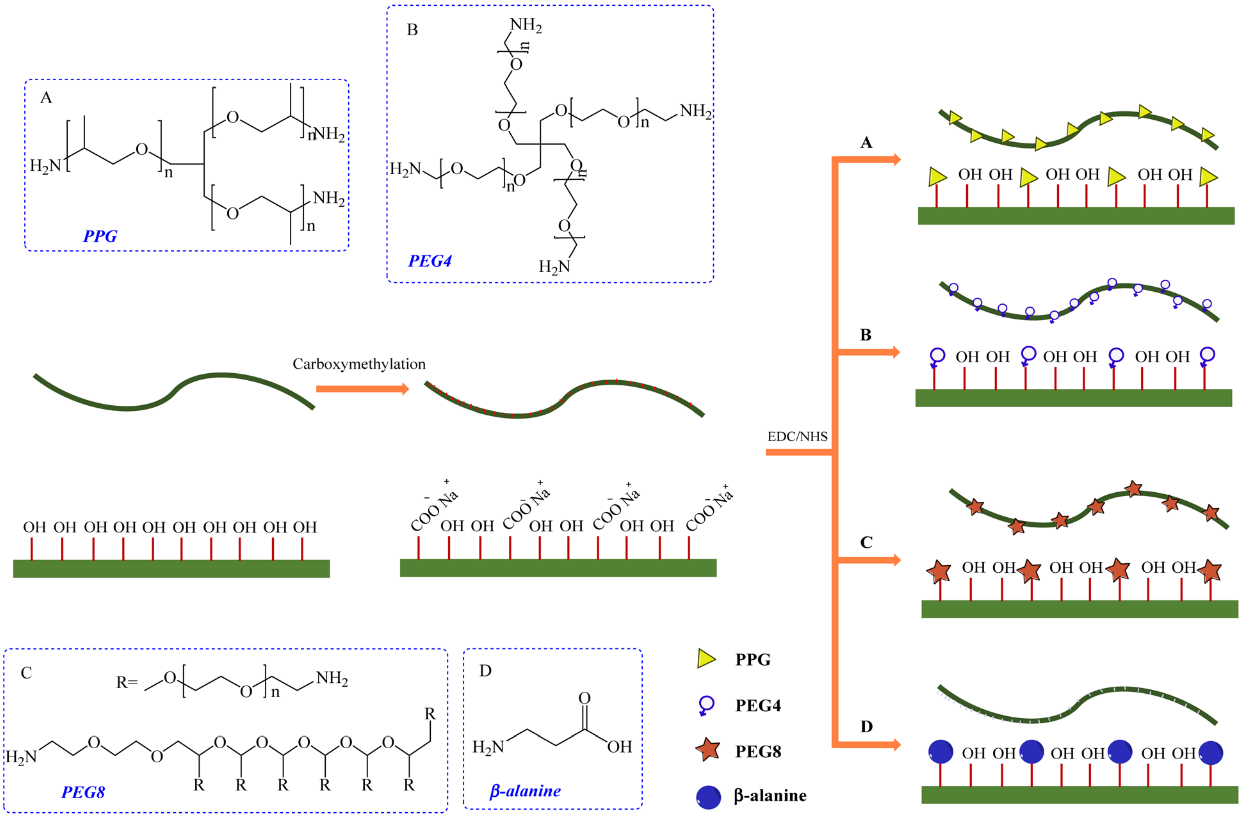

Fig. 17 Surface modification of nanocellulose fibrils.[250]

(Fig. 18).[252] By a maximum adsorption capacity of 6.45 mmol g^{-1} and freeze-drying, the sample displayed good adsorption performance.

Cheng *et al.* synthesized 3D network-shaped biomass-derived cellulose carbon aerogels from Typha Orientalis (TO).[253] The results showed that the material possessed 0.6 wt% hydrogen storage capacity at ambient temperature and adsorption capacities of 16 mmol g^{-1}, 123.31 and 124.57 mg g^{-1} for o-xylene and o-dichlorobenzene, respectively.

In 2022, by *tert*-butanol substitution, gradual heating, high-temperature activation, and freeze-drying, Zhang *et al.* fabricated a cellulose nanofiber (CNF)/PVA/GO aerogel.[254] The amount of GO in the material improved its HSSA (392.41 m^2 g^{-1}) and CO_2 adsorption capacity (432.76 cm^3 g^{-1} at 273 K). In fact, the novelty of this work is the presence of GO, which improves SSA.

Sun and colleagues used a simple vacuum impregnation approach along with a directional freeze-drying procedure to form a novel composite aerogel made of konjac glucomannan (KGM)/TEMPO-oxidized cellulose nanofibers (TOCNF) @HKUST-1 (KTA@HKUST-1) utilizing KGM and TOCNF as starting materials.[255] The CO_2 adsorption capacity of KTA@HKUST-1-10 (KTA@H10) may be as high as 3.50 mmol g^{-1} at 1 bar and 298 K and the adsorption capacity retention rate can be as high as 91.43% after 7 cycles, according to the experimental findings.

By employing BC as a template, Gong *et al.* developed a hydrothermal synthesis method to quickly construct hierarchical pompon-like SAPO-34. To prepare SAPO-34, SiO_2-loaded BC aerogel was synthesized and employed as a silicon source.[256] Furthermore, the CO_2 adsorption capacity of the hierarchical pompon-like SAPO-34 crystals was 2.26 mmol g^{-1} at 100 kPa and 298 K, and the corresponding CO_2/CH_4 ideal separation factor was 5.7, which was greater than that of trigonal SAPO-34 crystals. In a study by Othaman *et al.*, they prepared nanocrystalline cellulose (NCC) from oil palm empty fruit bunch fiber (OPEFB) and grafted it with three different aminosilanes; namely, 3-(aminopropyl) trimethoxysilane (APTMS), 3-(2-aminoethylamino) propyl-dimethoxymethylsilane (AEAPDMS), and *N*-(3-trimethoxysilylpropyl)diethylenetriamine (DET3)).[257] According to these findings, APTMS-NCC aerogel has a greater CO_2 adsorption (0.20 mmol g^{-1}) than NCC aerogel, which has not been changed (0.010 mmol g^{-1}).

Jiang and colleagues used a phase inversion-induced sol–gel method with supercritical drying to synthesize a cellulose aerogel. 3-Aminopropyltriethoxysilane (APTES) was grafted onto the cellulose gel structure to produce an amine-grafted cellulose aerogel (AGCA).[258] AGCA demonstrated remarkable stability within 20 adsorption–desorption cycles, reaching a CO_2 adsorption capacity of 1.20 mmol g^{-1} with dry 1% CO_2. In another study, Zhou *et al.* produced cellulose whiskers/silica by a sol–gel technique. Tetraethyl orthosilicate (TEOs) and an

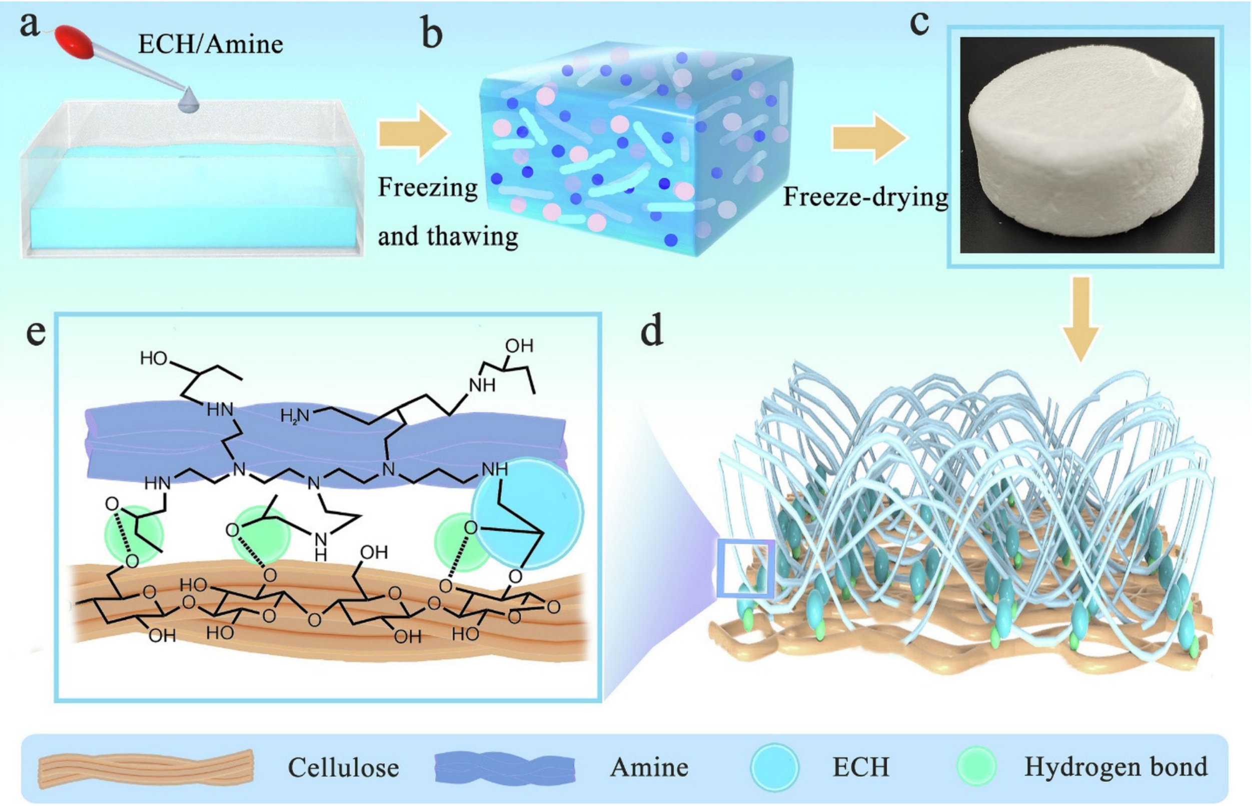

Fig. 18 Synthesis of epoxy-functionalized PEI-modified epichlorohydrin-cross-linked cellulose aerogel. Reproduced from ref. 252 with permission from Elsevier, copyright 2023.

alkaline silica solution were used to form solid aerogels from skim cotton (Fig. 19).[259] Achieving a maximum adsorption capacity of 2.25 mmol g^{-1}, the sample CSA-TEPA-70% showed good adsorption capacity.

Xu and colleagues were able to functionalize CNC aerogel by employing aminosilane in a vapor-phase process.[260] At 25 °C and 101.33 kPa, the adsorption capacity reached 2.57 mmol CO_2 and was completely dominated by chemisorption. The adsorption capacity was reduced only 3–4% after six cycles. In addition, Zhu *et al.* prepared an amino CNC aerogel using 3-(2-aminoethylamino)-propylmethyldimethoxy silane (APS) as the modifier *via* chemical vapor deposition, which maintained the CO_2 adsorption performance while improving the utilization ratio of the modifier.[261] The CNC aerogel grafted with APS showed a CO_2 adsorption capacity of 1.5034 mmol g^{-1} at 25 °C, 1 bar, and a pure dry CO_2 environment. After 10 cycles, the APS-CNC aerogel demonstrated outstanding CO_2 adsorption/desorption recyclability. According to the results obtained in this study, the adsorbent had a high stability up to 10 cycles.

For the *in situ* preparation of a variety of silica/cellulose aerogels in a NaOH/urea solution, Miao *et al.* employed fly ash-based fresh wet silica gel and cellulose derived from old corrugated containers.[262] With a CO_2 adsorption value of 3.68 mmol g^{-1} at 25 °C and 1 atm, the CA-Si-0 (Si-free aerogel) sample showed the highest adsorption.

In 2020, Zhang and colleagues used a facile amine gas phase modification technique to prepare a biomass-based nano cellulose aerogel with excellent CO_2 adsorption capability.[263] The modified nano cellulose aerogel adsorption capacity for CO_2 improved from 0.19 to 1.59 mmol g^{-1}, a factor of 7.4, compared to the unaltered one. Furthermore, Li and co-workers used *N*-(2-aminoethyl)-3-aminopropylmethyldimethoxysilane (APMDS) to add amines to CNFs during the functionalization process.[264] The uptakes of CO_2 by chemical and physical interactions at 15 kPa and 25 °C were 1.01 and 0.35 mmol g^{-1}, respectively. In another study, Tang *et al.* functionalized cellulose with acrylamide in the 1-butyl-3-methylimidazolium chloride (BMIMCl) ionic liquid system by free radical grafting polymerization.[265] At 313.15 K and 190 kPa, aerocellulose had an adsorption capacity of 0.52 mmol g^{-1}. The sorption of AM-*g*-AC (38.59%), which was 2.06 times higher than that of AC, was 1.07 mmol g^{-1} under the same conditions.

Miao and colleagues synthesized a series of aerogels with different cellulose concentrations in NaOH/urea solution using old corrugated containers (OCCs) with small recycling potential as the starting material by freeze-drying method (Scheme 1a).[266] At room temperature and pressure, the aerogels exhibited excellent CO_2 adsorption capacities in the range of 1.96–11.78 mmol g^{-1}.

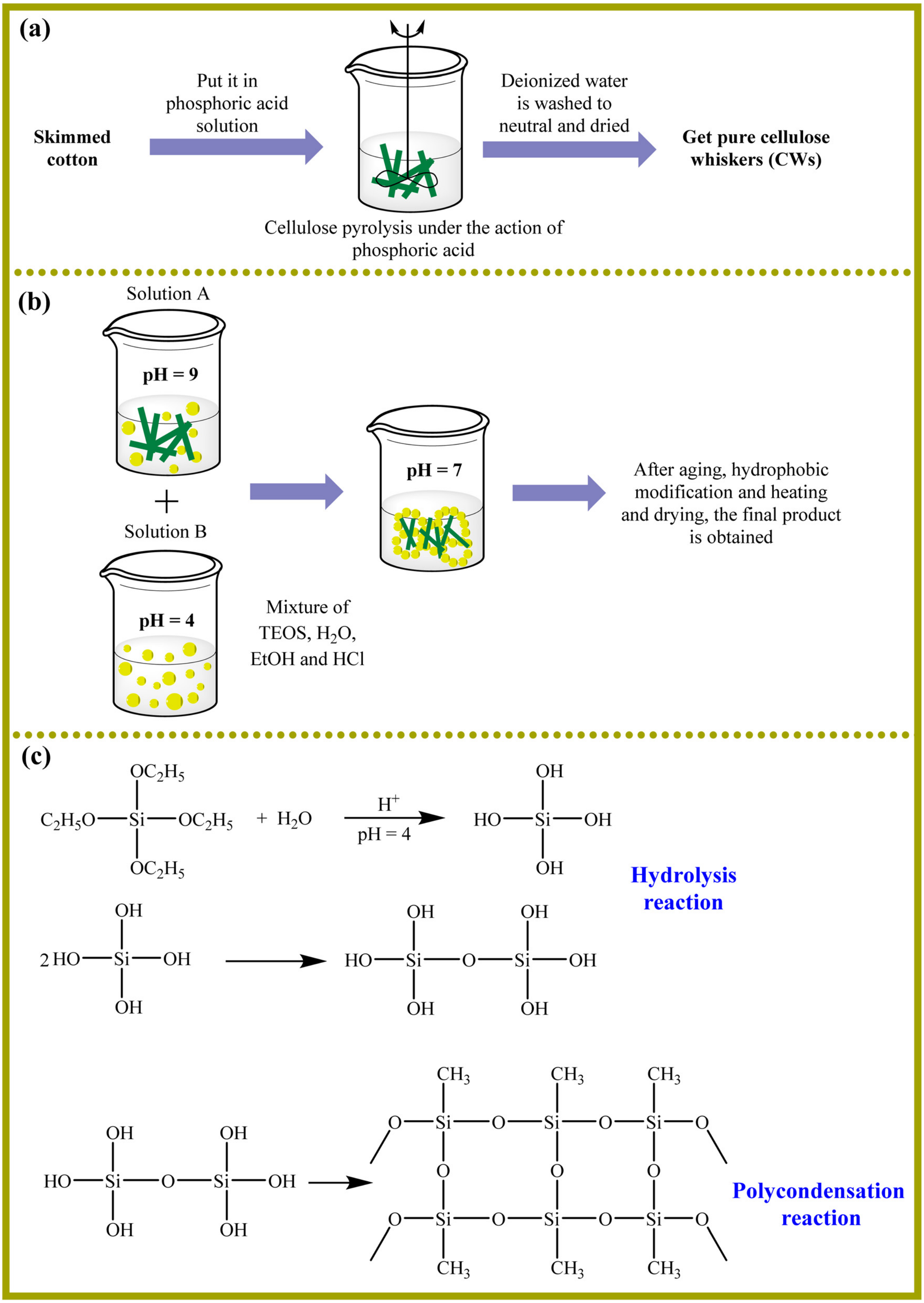

Fig. 19 The preparation of (a) CWs and (b and c) CSA.[259]

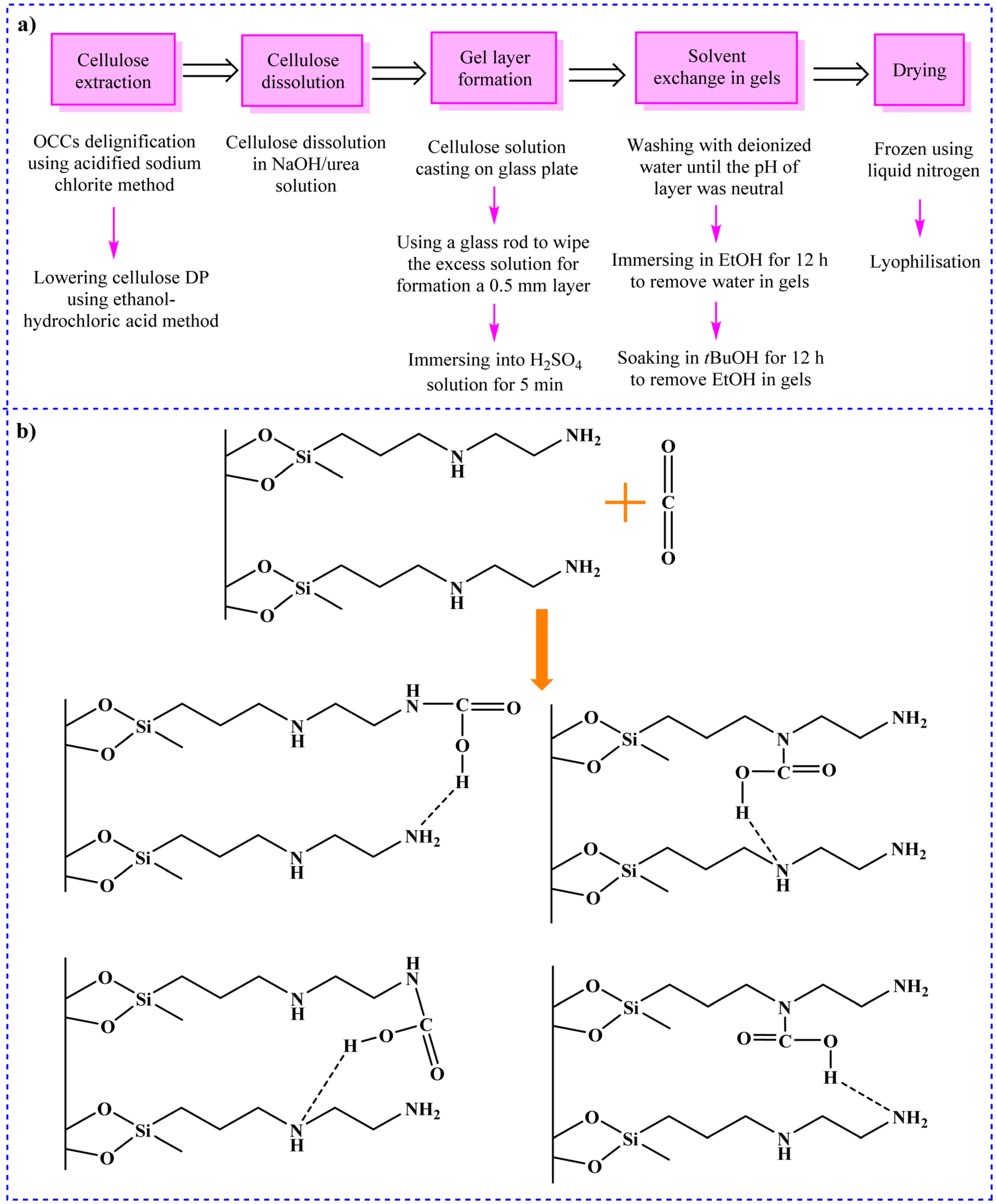

Scheme 1 Synthesis of (a) cellulose aerogel from OCCs[266] and (b) the CO_2 adsorption mechanism of A-CNC-aerogel.[267]

Zhang *et al.* developed a method for the preparation of CNC aerogel spheres modified with *N*-(2-aminoethyl)-3-aminopropylmethyldimethoxysilane (AEAPMDS) using a water phase heat treatment.[267] The amount of CO_2 adsorbed at a pressure of 3 bar by the modified aerogel (2.63 mmol g^{-1}) was significantly higher than that of the unmodified aerogel (0.26 mmol g^{-1}). Scheme 1b displayed the CO_2 adsorption mechanism of A-CNC-aerogel. According to this Scheme, the in anhydrous conditions, the π bond in the chemical structure of CO_2 was broken owing to the attacking of the lone pair electrons of the N in the structure of the A-CNC-aerogel to the C atom on the acid gas CO_2 which led to formation of the carbamate.

Wang and Okubayashi used the sol–gel method, hydrolysis, and cross-linking to develop a novel PEI-cross-linked cellulose (PCC) aerogel sorbent. The CO_2 adsorption capacity of PCC aerogel was 2.31 mmol g^{-1} at 25 °C in an environment with only dry, pure CO_2.[268] After 10 cycles, the PCC aerogel displayed excellent CO_2 adsorption–desorption recyclability.

In 2018, unique amine-based aerogels, which may be employed as CO_2 adsorbents, were synthesized by Wu and colleagues using CNFs (Scheme 2a).[269] A significant CO_2 adsorption capacity of 1.91 mmol g^{-1} at 25 °C and 1 bar was observed in CNF grafted with aminosilane. In addition, heating the aerosol to 80 °C facilitated the regeneration process.

Using eucalyptus pulp as a starting material, Liu *et al.* produced cellulose nanofibres *via* a chemical mechanical process. Subsequently, using the suspension titration approach, the spherical CNFs hydrogel was generated.[270] Amino-modified bio-spherical CNF aerogels were then produced using the freeze-drying technology and the grafting modification process. The aerogels exhibited good regeneration of more than 10 cycles and their highest CO_2 adsorption capacity was 1.78 mmol g^{-1}. Moreover, Jiang *et al.* developed CNF-silica aerogels using a one-step *in situ* aqueous sol–gel method, which involved polymerization as well as aging the silica precursor in the presence of CNFs (Scheme 2b).[271] CNF aerogels showed great flexibility and dry compressive strength and silica aerogels have had high thermal stability. Organosilane functionalization of CNF-silica aerogels resulted in the introduction of primary amine groups with an adsorption capacity of 1.49 mmol g^{-1} for CO_2.

In 2017, Wu and colleagues grafted *N*-(2-aminoethyl)-3-aminopropylmethyldimethoxysilane (AEAPMDS) onto CNC derived from hybrid poplar residue.[272] High CO_2 adsorption capacities of 1.7 and 2.6 mmol g^{-1} were determined at 1 bar at temperatures of 25 and 0 °C, respectively. By carbonizing and activation with CO_2, Dassanayake *et al.* could prepare AC from monoliths of cellulose-based aerogel (aerocellulose) (Fig. 20a).[273] The aerocellulose retained its monolithic structure during the carbonization and activation operations. With CO_2 adsorption capacities of 5.8 and 3.7 mmol g^{-1} at 0 °C, 1 atm and 25 °C, 1.2 atm, respectively, the resultant AC demonstrated outstanding adsorption characteristics toward CO_2.

In 2016, Hu and colleagues developed a quick and convenient method for producing hierarchical porous N-doped carbons from cellulose to prepare high-performance supercapacitor and CO_2 capture applications. According to this procedure, hierarchical porous cellulose aerogels were first synthesized using a dissolving-gelling process, followed by carbonization in an atmosphere of NH_3 to produce hierarchical porous N-doped carbon aerogels with more linked mecropores and micropores (Fig. 20b).[274] The CO_2 adsorption capacity of N-doped carbon aerogels was 4.99 mmol g^{-1}, which is substantially greater than that of other porous carbons. The innovation of this study is that a double compound acting as both a supercapacitor and a CO_2 absorber has been designed.

4.1.6.5 Cellulose-based ZIF materials. A potential method to fabricate hybrid materials, which blend organic and conventional materials, is the crystal development of zeolitic imidazolate frameworks (ZIFs) on cellulose. In 2019, Valencia and Abdelhamid reported the one-pot synthesis of gelatin/nanocellulose leaf-like ZIF-L foams and ZIF-L stands to Zn $(mim)_2(Hmim)_{1/2}(H_2O)_{3/2}$, in which Hmim stands for 2-methylimidazole.[275] As a model for nanocellulose, TOCNF was employed. Using water as the solvent, the *in situ* growth of ZIF-L into TOCNF was accomplished at room temperature.

In 2021, Abdelhamid and Mathew used a derivative of cellulose named TOCNF to modulate the crystal growth of ZIF-8 and ZIF-L, called CelloZIF-8 and CelloZIF-L, respectively.[276] At room temperature, the synthesis process was carried out in the presence or absence of NaOH in water. CO_2, metal ions, and colors were all adsorbed using the resultant CelloZIFs materials.

In the same year, Mubashir *et al.* synthesized CA-based membranes by interfacial engineering and integration of ZIF-62 glass NPs for CO_2 separation.[277] The maximum CO_2 permeability and CO_2/CH_4 ideal selectivity were also provided by this set of membranes at 84.8 Barrer and 35.3, an increase of 436.7 and 189.3%, respectively. In another study, BC, a renewable and biodegradable material, was employed by Ma and co-workers as the substrate for ZIF growth. Using an *in situ* growth technique, amino-functionalized ZIF-8 (ZIF-8-NH_2) was generated inside the BC substrate. The chelating action among zinc metal ions and –OH groups gives the composites great interface affinity and compatibility. Cellulose fibers were evenly covered with ZIF crystals.[278] The final foams, produced at 25 °C and 1 bar, showed a high CO_2 adsorption capacity of 1.63 mmol g^{-1}.

4.1.6.6 Cellulose-based pellet materials. To capture CO_2, Zeng *et al.* prepared graphite-casted K_2CO_3-based adsorbent pellets with SiO_2, ZrO_2 and TiO_2 as porous supports.[279] The ZrO_2-supported, 30 wt% K_2CO_3-loaded pellets showed the greatest CO_2 adsorption capacity, around 0.93 mmol g^{-1}, in contrast to the K_2CO_3 pellets supported by TiO_2 or SiO_2. The SiO_2-supported K_2CO_3 adsorbent pellets with a 30 wt% K_2CO_3 loading and 500 °C calcination showed an adsorption capability of 0.38 mmol g^{-1}. Furthermore, in 2022, Zheng *et al.* synthesized composite adsorbent pellets containing alkali metal salts (AMS) and MgO using the extrusion-spheronization technique.[280] To enhance the porosity, morphologies, and CO_2 uptakes of the AMS-MgO pellets, pore-forming templates composed of MCC, urea (UA), ammonium bicarbonate (AB), and citric acid (CA) were used. A fixed-bed reactor was used to study the CO_2 uptakes and adsorption kinetics of the adsorbent pellets. At 340 °C and 50% CO_2, the ideal AMS-MgO-MC pellets modified with an MC template had a significant CO_2 absorption of 7.54 mmol g^{-1}, CO_2 absorption being maintained at 5 mmol g^{-1} throughout the course of 20 cycles. In addition, Sun *et al.* produced CaO-based pellets using an extrusion–spheronization technique. Although the addition of a cellulose template helped increase the CO_2 absorption of CaO-based sorbent pellets above 0.32 g CO_2 per g sorbent after 25 cycles, the impact of the cellulose particle size in improving CO_2 capture performance was limited.[281]

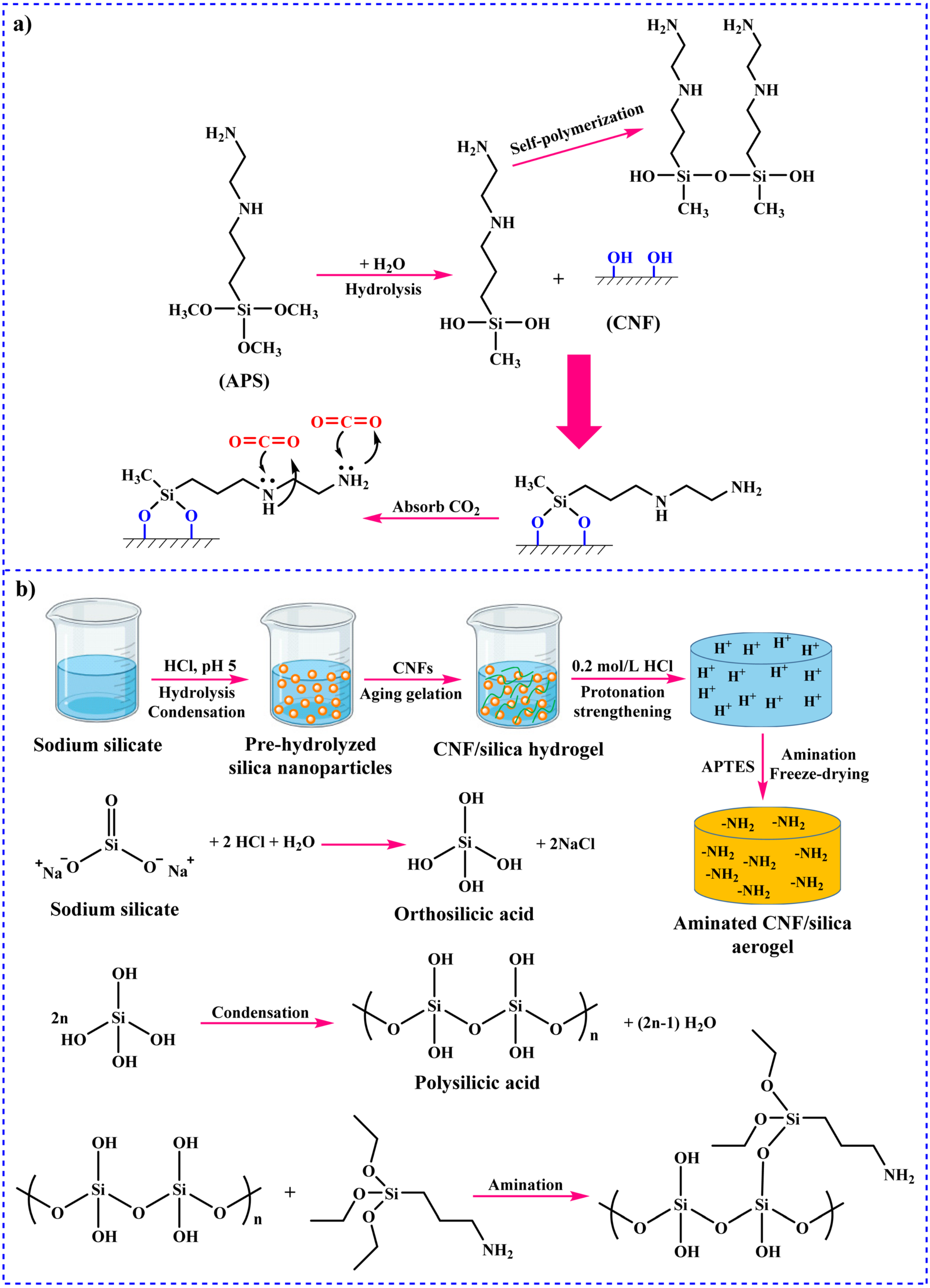

Scheme 2 Synthesis of (a) polymer aerogel[269] and (b) aminated CNF/silica aerogel.[271]

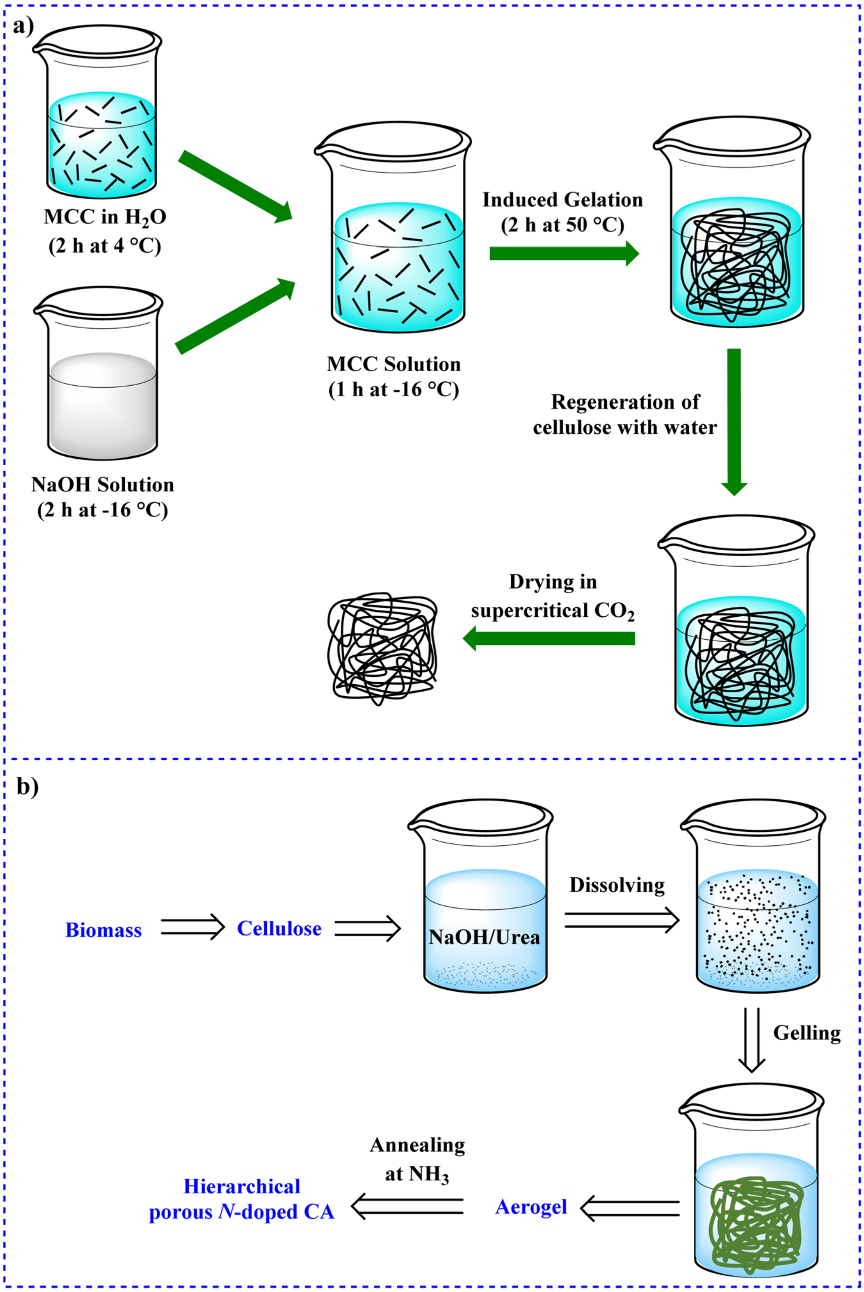

Fig. 20 Synthesis of (a) aerocellulose monoliths[273] and (b) hierarchical porous N-doped carbon aerogels.[274]

In 2018, by using a surfactant-assisted steam explosion technique, Helmlinger *et al.* developed a unique method for the rapid and economical preparation of amine-functionalized cellulose pellets.[282] A new laboratory reactor was used for capacity testing, and the results showed that the CO_2 capacity was 1 mmol g^{-1}, which is equivalent to those of other cellulose-based adsorbents reported in the literature. In another study, Hu and colleagues developed a facile gel-casting method to produce highly effective CaO-based sorbent pellets in a single step.[283] In comparison to the unmodified pellets, the pellets modified with microcrystalline cellulose (CaOMC) achieved a significant CO_2 capture capacity of 0.48 g/g at the 25th cycle under mild calcination conditions and maintained a reasonably exceptional efficiency of 0.41 g/g through 25 medium-cycle tests (CaO-pellets).

Sun *et al.* synthesized CaO-based pellets from residual carbide slag using a model extrusion-spheronization technique.[284] For the first time, the pore architectures of the pellets were altered to improve their CO_2 adsorption capacity. These modifications involved the use of two different types of biomass-based pore-forming materials (MCC and rice husk).

Other examples of CO_2 collection using cellulose-based materials are shown in Table 2.

4.1.6.7 Summary of this section. Various types of cellulose such as carboxymethylcellulose and microcrystalline cellulose

Table 2 Cellulose-based materials for CO_2 capture

Entry	Cellulose-based sorbent	Operating conditions (temperature and pressure (bar))	Capacity (mmol g^{-1})	Ref.
1	Cellulose@$CaCO_3$ composite	—	7.3	285
2	Cellulose gelation in NaOH (aq)	—	—	286
3	PEI-functionalized cellulose materials[a]	80 °C	$0.026\ mg_{CO2}\ mg_{adsorbent}^{-1}$	287
4	CNF-TBFA[b]	—	6.52	288
5	TRCNF/PEIA[c]	60 °C	6.74	289
6	Biochar derived cellulose	25 °C and 760 mm Hg	3.6	290
7	CNC	25–45 °C	1.81	291
8	CNC-COOH	25–45 °C	3.19	291
9	CNC-NH_2	25–45 °C	3.46	291
10	PAMAM functionalized CNC	25–45 °C	3.54	291
11	Cell-UK[d]	273 K and 1	297.1 mg g^{-1}	292
12	CP-AC[e]	25 °C and 35	14.3	293
13	J-AC[f]	25 °C and 35	18.4	293
14	K-AC[g]	25 °C and 35	17.8	293
15	Cellulose fibers/IL/TEA or MEA[h]	25 °C and 25	141 mg of CO_2 per g of fiber	294
16	Phthalimide-modified CNF	—	—	295
17	Quaternized bamboo cellulose	—	—	296
18	Cellulose-TiO_2	298.15 K and 30	184.1 mg g^{-1}	297
19	Cellulose-Fe_3O_4	298.15 K and 30	130.6 mg g^{-1}	297
20	Formaldehyde-free decorative paper coated with AEAPMDS-CNCs[i]	25 °C and 1	1.806	298
21	75 wt% cellulose-supported $[N_{1888}][Ac]$	298 K and 30	30 g kg^{-1}	299
22	75 wt% cellulose-supported $[N_{4444}][Ac]$	298 K and 30	31.6 g kg^{-1}	299
23	70 wt% cellulose-supported $[N_{8888}]Br$	298 K and 30	19.8 g kg^{-1}	299
24	75 wt% cellulose-supported [Bmim]Br	298 K and 30	28.8 g kg^{-1}	299
25	CH-CNF-DAMO[j]	—	0.89	300
26	OH-CNF-DAMO[k]	—	1.27	300
27	KP-CNF-DAMO[l]	—	2.11	300
28	CaO-based sorbent pellets	—	0.1 g CO_2 per g of sorbent	301
29	Cellulose dissolved in NaOH (aq)	—	—	302
30	AC-derived *Cladophora* cellulose	273 K and 1	5.52	303
31	NCC-AO composite	120 °C and 1 atm	5.54	304
32	Cross-linked-TBA	25 °C and 3 MPa	71 mg g^{-1}	305
33	Organoclay-TOCNF	—	—	306
34	NCC-AEAPDMS[m]	—	—	307
35	Ammonia activation of carbonized cellulose	—	2.44	308
36	Cellulose fiber-based porous carbon	298 K and 1	3.776	309
37	Nanofibrillated cellulose-polyethylenimine foams	—	2.22	310
38	Amine-functionalized nanofibrillated cellulose	—	—	311
39	Amine-functionalized nanofibrillated cellulose	90 °C and 30 mbar	0.90	312
40	Hollow fibres of deacetylated CA	—	—	313
41	Microfibrillated cellulose/Lupamin	—	—	314

[a] Poly(ethyleneimine) (PEI) immobilized on cellulose, cellulose tosylate (CT), and cellulose carbamate (CC). [b] CNF-based thermoresponsive bionic fiber. [c] Thermoresponsive cellulose nanofiber (TRCNF)-based PEI. [d] Cellulose impregnated with urea and KOH. [e] Cotton pulp as carbon fibers activated with KOH/C. [f] Jute as carbon fibers activated with KOH/C. [g] Kenaf as carbon fibers activated with KOH/C. [h] Ionic liquid 1-butyl-3-methylimidazolium tetrafluoroborate $[BMIM][BF_4]$ and monoethanolamine or triethanolamine dropped cellulose fibers. [i] *N*-(2-Aminoethyl) (3-aminopropyl) methyldimethoxysilane (AEAPMDS) grafted onto the CNCs. [j] CNF films modified with diaminosilane *N*-[3-(trimethoxysilyl)propyl]ethylenediamine (DAMO) from corn husks (CH). [k] CNF films modified with DAMO from oat hulls (OH). [l] CNF films modified with DAMO from Kraft pulp (KP). [m] Nanocrystalline cellulose (NCC) modified with aminosilane, 3-(2-aminoethylamino)propyl-dimethoxymethylsilane (AEAPDMS).

have been used to prepare sorbent materials for CO_2 capture. The use of cellulose as an edifice material offers new opportunities expanding the prospects of cellulose for CO_2 capture. However, in future studies, new composites based on cellulose can be prepared and their efficiency of CO_2 absorption can be improved to a great extent. The combination of cellulose and MOF has performed relatively well for carbon dioxide absorption. Cellulose-based membranes used for gas separation have shown good selectivity and CO_2 capture efficiency. Studies conducted in the field of making cellulose-based aerogels show that cellulose is a suitable material for making aerogels in addition to possessing a high efficiency in absorbing and CO_2 trapping. Studies have also been performed on cellulose-based pellets, but much work remains to be done. In general, cellulose and cellulosic sources are the appropriate and predominant biopolymers for making materials for carbon capture.

4.2 Lignin-based materials for CO_2 capture

Lignin is a complex lignocellulosic biomass. After cellulose, lignin is the most abundant aromatic natural polymer. The sources of lignin are plant cell walls as well as a by-product of biorefineries and pulp manufacturing. In the structure of lignin, there are some functional groups such as carboxyl, hydroxyl, aldehyde, phenolic, and methoxy groups, which make this natural polymer very useful. Lignin has various properties such as biodegradability, low price, accessibility, HSSA, and stability, making it an attractive material applied in different industries including food packaging, medicine, catalysis, adsorption, *etc*. About 85% of the world's annual production of lignin is Kraft lignin although lignosulfonates are the prominent commercially available lignin source with a crop of about ~1 million tons.[315–319] In this section, we review recent studies regarding lignin-based materials for CO_2 capture applications.

4.2.1 Lignin-based composite materials. HKUST-1 is a type of MOF. In 2022, López-Monreal and Loera-Serna investigated the synthesis of a bio-nanocomposite using HKUST-1 and lignin.[320] They synthesized HKUST-1-supported lignin (HKUST-1@lignin) for CO_2 capture. Since HKUST-1 does not have a HSSA to act as an adsorbent, HKUST-1 was coated on the lignin surface to improve this property.

4.2.2 Lignin-based doped materials. The preparation of sulfur-doped (S-D) nano porous carbons through one-step synthesis (Fig. 21) was performed by Saha and colleagues.[321] For this aim, they used lignin as the precursor for the synthesis of nano porous carbons. Sodium thiosulfate and KOH were applied as sulfurizing and activating agents, respectively. The prepared S-D materials were applied for the CO_2 adsorption, N_2, and CH_4. At 298 K and 760 torr, the experimental results indicated that the equilibrium capture capacity of CO_2 was ~11 mmol g^{-1}.

In 2023, Gong and Bao reported the synthesis of the N,O-codoped porous carbon from lignin for CO_2 capture application.[322] For this work, they used precarbonization, pyrolysis, and chemical activation with KOH. Their results displayed that the CO_2 adsorption activity of the materials was considerably improved by the precarbonization of lignin. The adsorption capacity of the materials was 5.82 (at 273 K) and 3.98 mmol g^{-1} (at 298 K) at 1 bar.

In another study, Demir and co-workers fabricated heteroatom-doped porous carbons (LHPCs) by hydrothermal carbonization following chemical activation.[323] The prepared carbons have 2.5–5.6 and 54 wt% nitrogen and oxygen, respectively. The prepared materials possessed micro– and mesoporous structures. LHPCs were applied as CO_2 adsorbents and electrodes for supercapacitors. The adsorption capacity of the materials was 4.8 mmol g^{-1} at 1 bar and 298 K. The innovation of this study is that a double compound functioning as both a capacitor and a CO_2 absorber has been designed.

Park *et al.* reported the synthesis of the N-doped ultraporous carbon derived from lignin by hydrothermal carbonization and activation using KOH.[324] The fabricated materials were applied for CO_2 adsorption. The adsorption capacity of the materials was 13.6 mmol g^{-1} at 25 °C up to 10 atm and they showed high stability through 10 adsorption/desorption cycles. The results displayed that N-doped porous carbon had a high performance compared with non-doped porous carbon, indicating the enhancement of CO_2 adsorption by functionalization with N.

In 2017, Saha and colleagues prepared N-doped and hierarchical porous carbons using lignin as the precursor and KOH and NH_3 as activation agents.[325] They used pyridinic, amino, and pyrrolic/pyridone materials for the functionalization of porous carbon. The materials prepared were applied for CO_2 adsorption. The adsorption capacities were 5.48 and 8.6 mmol g^{-1} at 298 and 273 K and 1 bar, respectively.

4.2.3 Lignin-based aerogel materials. Geng and colleagues investigated the synthesis of high-performance multifunctional carbon aerogels using Kraft lignin and cellulose nanofibers through ice-templating and carbonization

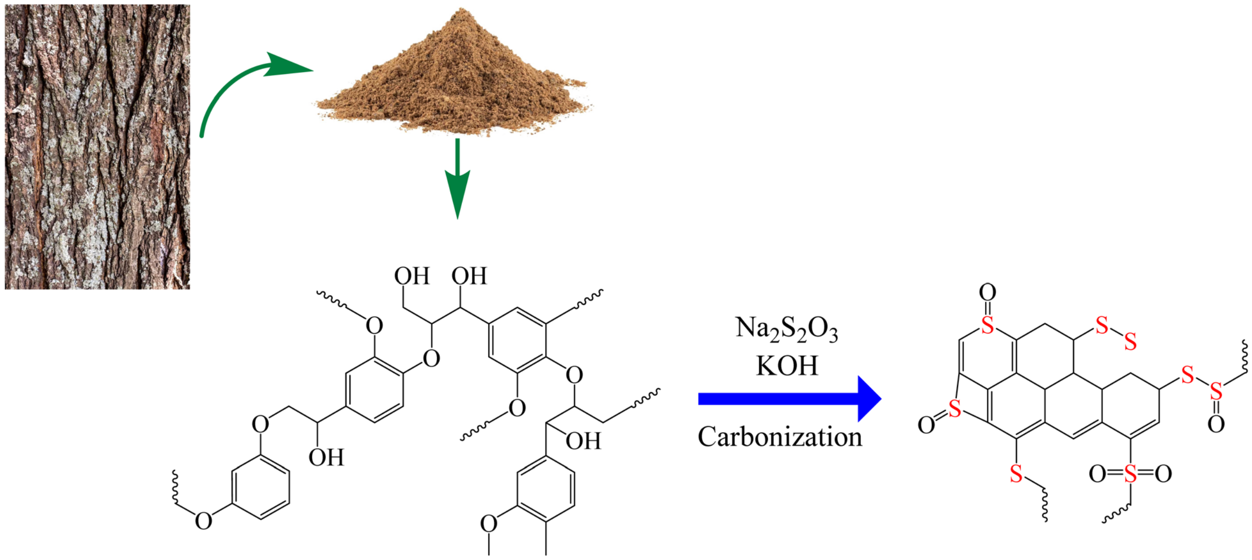

Fig. 21 Schematic of one-step preparation of S-D nano porous carbon from lignin.[321]

approaches.[326] Cellulose and lignin were extracted from renewable resources. The prepared carbon aerogels were used for CO_2 capture as well as capacitive energy storage. At 273 K and 100 kPa, the results displayed excellent performance with adsorption capacity of 5.23 mmol g^{-1}.

4.2.4 Lignin-based other materials. Preparation of several types of porous carbon materials using black liquor lignin by chemical activation following the template technique was performed by Wang and co-workers.[327] They used KOH as an activator for the synthesis of porous carbon (C-BLL-KOH), which has a HSSA (1336.5 m^2 g^{-1}) as well as high microporosity. These properties make the prepared materials very suitable for CO_2 adsorption applications. According to the results, C-BLL-KOH showed high performance in CO_2 capture and the maximum adsorption capacities were 5.20, 3.60, and 2.23 mmol g^{-1} at 0, 25, and 50 °C at 100 kPa pressure, respectively.

Sun *et al.* studied the synthesis of ordered mesoporous carbons using lignin and siliceous mesostructured cellular foam as precursor and template, respectively, through a solvothermal procedure.[328] The synthesized lignin carbon materials showed a 3D large mesopore system as well as thin pore size distribution center. The fabricated mesoporous lignin carbon can be used as a support for CO_2 adsorption. The results indicated that 60 wt% polyamines (polyethyleneimine (PEI)) could be loaded on the support and applied for CO_2 adsorption. The adsorption capacity was 129.9 mg or 2.95 mmol CO_2 per g-adsorbent at 75 °C. The meso porous carbon functionalized with PEI was highly stable and only 6% of the performance decreased after 50 runs.

In 2023, Liu and colleagues reported the preparation of lignin-based absorbents using grafted active amine group on a lignin-derived compound (vanillin and alkali lignin) and applied it for CO_2 absorption (Fig. 22a).[329] The results displayed that the vanillin-functionalized acrylamide had high adsorption capacity of CO_2 (0.114 g CO_2 per g of absorbent at 25 °C and 100 kPa). The synthesized absorbent was highly stable even after 6 cycles.

In 2022, Sun and co-workers carried out the synthesis of several types of bio-carbon materials using Kraft lignin precursor through a chemical activation procedure.[330] The Kraft lignin-derived carbons were applied for CO_2 adsorption. The adsorption capacities of the carbon synthesized at 600 °C were 3.29 and 2.01 mmol g^{-1} at 0 and 25 °C at 15 kPa, respectively.

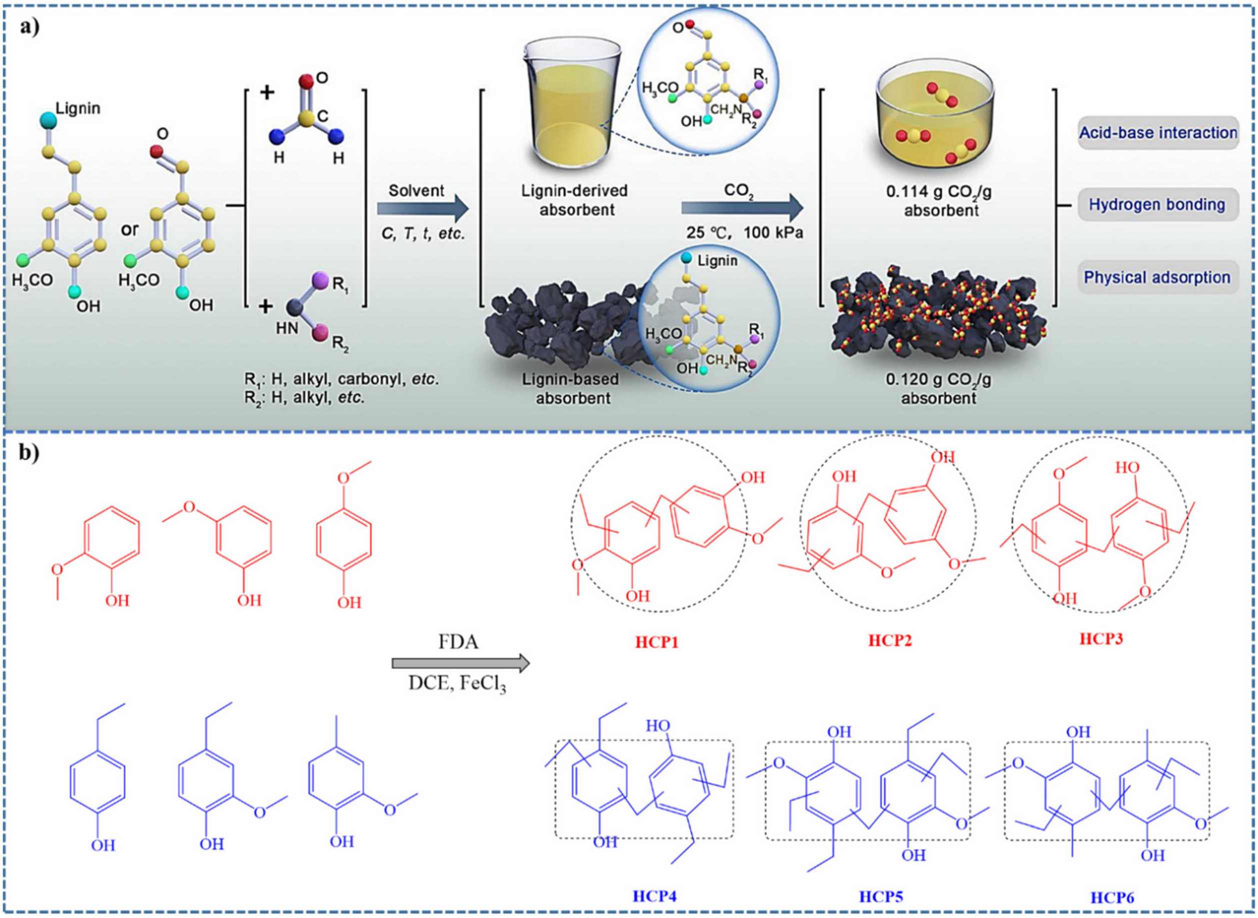

Fig. 22 (a) The schematic representation of the synthesis of absorbent and CO_2 absorption process. Reproduced from ref. 329 with permission from Elsevier, copyright 2023 and (b) representation demonstration for the preparation process of HCP1~HCP6 over Friedel–Crafts reaction.[331]

Table 3 Non-polysaccharide and lignin-based materials for CO_2 capture

Entry	Non-polysaccharide and lignin-based sorbent	Operating conditions (temperature and pressure (bar))	Capacity (mmol g^{-1})	Ref.
1	N-doped graphene composite	298 K and 1	2.7	334
2	Borane-modified graphene-based materials	1	1.82	335
3	Zeolite 13X (13X-C)	25 °C and 1	6.2	336
4	Zeolite 13X (13X-B)	25 °C and 1	4.8	336
5	Dispersing CaO on γ-Al_2O_3 support	650 °C	6.4	337
6	Polyethyleneimine-graphene-silica	75 °C and 7.5 bar	4.3	338
7	Polyethyleneimine-F-Ce-2.5 nanosheets	35 °C and 2 bar	1.32	339
8	MCF@G-PEI[a]	50 °C	2.78	340
9	SSMMP[b]-Ni 50%-ammonium Br	25 °C and 1	1.91	341
10	SSMMP-Ni 50%-imidazolium Br	25 °C and 1	1.64	341

[a] Co-grafting of polyethyleneimine (PEI) on mesocellular silica foam (MCF), and (3-glycidyloxypropyl)triethoxysilane (GPTES). [b] Synthetic silico-metallic mineral particles.

In the same year, the synthesis of the 6 aromatic units prepared from the depolymerization of the liquid products of lignin was performed by Chen and co-workers.[331] They synthesized O-rich hyper-cross-linked polymers (HCPs) through a one-pot Friedel–Crafts reaction using formaldehyde dimethyl acetal (FDA) as a crosslinker (Fig. 22b). The prepared HCPs exhibited high CO_2 uptake and selectivity of 64.1 mg g^{-1} and 35.2 at 273 K, respectively.

Atta-Obeng and colleagues developed an efficient process for the synthesis of amine-functionalized carbons derived from technical lignin.[332] For this purpose, they first synthesized carbonaceous materials (CMs) from lignin using hydrothermal treatment, following activation by KOH. Afterward, they functionalized CMs using PEI, which is appropriate for CO_2 capture applications. The optimum amount of PEI for loading was 5% and a further increase in the amount of PEI decreased CO_2 absorption.

4.2.5 Summary of this section. Lignin is a natural polymer possessing many functional groups in its structure, which can be functionalized with various materials. However, there are relatively few studies in the field of making lignin composites for carbon capture. Given the unique capacities and characteristics of lignin, future studies in the field of preparing lignin-based composites are necessary. For example, lignin can be easily aminated through the Mannich reaction and these structures can be very beneficial for CO_2 capture. Moreover, in other studies, lignin has been used as a source of carbon and various atoms have been doped on it, yielding relatively effective materials. In general, considering the high potential of lignin as well as its many properties, there is a lot of work to be done in the future.

5. Summary and discussion

Since CO_2 is a toxic and dangerous gas for the environment and humans, it is necessary to identify routes to capture or convert it into useful materials.[333] The materials used for CO_2 capture have been summarized in this review. In other words, in this review, the applications of polysaccharides and lignin-based materials, which are environmentally friendly and biodegradable, for capturing CO_2 have been reviewed. Different structures based on polysaccharides and lignin have been prepared and used for this purpose. The results have shown that the more nitrogen groups there are in the structure, the higher the ability to capture CO_2. On the other hand, the more porous the structure, the greater the ability to capture it. Polysaccharides and lignin are important for CO_2 removal because they are natural materials and do not harm the environment. The results also showed that they have a high absorption capacity and are thus suitable for CO_2 capture. There are other materials, which can capture CO_2. These materials are not made of natural materials, and in some cases, they may have relatively good absorbency. However, toxic, non-environmentally friendly materials may have been used in the process of making them, making them undesirable materials. In addition, other materials are not cost-effective. Other materials may have complex and expensive methods of preparation and purification, but polysaccharides and lignin are readily available because they are natural, affordable, and economical. A number of different materials, which do not have polysaccharides and lignin-based materials used for CO_2 capture, are reported in Table 3. Generally, these materials including graphene, MOF, zeolite, *etc.*, are porous. The absorbability of these materials is not very high compared to polysaccharides and lignin-based materials, and are not very suitable because most of them do not have a natural source.

6. Conclusion and future prospects

Climate change, largely linked to the emission of greenhouse gases, including CO_2, is disrupting our planet, threatening the lives of humans and other living beings. This review highlights interesting points to explore further and gaps to fill. As pointed out, many workers are interested in the separation of CO_2 *via* post-combustion processes for CO_2 capture. Various classes of materials, which could be used for the capture and removal of CO_2 by adsorption (or absorption) have received a great deal of attention in recent years. These materials can be in different forms including composites, aerogels, hydrogels, pellets, heteroatom-doped materials, membranes, MOFs, porous carbons, *etc*. Among the materials already used or under examination, polysaccharides and lignin, which are classified as biopolymers, are of great interest to researchers because they have many advantages such as biodegradability, environmental friendliness, availability, low cost, and non-toxicity. As a result, making compounds using polysaccharides and lignin to capture CO_2 is a very effective method. In this review, recent publications regarding the application of polysaccharide and lignin-based materials for CO_2 capture have been reviewed. In other words, in these studies, researchers have used environmentally friendly materials to protect the environment by capturing CO_2.

Various polysaccharides such as alginate, starch, pectin, gum, chitosan, and cellulose have been used for CO_2 capture. According to the existing studies, starch, pectin and gum have rarely been used for this purpose. However, chitosan and cellulose were more frequently used; especially in the form of aerogel. This highlights the suitability, appropriability, and efficiency of chitosan and cellulose, as well as their aerogels, compared to other polysaccharides for CO_2 capture.

Undoubtedly, in gas separation applications, membranes offer the greatest potential. The studies conducted reveal that cellulose-based materials have been among the most studied in this field, and that the newly developed cellulose-based membrane materials have superior performance to most conventional commercial membranes. Studies on lignin have been less numerous and used lignin as a source for porous carbon supra-particle production. Nonetheless, lignin-based CO_2 sorbents have been synthesized by functionalization of the functional groups in the structure of lignin (such as hydroxyl, carbonyl, sulfur, aldehyde, *etc.*). It should be noted that there is still much work to be done in this field.

Although relatively many studies have been conducted in the field of the application of polysaccharides (especially cellulose and chitosan) and lignin to capture CO_2, there is still much work to be done in this field, which include:

- The combination of polysaccharides and lignin to increase the surface as well as mechanical and chemical properties.
- More use of pectin polysaccharides and gums for CO_2 capture.
- Using polysaccharides and lignin on an industrial scale for CO_2 capture
- These materials have been used as absorbents for CO_2 capture, but CO_2 can be converted into valuable compounds. Thus, these compounds can be made in such a way that after adsorbing (or absorbing) CO_2, they can convert it into valuable compounds.
- Using other biopolymers for CO_2 capture, such as collagen and gelatin, which are in the category of proteins.

Conflicts of interest

There are no conflicts to declare.

Acknowledgements

The supports from Iranian Nano Council, Iran University of Science and Technology and the University of Qom are appreciated. The authors also acknowledge the financial support from the "Belt and Road" Innovative Talents Exchange Foreign Experts Project of China (Grant No. DL2022026005L).

References

1 Z. Sun, T. Wang, R. Zhang, H. Li, Y. Wu, S. Toan and Z. Sun, *Bioresour. Technol.*, 2023, **382**, 129197.

2 A. George, B. Shen, M. Craven, Y. Wang, D. Kang, C. Wu and X. Tu, *Renewable Sustainable Energy Rev.*, 2021, **135**, 109702.

3 L. Jeffry, M. Y. Ong, S. Nomanbhay, M. Mofijur, M. Mubashir and P. L. Show, *Fuel*, 2021, **301**, 121017.

4 F. C. Özbuğday and B. C. Erbas, *Energy*, 2015, **82**, 734–745.

5 U. Kamran and S.-J. Park, *J. Cleaner Prod.*, 2021, **290**, 125776.

6 L. Li, N. Zhao, W. Wei and Y. Sun, *Fuel*, 2013, **108**, 112–130.

7 K. Riahi, E. S. Rubin and L. Schrattenholzer, in *Greenhouse Gas Control Technologies-6th International Conference*, Elsevier, 2003, pp. 1095–1100.

8 Y. Qin, G. Niu, X. Wang, D. Luo and Y. Duan, *J. CO_2 Util.*, 2018, **28**, 283–291.

9 M. K. Mondal, H. K. Balsora and P. Varshney, *Energy*, 2012, **46**, 431–441.

10 X. Shen, H. Du, R. H. Mullins and R. R. Kommalapati, *Energy Technol.*, 2017, **5**, 822–833.

11 A. Nosrati, S. Javanshir, F. Feyzi and S. Amirnejat, *ACS Omega*, 2023, **8**, 3981–3991.

12 B. Dutcher, M. Fan and A. G. Russell, *ACS Appl. Mater. Interfaces*, 2015, **7**, 2137–2148.

13 I. S. Omodolor, H. O. Otor, J. A. Andonegui, B. J. Allen and A. C. Alba-Rubio, *Ind. Eng. Chem. Res.*, 2020, **59**, 17612–17631.

14 P. R. Yaashikaa, P. S. Kumar, S. J. Varjani and A. Saravanan, *J. CO_2 Util.*, 2019, **33**, 131–147.

15 S. Saeidi, N. A. S. Amin and M. R. Rahimpour, *J. CO_2 Util.*, 2014, **5**, 66–81.

16 A. Alok, R. Shrestha, S. Ban, S. Devkota, B. Uprety and R. Joshi, *J. Environ. Chem. Eng.*, 2022, **10**, 106922.

17 K. Sumida, D. L. Rogow, J. A. Mason, T. M. McDonald, E. D. Bloch, Z. R. Herm, T.-H. Bae and J. R. Long, *Chem. Rev.*, 2012, **112**, 724–781.

18 C. M. White, B. R. Strazisar, E. J. Granite, J. S. Hoffman and H. W. Pennline, *J. Air Waste Manage. Assoc.*, 2003, **53**, 645–715.

19 P. Markewitz, W. Kuckshinrichs, W. Leitner, J. Linssen, P. Zapp, R. Bongartz, A. Schreiber and T. E. Müller, *Energy Environ. Sci.*, 2012, **5**, 7281–7305.

20 N. MacDowell, N. Florin, A. Buchard, J. Hallett, A. Galindo, G. Jackson, C. S. Adjiman, C. K. Williams,

N. Shah and P. Fennell, *Energy Environ. Sci.*, 2010, **3**, 1645–1669.
21 E. S. Rubin, H. Mantripragada, A. Marks, P. Versteeg and J. Kitchin, *Prog. Energy Combust. Sci.*, 2012, **38**, 630–671.
22 J. C. M. Pires, F. G. Martins, M. C. M. Alvim-Ferraz and M. Simões, *Chem. Eng. Res. Des.*, 2011, **89**, 1446–1460.
23 A. A. Olajire, *Energy*, 2010, **35**, 2610–2628.
24 Z. Zhang, T. N. Borhani and A. G. Olabi, *Energy*, 2020, **205**, 118057.
25 N. P. Wickramaratne and M. Jaroniec, *ACS Appl. Mater. Interfaces*, 2013, **5**, 1849–1855.
26 J. M. Kolle, M. Fayaz and A. Sayari, *Chem. Rev.*, 2021, **121**, 7280–7345.
27 A. Saravanan, D.-V. N. Vo, S. Jeevanantham, V. Bhuvaneswari, V. A. Narayanan, P. R. Yaashikaa, S. Swetha and B. Reshma, *Chem. Eng. Sci.*, 2021, **236**, 116515.
28 J. Ma, N. Sun, X. Zhang, N. Zhao, F. Xiao, W. Wei and Y. Sun, *Catal. Today*, 2009, **148**, 221–231.
29 B. Li, Y. Duan, D. Luebke and B. Morreale, *Appl. Energy*, 2013, **102**, 1439–1447.
30 A. A. Chaugule, A. H. Tamboli and H. Kim, *Fuel*, 2017, **200**, 316–332.
31 G. Zhao, Z. Li, B. Cheng, X. Zhuang and T. Lin, *Sep. Purif. Technol.*, 2023, **315**, 123754.
32 M. Li, Q. Xia, S. Lv, J. Tong, Z. Wang, Q. Nie and J. Yang, *Green Chem.*, 2022, **24**, 7500–7518.
33 S. Zhang, X. Bai, C. Zhao, Q. Tan, G. Luo, J. Wang, Q. Li, L. Wu, F. Chen and C. Li, *Earth's Future*, 2021, **9**, e2020EF001938.
34 M. Xi, C. He, H. Yang, X. Fu, L. Fu, X. Cheng and J. Guo, *Chin. Chem. Lett.*, 2022, **33**, 2595–2599.
35 C. Zhao, M. Xi, J. Huo, C. He and L. Fu, *Chin. Chem. Lett.*, 2023, **34**, 107213.
36 J. H. Choe, H. Kim and C. S. Hong, *Mater. Chem. Front.*, 2021, **5**, 5172–5185.
37 Z. Hu, Y. Wang, B. B. Shah and D. Zhao, *Adv. Sustainable Syst.*, 2019, **3**, 1800080.
38 N. H. Khdary, A. S. Alayyar, L. M. Alsarhan, S. Alshihri and M. Mokhtar, *Catalysts*, 2022, **12**, 300.
39 R. Balasubramanian and S. Chowdhury, *J. Mater. Chem. A*, 2015, **3**, 21968–21989.
40 S. Kumar, R. Srivastava and J. Koh, *J. CO_2 Util.*, 2020, **41**, 101251.
41 L. Yin, D. Li, S. Li, F. Gai, T. Zhang, Y. Liu and X. Zhao, *J. Dispersion Sci. Technol.*, 2022, **44**, 2303–2310.
42 E. Magnanelli, Ø. Wilhelmsen, E. Johannessen and S. Kjelstrup, *J. Membr. Sci.*, 2016, **513**, 129–139.
43 Y. Han and W. S. W. Ho, *J. Membr. Sci.*, 2021, **628**, 119244.
44 S. Yu, X. Zhao, J. Zhang, S. Liu, Z. Yuan, X. Liu, B. Liu and X. Yi, *Cellulose*, 2022, **29**, 6783–6796.
45 A. Primo, A. Forneli, A. Corma and H. García, *ChemSusChem*, 2012, **5**, 2207–2214.
46 S. Manzoor, M. Talib, A. V. Arsenin, V. S. Volkov and P. Mishra, *ACS Omega*, 2023, **8**, 893–906.
47 Q. Yang, D. Teng, J. Qu, P. Li and Y. Cao, *Ind. Eng. Chem. Res.*, 2021, **60**, 13023–13030.
48 J. Shen, Y. Yuan and S. Salmon, *ACS Sustainable Chem. Eng.*, 2022, **10**, 7772–7785.
49 D. E. F. Oliveira, J. A. O. Chagas, A. L. De Lima and C. J. A. Mota, *Ind. Eng. Chem. Res.*, 2022, **61**, 10522–10530.
50 Z. Dai, J. Deng, Y. Ma, H. Guo, J. Wei, B. Wang, X. Jiang and L. Deng, *Ind. Eng. Chem. Res.*, 2022, **61**, 9067–9076.
51 X. Qiu, S. Wang and S. Chen, *Cellulose*, 2022, **29**, 5645–5658.
52 J. Ralph, C. Lapierre and W. Boerjan, *Curr. Opin. Biotechnol.*, 2019, **56**, 240–249.
53 S.-J. Sun, P. Deng, C.-E. Peng, H.-Y. Ji, L.-F. Mao and L.-Z. Peng, *Polymers*, 2022, **14**, 2899.
54 M. Nasrollahzadeh, N. S. S. Bidgoli, N. Shafiei and F. Momenbeik, *Int. J. Biol. Macromol.*, 2021, **182**, 59–64.
55 B. Jaleh, A. Moradi, M. Eslamipanah, S. Khazalpour, H. Tahzibi, S. Azizian and M. B. Gawande, *J. Magnesium Alloys*, 2023, **11**, 2072–2083.
56 A. Nasri, B. Jaleh, S. Khazalpour, M. Nasrollahzadeh and M. Shokouhimehr, *Int. J. Biol. Macromol.*, 2020, **164**, 3012–3024.
57 M. Dohendou, K. Pakzad, Z. Nezafat, M. Nasrollahzadeh and M. G. Dekamin, *Int. J. Biol. Macromol.*, 2021, **192**, 771–819.
58 Y. Orooji, Z. Nezafat, M. Nasrollahzadeh and T. A. Kamali, *Int. J. Biol. Macromol.*, 2021, **188**, 950–973.
59 M. Nasrollahzadeh, N. Shafiei, Z. Nezafat and N. S. S. Bidgoli, *Mol. Catal.*, 2020, **489**, 110942.
60 G. A. M. Mersal, H. S. El-Sheshtawy, I. S. Yahia and K. I. Assaf, *Comput. Theor. Chem.*, 2021, **1204**, 113413.
61 P. Thiyam, C. Persson, D. F. Parsons, D. Huang, S. Y. Buhmann and M. Boström, *Colloids Surf., A*, 2015, **470**, 316–321.
62 M. Sajjadi, F. Ahmadpoor, M. Nasrollahzadeh and H. Ghafuri, *Int. J. Biol. Macromol.*, 2021, **178**, 394–423.
63 H. Rasoulzadeh, S. Motesaddi Zarandi, M. Massoudinejad, M. M. Amini and A. Sheikhmohammadi, *Int. J. Environ. Anal. Chem.*, 2021, DOI: 10.1080/03067319.2021.2004408.
64 D. Bi, X. Yang, L. Yao, Z. Hu, H. Li, X. Xu and J. Lu, *Mar. Drugs*, 2022, **20**, 564.
65 H. Wang, J. Qian and F. Ding, *J. Agric. Food Chem.*, 2018, **66**, 395–413.
66 X. Qiu, X. Wang and S. Chen, *New J. Chem.*, 2022, **46**, 6956–6965.
67 P. Jia, J. Xu, X. Wang, Z. Chen, Z. Xie and H. Jiang, *J. Porous Mater.*, 2022, **29**, 745–758.
68 K. Malini, M. Sasi, R. Meghanath, D. Selvakumar and N. S. Kumar, *Int. J. Environ. Anal. Chem.*, 2021, DOI: 10.1080/03067319.2021.1965595.
69 A. Verma, S. Thakur, G. Goel, J. Raj, V. K. Gupta, D. Roberts and V. K. Thakur, *Curr. Res. Green Sustainable Chem.*, 2020, **3**, 100027.
70 Y. Chen, Y. Long, J. Sun, S. Bai, Y. Chen, Z. Chen and C. Zhao, *Energy Fuels*, 2021, **35**, 13215–13223.

71 S. Ren, C. Li, Z. Tan, Y. Hou, S. Jia and J. Cui, *J. Agric. Food Chem.*, 2019, **67**, 3372–3379.

72 N. A. Rashidi, S. Yusup and B. H. Hameed, *Energy*, 2013, **61**, 440–446.

73 Q. B. Meng and J. Weber, *ChemSusChem*, 2014, **7**, 3312–3318.

74 B. Zhao, M. Borghei, T. Zou, L. Wang, L.-S. Johansson, J. Majoinen, M. H. Sipponen, M. österberg, B. D. Mattos and O. J. Rojas, *ACS Nano*, 2021, **15**, 6774–6786.

75 J. Yi, D.-L. Zhong, J. Yan and Y.-Y. Lu, *Energy*, 2019, **171**, 61–68.

76 B. Zhu, J. Huang, J. Lu, D. Zhao, L. Lu, S. Jin and Q. Zhou, *Int. J. Electrochem. Sci.*, 2017, **12**, 11102–11107.

77 W. H. Arnawtee, B. Jaleh, M. Nasrollahzadeh, R. Bakhshali-Dehkordi, A. Nasri and Y. Orooji, *Sep. Purif. Technol.*, 2022, **290**, 120793.

78 X. Wang, M. Tarahomi, R. Sheibani, C. Xia and W. Wang, *Int. J. Biol. Macromol.*, 2023, **241**, 124472.

79 Y. Wu, A. Parandoust, R. Sheibani, F. Kargaran, Z. Khorsandi, Y. Liang, C. Xia and Q. Van Le, *Carbohydr. Polym.*, 2023, **318**, 121102.

80 C. Xu, M. Nasrollahzadeh, M. Selva, Z. Issaabadi and R. Luque, *Chem. Soc. Rev.*, 2019, **48**, 4791–4822.

81 B. Jaleh, M. Nasrollahzadeh, A. Nasri, M. Eslamipanah, A. Moradi and Z. Nezafat, *Int. J. Biol. Macromol.*, 2021, **182**, 1056–1090.

82 R. Mohami, A. Shakeri and M. Nasrollahzadeh, *Sep. Purif. Technol.*, 2022, **285**, 120373.

83 M. Nasrollahzadeh, N. S. S. Bidgoli and M. M. Karimkhani, *Biomass Convers. Biorefin.*, 2023, **13**, 9675–9688.

84 A. Khan, M. Goepel, J. C. Colmenares and R. Gläser, *ACS Sustainable Chem. Eng.*, 2020, **8**, 4708–4727.

85 F. Freitas, V. D. Alves, M. A. Reis, J. G. Crespo and I. M. Coelhoso, *J. Appl. Polym. Sci.*, 2014, **131**, 40047.

86 Z. Nezafat, B. F. Mohazzab, B. Jaleh, M. Nasrollahzadeh, T. Baran and M. Shokouhimehr, *Inorg. Chem. Commun.*, 2021, **130**, 108746.

87 C. Zhao, X. Chen, E. J. Anthony, X. Jiang, L. Duan, Y. Wu, W. Dong and C. Zhao, *Prog. Energy Combust. Sci.*, 2013, **39**, 515–534.

88 Q. Wang, J. Luo, Z. Zhong and A. Borgna, *Energy Environ. Sci.*, 2011, **4**, 42–55.

89 A. E. Creamer and B. Gao, *Environ. Sci. Technol.*, 2016, **50**, 7276–7289.

90 C. H. Lee, S. Mun and K. B. Lee, *Chem. Eng. J.*, 2014, **258**, 367–373.

91 R. V. Siriwardane, M.-S. Shen, E. P. Fisher and J. Losch, *Energy Fuels*, 2005, **19**, 1153–1159.

92 M. S. Duyar, S. Wang, M. A. Arellano-Trevino and R. J. Farrauto, *J. CO_2 Util.*, 2016, **15**, 65–71.

93 W. Zhang, H. Liu, Y. Sun, J. Cakstins, C. Sun and C. E. Snape, *Appl. Energy*, 2016, **168**, 394–405.

94 P. Luis, T. Van Gerven and B. Van der Bruggen, *Prog. Energy Combust. Sci.*, 2012, **38**, 419–448.

95 Y. Han and W. S. W. Ho, *Chin. J. Chem. Eng.*, 2018, **26**, 2238–2254.

96 R. J. Littel, G. F. Versteeg and W. P. M. Van Swaaij, *Chem. Eng. Sci.*, 1992, **47**, 2037–2045.

97 M. Caplow, *J. Am. Chem. Soc.*, 1968, **90**, 6795–6803.

98 H.-B. Xie, Y. Zhou, Y. Zhang and J. K. Johnson, *J. Phys. Chem. A*, 2010, **114**, 11844–11852.

99 N. J. M. C. Penders-van Elk, S. Fradette and G. F. Versteeg, *Chem. Eng. J.*, 2015, **259**, 682–691.

100 P. Khakharia, L. Brachert, J. Mertens, C. Anderlohr, A. Huizinga, E. S. Fernandez, B. Schallert, K. Schaber, T. J. H. Vlugt and E. Goetheer, *Int. J. Greenhouse Gas Control*, 2015, **34**, 63–74.

101 A. García-Abuín, D. Gomez-Diaz, A. B. López, J. M. Navaza and A. Rumbo, *Ind. Eng. Chem. Res.*, 2013, **52**, 13432–13438.

102 L. Zhu, G. W. Schade and C. J. Nielsen, *Environ. Sci. Technol.*, 2013, **47**, 14306–14314.

103 J. E. Crooks and J. P. Donnellan, *J. Chem. Soc., Perkin Trans. 2*, 1989, 331–333.

104 E. F. Da Silva and H. F. Svendsen, *Ind. Eng. Chem. Res.*, 2004, **43**, 3413–3418.

105 B. Arstad, R. Blom and O. Swang, *J. Phys. Chem. A*, 2007, **111**, 1222–1228.

106 H. Guo, Z. Zhou and G. Jing, *Int. J. Greenhouse Gas Control*, 2013, **16**, 197–205.

107 S. Kasahara, E. Kamio and H. Matsuyama, *J. Membr. Sci.*, 2014, **454**, 155–162.

108 H. Sun, X. Zhou, Z. Xue, Z. Zhou and T. Mu, *Int. J. Greenhouse Gas Control*, 2014, **20**, 43–48.

109 B. Lv, B. Guo, Z. Zhou and G. Jing, *Environ. Sci. Technol.*, 2015, **49**, 10728–10735.

110 S.-J. Han and J.-H. Wee, *Environ. Sci. Pollut. Res.*, 2020, **27**, 44951–44968.

111 T. L. Donaldson and Y. N. Nguyen, *Ind. Eng. Chem. Fundam.*, 1980, **19**, 260–266.

112 R. Yang, W. Fan, Y. Zheng, T. Wang, Y. Wang, T. Shi, D. Yao, L. Chen and A. Zhang, *J. Mater. Sci.*, 2018, **53**, 5172–5182.

113 J.-S. Yang, Y.-J. Xie and W. He, *Carbohydr. Polym.*, 2011, **84**, 33–39.

114 K. Y. Lee and D. J. Mooney, *Prog. Polym. Sci.*, 2012, **37**, 106–126.

115 M. G. Dekamin, S. Ilkhanizadeh, Z. Latifidoost, H. Daemi, Z. Karimi and M. Barikani, *RSC Adv.*, 2014, **4**, 56658–56664.

116 B. Wang, Y. Wan, Y. Zheng, X. Lee, T. Liu, Z. Yu, J. Huang, Y. S. Ok, J. Chen and B. Gao, *Crit. Rev. Environ. Sci. Technol.*, 2019, **49**, 318–356.

117 N. T. T. Uyen, Z. A. A. Hamid, N. X. T. Tram and N. Ahmad, *Int. J. Biol. Macromol.*, 2020, **153**, 1035–1046.

118 J. Venkatesan, I. Bhatnagar, P. Manivasagan, K.-H. Kang and S.-K. Kim, *Int. J. Biol. Macromol.*, 2015, **72**, 269–281.

119 L. Wang, Y. Hou, X. Zhong, J. Hu, F. Shi and H. Mi, *Carbohydr. Polym.*, 2019, **208**, 42–49.

120 Y. Qin, J. Jiang, L. Zhao, J. Zhang and F. Wang, in *Biopolymers for Food Design*, Elsevier, 2018, pp. 409–429.

121 T. Ramdhan, S. H. Ching, S. Prakash and B. Bhandari, *Trends Food Sci. Technol.*, 2020, **106**, 150–159.

122 X. Guo, Y. Wang, Y. Qin, P. Shen and Q. Peng, *Int. J. Biol. Macromol.*, 2020, **162**, 618–628.

123 A. Benettayeb, E. Guibal, A. Morsli and R. Kessas, *Chem. Eng. J.*, 2017, **316**, 704–714.

124 Z. Belattmania, F. Bentiss, C. Jama, M. Barakate, C. Katif, A. Reani and B. Sabour, *Bionanoscience*, 2018, **8**, 617–623.

125 J. Venkatesan, S. Anil and S.-K. Kim, *Seaweed Polysaccharides: Isolation, biological and biomedical applications*, Elsevier, 2017.

126 H. Rasoulzadeh, S. Motesaddi Zarandi, M. Massoudinejad and M. M. Amini, *Int. J. Environ. Anal. Chem.*, 2021, **103**, 3740–3761.

127 S. Hosseini, F. E. Babadi, S. M. Soltani, M. K. Aroua, S. Babamohammadi and A. M. Moghadam, *Process Saf. Environ. Prot.*, 2017, **109**, 387–399.

128 Y. Li, J. Wang, S. Fan, F. Wang, Z. Shen, H. Duan, J. Xu and Y. Huang, *J. Energy Chem.*, 2021, **53**, 168–174.

129 Y. Wu, Z. Chen, Y. Liu, Y. Xu and Z. Liu, *Fuel*, 2018, **233**, 574–581.

130 X. Ma, Y. Li, M. Cao and C. Hu, *J. Mater. Chem. A*, 2014, **2**, 4819–4826.

131 Z. Li, W. Sun, C. Chen, Q. Guo, X. Li, M. Gu, N. Feng, J. Ding, H. Wan and G. Guan, *Appl. Surf. Sci.*, 2019, **480**, 770–778.

132 J. M. Park, D. K. Yoo and S. H. Jhung, *Chem. Eng. J.*, 2020, **402**, 126254.

133 P. Chen, X. He, M. Pang, X. Dong, S. Zhao and W. Zhang, *ACS Appl. Mater. Interfaces*, 2020, **12**, 20429–20439.

134 K. Wang, Y. Tang, Q. Jiang, Y. Lan, H. Huang, D. Liu and C. Zhong, *J. Energy Chem.*, 2017, **26**, 902–908.

135 A. Kidanemariam, J. Lee and J. Park, *Polymers*, 2019, **11**, 2090.

136 S. Xiao, M. Li, H. Cong, L. Wang, X. Li and W. Zhang, *Polymers*, 2021, **13**, 4075.

137 S. Salehi and M. Hosseinifard, *Chem. Eng. J.*, 2021, **410**, 128315.

138 G. Mondino, A. I. Spjelkavik, T. Didriksen, S. Krishnamurthy, R. E. Stensrød, C. A. Grande, L. O. Nord and R. Blom, *Ind. Eng. Chem. Res.*, 2020, **59**, 7198–7211.

139 J. Xue, T. Wu, Y. Dai and Y. Xia, *Chem. Rev.*, 2019, **119**, 5298–5415.

140 A. Suratman, D. N. Astuti, R. Jonathan, A. Kuncaka and Y. Yusuf, *Indones. J. Chem.*, 2022, **22**, 317–330.

141 F. V. L. Koly and A. Suratman, Suyanta, *Mor. J. Chem.*, 2020, **8**, 053–063.

142 S. Wanjari, C. Prabhu, R. Yadav, T. Satyanarayana, N. Labhsetwar and S. Rayalu, *Process Biochem.*, 2011, **46**, 1010–1018.

143 S. Zhang, Z. Zhang, Y. Lu, M. Rostam-Abadi and A. Jones, *Bioresour. Technol.*, 2011, **102**, 10194–10201.

144 D. Dziedzic, K. B. Gross, R. A. Gorski and J. T. Johnson, *J. Air Waste Manage. Assoc.*, 2006, **56**, 1631–1641.

145 N. Liu, G. M. Bond, A. Abel, B. J. McPherson and J. Stringer, *Fuel Process. Technol.*, 2005, **86**, 1615–1625.

146 Y. Zhu, W. Li, G. Sun, Q. Tang and H. Bian, *Int. J. Greenhouse Gas Control*, 2016, **49**, 290–296.

147 A. Hussain and M.-B. Hägg, *J. Membr. Sci.*, 2010, **359**, 140–148.

148 Y. Zhang, Z. Wang and S. Wang, *Chem. Lett.*, 2002, **31**, 430–431.

149 Z. H. U. Yaqun, W. Zhi, C. Zhang, W. Jixiao and W. Shichang, *Chin. J. Chem. Eng.*, 2013, **21**, 1098–1105.

150 P. Mahajan, M. B. Bera, P. S. Panesar and A. Chauhan, *Int. J. Biol. Macromol.*, 2021, **180**, 61–79.

151 B. Dereje, *Int. J. Biol. Macromol.*, 2021, **187**, 911–921.

152 M. Nasrollahzadeh, N. Shafiei, Z. Nezafat, N. S. S. Bidgoli and F. Soleimani, *Carbohydr. Polym.*, 2020, **241**, 116353.

153 F. Xie, E. Pollet, P. J. Halley and L. Averous, *Prog. Polym. Sci.*, 2013, **38**, 1590–1628.

154 W. Dang, Q. Lin, H. Pan and D. Zhang, *J. Mater. Sci.*, 2022, **57**, 12438–12448.

155 G. Nazir, A. Rehman and S.-J. Park, *J. CO_2 Util.*, 2021, **51**, 101641.

156 S. A. Anuar, W. N. R. W. Isahak and M. S. Mastar, in *IOP Conference Series: Earth and Environmental Science*, IOP Publishing, 2019, vol. 268, p. 12093.

157 N. Rong, Y. Wu, J. Wang, L. Han and G. Wang, *Energy Fuels*, 2021, **35**, 6056–6067.

158 R. Rajamathi, Bhojaraj and C. Nethravathi, *ACS Appl. Nano Mater.*, 2021, **4**, 10969–10975.

159 A. Alabadi, S. Razzaque, Y. Yang, S. Chen and B. Tan, *Chem. Eng. J.*, 2015, **281**, 606–612.

160 M. Sevilla and A. B. Fuertes, *Energy Environ. Sci.*, 2011, **4**, 1765–1771.

161 R. Mohammadinejad, A. Kumar, M. Ranjbar-Mohammadi, M. Ashrafizadeh, S. S. Han, G. Khang and Z. Roveimiab, *Polymers*, 2020, **12**, 176.

162 F. Hussin, N. N. Hazani and M. K. Aroua, *Mater. Today: Proc.*, 2023, DOI: 10.1016/j.matpr.2023.01.094.

163 T. Prasankumar, D. Salpekar, S. Bhattacharyya, K. Manoharan, R. M. Yadav, M. A. C. Mata, K. A. Miller, R. Vajtai, S. Jose and S. Roy, *Carbon*, 2022, **199**, 249–257.

164 J. Chen, W. Liu, C.-M. Liu, T. Li, R.-H. Liang and S.-J. Luo, *Crit. Rev. Food Sci. Nutr.*, 2015, **55**, 1684–1698.

165 C. F. de Oliveira, D. Giordani, R. Lutckemier, P. D. Gurak, F. Cladera-Olivera and L. D. F. Marczak, *LWT–Food Sci. Technol.*, 2016, **71**, 110–115.

166 M. Nasrollahzadeh, M. Sajjadi, S. Iravani and R. S. Varma, *Carbohydr. Polym.*, 2021, **251**, 116986.

167 M. Vafaeinia, M. S. Khosrowshahi, H. Mashhadimoslem, H. B. M. Emrooz and A. Ghaemi, *RSC Adv.*, 2022, **12**, 546–560.

168 J. A. K. P. Jovellana and B. B. Pajarito, *Key Eng. Mater.*, 2019, **801**, 179–184.

169 A. Lagazzo, E. Finocchio, P. Petrini, C. Ruggiero and L. Pastorino, *Mater. Lett.*, 2016, **171**, 212–215.

170 K. V. H. Prashanth and R. N. Tharanathan, *Trends Food Sci. Technol.*, 2007, **18**, 117–131.

171 F. Gu, J. Geng, M. Li, J. Chang and Y. Cui, *ACS Omega*, 2019, **4**, 21421–21430.

172 M. J. Ahmed, B. H. Hameed and E. H. Hummadi, *Carbohydr. Polym.*, 2020, **247**, 116690.

173 K. Kurita, *Mar. Biotechnol.*, 2006, **8**, 203–226.

174 X. Liu, X. Zhao, Y. Liu and T. Zhang, *Polym. Bull.*, 2022, **79**, 2633–2665.

175 L. A. El-Azzami and E. A. Grulke, *J. Polym. Sci., Part B: Polym. Phys.*, 2007, **45**, 2620–2631.

176 M. H. Al Marzouqi, M. A. Abdulkarim, S. A. Marzouk, M. H. El-Naas and H. M. Hasanain, *Ind. Eng. Chem. Res.*, 2005, **44**, 9273–9278.

177 E. Luzzi, P. Aprea, M. Salzano de Luna, D. Caputo and G. Filippone, *ACS Appl. Mater. Interfaces*, 2021, **13**, 20728–20734.

178 Z. Liu, R. Ma, W. Du, G. Yang and T. Chen, *RSC Adv.*, 2021, **11**, 20486–20497.

179 W. Du, R. Ma, Z. Liu, G. Yang and T. Chen, *Materials*, 2021, **14**, 3224.

180 N. Hsan, P. K. Dutta, S. Kumar, R. Bera and N. Das, *Int. J. Biol. Macromol.*, 2019, **125**, 300–306.

181 J. Song, J. Liu, W. Zhao, Y. Chen, H. Xiao, X. Shi, Y. Liu and X. Chen, *Ind. Eng. Chem. Res.*, 2018, **57**, 4941–4948.

182 A. A. Alhwaige, H. Ishida and S. Qutubuddin, *ACS Sustainable Chem. Eng.*, 2016, **4**, 1286–1295.

183 A. A. Alhwaige, T. Agag, H. Ishida and S. Qutubuddin, *RSC Adv.*, 2013, **3**, 16011–16020.

184 S. Kumar, M. Y. Wani, J. Koh, J. M. Gil and A. J. F. N. Sobral, *J. Environ. Sci.*, 2018, **69**, 77–84.

185 S. Kunalan, K. Palanivelu, E. K. Sachin, D. A. Syrtsova and V. V. Teplyakov, *J. Appl. Polym. Sci.*, 2022, **139**, 52024.

186 H. Wen, L. Zhang, Y. Du, Z. Wang, Y. Jiang, H. Bian, J. Cui and S. Jia, *J. CO_2 Util.*, 2020, **39**, 101171.

187 N. Li, Z. Wang and J. Wang, *J. Membr. Sci.*, 2022, **642**, 119946.

188 Y. Shen, H. Wang, J. Liu and Y. Zhang, *ACS Sustainable Chem. Eng.*, 2015, **3**, 1819–1829.

189 M. C. Singo, X. C. Molepo, O. O. Oluwasina and M. O. Daramola, *Energy Procedia*, 2017, **114**, 2429–2440.

190 K. O. Yoro, M. Singo, M. O. Daramola and J. L. Mulopo, in *Proceedings of the 33rd annual international pittsburgh coal conference. Omnipress, Capetown, South Africa*, 2016.

191 K. Malini, D. Selvakumar and N. S. Kumar, *J. Porous Mater.*, 2022, **29**, 1539–1550.

192 C. Yang, T. Zhao, H. Pan, F. Liu, J. Cao and Q. Lin, *Chem. Eng. J.*, 2022, **432**, 134347.

193 J. Li, A. Bao, J. Chen and Y. Bao, *J. Environ. Chem. Eng.*, 2022, **10**, 107021.

194 J. Xiao, Y. Wang, T. C. Zhang, L. Ouyang and S. Yuan, *J. Power Sources*, 2022, **517**, 230727.

195 S. He, G. Chen, H. Xiao, G. Shi, C. Ruan, Y. Ma, H. Dai, B. Yuan, X. Chen and X. Yang, *J. Colloid Interface Sci.*, 2021, **582**, 90–101.

196 J. Shi, H. Cui, J. Xu, N. Yan, C. Zhang and S. You, *Fuel*, 2021, **305**, 121505.

197 G. Nazir, A. Rehman and S.-J. Park, *J. Environ. Manage.*, 2021, **299**, 113661.

198 Q. Wu, G. Zhang, M. Gao, L. Huang, L. Li, S. Liu, C. Xie, Y. Zhang and S. Yu, *J. Alloys Compd.*, 2019, **786**, 826–838.

199 J. Fujiki and K. Yogo, *Chem. Commun.*, 2016, **52**, 186–189.

200 X. Fan, L. Zhang, G. Zhang, Z. Shu and J. Shi, *Carbon*, 2013, **61**, 423–430.

201 J. A. Thote, R. V. Chatti, K. S. Iyer, V. Kumar, A. N. Valechha, N. K. Labhsetwar, R. B. Biniwale, M. K. N. Yenkie and S. S. Rayalu, *J. Environ. Sci.*, 2012, **24**, 1979–1984.

202 M. Helmi, F. Moazami, A. Ghaemi and A. Hemmati, *Fuel*, 2023, **338**, 127300.

203 M. Lopes, A. Cecílio, M. Zanatta and M. C. Corvo, *J. Cleaner Prod.*, 2022, **367**, 132977.

204 I. Barroso-Martín, J. A. Cecilia, E. Vilarrasa-García, D. Ballesteros-Plata, C. P. Jiménez-Gómez, Á. Vílchez-Cózar, A. Infantes-Molina and E. Rodríguez-Castellón, *Polymers*, 2022, **14**, 5240.

205 J. A. O. Chagas, G. O. Crispim, B. P. Pinto, R. A. S. San Gil and C. J. A. Mota, *ACS Omega*, 2020, **5**, 29520–29529.

206 P. Wang, G. Zhang, W. Chen, Q. Chen, H. Jiao, L. Liu, X. Wang and X. Deng, *ACS Omega*, 2020, **5**, 23460–23467.

207 N. Hsan, P. K. Dutta, S. Kumar, N. Das and J. Koh, *J. CO_2 Util.*, 2020, **41**, 101237.

208 I.-H. Tseng, Z.-C. Liu and P.-Y. Chang, *Carbohydr. Polym.*, 2020, **230**, 115584.

209 P. Jiamjirangkul, T. Inprasit, V. Intasanta and A. Pangon, *Chem. Eng. Sci.*, 2020, **221**, 115650.

210 A. Rehman and S.-J. Park, *Carbon*, 2020, **159**, 625–637.

211 G. Singh, S. Tiburcius, S. M. Ruban, D. Shanbhag, C. I. Sathish, K. Ramadass and A. Vinu, *Emergent Mater.*, 2019, **2**, 337–349.

212 L. Marin, B. Dragoi, N. Olaru, E. Perju, A. Coroaba, F. Doroftei, G. Scavia, S. Destri, S. Zappia and W. Porzio, *Eur. Polym. J.*, 2019, **120**, 109214.

213 H.-L. Peng, J.-B. Zhang, J.-Y. Zhang, F.-Y. Zhong, P.-K. Wu, K. Huang, J.-P. Fan and F. Liu, *Chem. Eng. J.*, 2019, **359**, 1159–1165.

214 M. A. Islam, Y. L. Tan, M. A. Islam, M. Romić and B. H. Hameed, *Colloids Surf., A*, 2018, **554**, 9–15.

215 K. Osler, N. Twala, O. O. Oluwasina and M. O. Daramola, *Energy Procedia*, 2017, **114**, 2330–2335.

216 S. Kumar, J. de A. e Silva, M. Y. Wani, J. M. Gil and A. J. F. N. Sobral, *Carbohydr. Polym.*, 2017, **175**, 575–583.

217 S. Kumar, J. de A. e Silva, M. Y. Wani, C. M. F. Dias and A. J. F. N. Sobral, *J. Dispersion Sci. Technol.*, 2016, **37**, 155–158.

218 G. Sneddon, A. Y. Ganin and H. H. P. Yiu, *Energy Technol.*, 2015, **3**, 249–258.

219 J. Fujiki and K. Yogo, *Energy Fuels*, 2014, **28**, 6467–6474.

220 M. Keramati and A. A. Ghoreyshi, *Phys. E*, 2014, **57**, 161–168.

221 C. Patkool, P. Chawakitchareon and R. Anuwattana, *Environ. Eng. Res.*, 2014, **19**, 289–292.

222 C.-C. Huang and S.-C. Shen, *J. Taiwan Inst. Chem. Eng.*, 2013, **44**, 89–94.

223 S. Kumar, K. Prasad, J. M. Gil, A. J. F. N. Sobral and J. Koh, *Carbohydr. Polym.*, 2018, **198**, 401–406.
224 C. Li, N. He, X. Zhao, X. Zhang, W. Li, X. Zhao and Y. Qiao, *ChemistrySelect*, 2022, **7**, e202103927.
225 H. P. S. A. Khalil, A. H. Bhat and A. F. I. Yusra, *Carbohydr. Polym.*, 2012, **87**, 963–979.
226 A. Gholampour and T. Ozbakkaloglu, *J. Mater. Sci.*, 2020, **55**, 829–892.
227 K. A. Adegoke, I. A. Bello, O. S. Bello, M. A. Balogun and N. W. Maxakato, *Sci. Afr.*, 2022, **16**, e01138.
228 B. Zhang, H. Chen, Q. Hu, L. Jiang, Y. Shen, D. Zhao and Z. Zhou, *Adv. Funct. Mater.*, 2021, **31**, 2105395.
229 S. Wohlhauser, G. Delepierre, M. Labet, G. Morandi, W. Thielemans, C. Weder and J. O. Zoppe, *Macromolecules*, 2018, **51**, 6157–6189.
230 A. H. Tayeb, E. Amini, S. Ghasemi and M. Tajvidi, *Molecules*, 2018, **23**, 2684.
231 D. Plackett, K. Letchford, J. Jackson and H. Burt, *Nord. Pulp Pap. Res. J.*, 2014, **29**, 105–118.
232 Z. Dai, V. Ottesen, J. Deng, R. M. L. Helberg and L. Deng, *Fibers*, 2019, **7**, 40.
233 Y. Habibi, L. A. Lucia and O. J. Rojas, *Chem. Rev.*, 2010, **110**, 3479–3500.
234 R. J. Moon, A. Martini, J. Nairn, J. Simonsen and J. Youngblood, *Chem. Soc. Rev.*, 2011, **40**, 3941–3994.
235 V. K. Thakur and M. K. Thakur, *Carbohydr. Polym.*, 2014, **109**, 102–117.
236 X.-F. Zhang, Z. Wang, M. Ding, Y. Feng and J. Yao, *J. Mater. Chem. A*, 2021, **9**, 23353–23363.
237 M. Babar, M. A. Bustam, A. Ali, A. S. Maulud, U. Shafiq, A. M. Shariff and Z. Man, *Cryogenics*, 2019, **101**, 79–88.
238 C. Gunathilake, R. S. Dassanayake, N. Abidi and M. Jaroniec, *J. Mater. Chem. A*, 2016, **4**, 4808–4819.
239 S. Q. Jabbar, H. Janani and H. Janani, *J. Polym. Environ.*, 2022, **30**, 4210–4224.
240 S. Wang, C. Wang and Q. Zhou, *ACS Appl. Mater. Interfaces*, 2021, **13**, 29949–29959.
241 A. Policicchio, M. Florent, M. F. Attia, D. C. Whitehead, J. Jagiello and T. J. Bandosz, *Adv. Mater. Interfaces*, 2020, **7**, 1902098.
242 Q. Yang, M. Zhang, S. Song and B. Yang, *Cellulose*, 2017, **24**, 3051–3060.
243 A. Brunetti, L. Lei, E. Avruscio, D. S. Karousos, A. Lindbråthen, E. P. Kouvelos, X. He, E. P. Favvas and G. Barbieri, *Chem. Eng. J.*, 2022, **448**, 137615.
244 A. Rehman, Z. Jahan, F. Sher, T. Noor, M. B. K. Niazi, M. A. Akram and E. K. Sher, *Chemosphere*, 2022, **307**, 135736.
245 C. Regmi, S. Ashtiani, F. Průša and K. Friess, *Sep. Purif. Technol.*, 2022, **282**, 120128.
246 A. Ali, M. Mubashir, A. Abdulrahman and P. E. Phelan, *Chemosphere*, 2022, **306**, 135482.
247 E. Akbarzadeh, A. Shockravi and V. Vatanpour, *Carbohydr. Polym.*, 2021, **252**, 117215.
248 A. Raza, S. Farrukh, A. Hussain, I. Khan, M. H. D. Othman and M. Ahsan, *Membranes*, 2021, **11**, 245.
249 A. Jamil, M. Zulfiqar, U. Arshad, S. Mahmood, T. Iqbal, S. Rafiq and M. Z. Iqbal, *Adv. Polym. Technol.*, 2020, **2020**, 8855577.
250 S. Janakiram, X. Yu, L. Ansaloni, Z. Dai and L. Deng, *ACS Appl. Mater. Interfaces*, 2019, **11**, 33302–33313.
251 S. Hafeez, X. Fan, A. Hussain and C. F. Martín, *J. Environ. Sci.*, 2015, **35**, 163–171.
252 X. Chen, J. Lin, H. Wang, Y. Yang, C. Wang, Q. Sun, X. Shen and Y. Li, *Carbohydr. Polym.*, 2023, **302**, 120389.
253 J. Cheng, X. Cheng, Z. Wang, M. B. Hussain and M. Wang, *Energy*, 2023, **263**, 125984.
254 Q. Zhang, W. Lu, M. Wu, G. Qi, Y. Yuan, J. Li, H. Su and H. Zhang, *J. Environ. Manage.*, 2022, **302**, 114044.
255 J. Sun, M. Shang, M. Zhang, S. Yu, Z. Yuan, X. Yi, S. Filatov and J. Zhang, *Carbohydr. Polym.*, 2022, **293**, 119720.
256 J. Gong, F. Tong, C. Zhang, M. S. Nobandegani, L. Yu and L. Zhang, *Microporous Mesoporous Mater.*, 2022, **331**, 111664.
257 N. H. Mohd, H. Kargazadeh, M. Miyamoto, S. Uemiya, N. Sharer, A. Baharum, T. L. Peng, I. Ahmad, M. A. Yarmo and R. Othaman, *J. Mater. Res. Technol.*, 2021, **13**, 2287–2296.
258 X. Jiang, Y. Kong, H. Zou, Z. Zhao, Y. Zhong and X. Shen, *J. Porous Mater.*, 2021, **28**, 93–97.
259 G. Zhou, K. Wang, R. Liu, Y. Tian, B. Kong and G. Qi, *Colloids Surf., A*, 2021, **631**, 127675.
260 J. Xu, P. Jia, X. Wang, Z. Xie, Z. Chen and H. Jiang, *J. Appl. Polym. Sci.*, 2021, **138**, 50891.
261 W. Zhu, Y. Yao, Y. Zhang, H. Jiang, Z. Wang, W. Chen and Y. Xue, *Ind. Eng. Chem. Res.*, 2020, **59**, 16660–16668.
262 Y. Miao, M. Pudukudy, Y. Zhi, Y. Miao, S. Shan, Q. Jia and Y. Ni, *Carbohydr. Polym.*, 2020, **236**, 116079.
263 T. Zhang, W. Zhang, Y. Zhang, M. Shen and J. Zhang, *Cellulose*, 2020, **27**, 2953–2958.
264 Y. Li, P. Jia, J. Xu, Y. Wu, H. Jiang and Z. Li, *Ind. Eng. Chem. Res.*, 2020, **59**, 2874–2882.
265 Y. Tang, S. Tang and T. Zhang, *Cellulose*, 2020, **27**, 3263–3275.
266 Y. Miao, H. Luo, M. Pudukudy, Y. Zhi, W. Zhao, S. Shan, Q. Jia and Y. Ni, *Carbohydr. Polym.*, 2020, **227**, 115380.
267 T. Zhang, Y. Zhang, H. Jiang and X. Wang, *Environ. Sci. Pollut. Res.*, 2019, **26**, 16716–16726.
268 C. Wang and S. Okubayashi, *Carbohydr. Polym.*, 2019, **225**, 115248.
269 Y. Wu, Y. Zhang, N. Chen, S. Dai, H. Jiang and S. Wang, *Carbohydr. Polym.*, 2018, **194**, 252–259.
270 S. Liu, Y. Zhang, H. Jiang, X. Wang, T. Zhang and Y. Yao, *Environ. Chem. Lett.*, 2018, **16**, 605–614.
271 F. Jiang, S. Hu and Y. Hsieh, *ACS Appl. Nano Mater.*, 2018, **1**, 6701–6710.
272 Y. Wu, F. Cao, H. Jiang and Y. Zhang, *Mater. Res. Express*, 2017, **4**, 85303.
273 R. S. Dassanayake, C. Gunathilake, T. Jackson, M. Jaroniec and N. Abidi, *Cellulose*, 2016, **23**, 1363–1374.

274 Y. Hu, X. Tong, H. Zhuo, L. Zhong, X. Peng, S. Wang and R. Sun, *RSC Adv.*, 2016, **6**, 15788–15795.

275 L. Valencia and H. N. Abdelhamid, *Carbohydr. Polym.*, 2019, **213**, 338–345.

276 H. N. Abdelhamid and A. P. Mathew, *Chem. Eng. J.*, 2021, **426**, 131733.

277 M. Mubashir, L. F. Dumée, Y. Y. Fong, N. Jusoh, J. Lukose, W. S. Chai and P. L. Show, *J. Hazard. Mater.*, 2021, **415**, 125639.

278 H. Ma, Z. Wang, X.-F. Zhang, M. Ding and J. Yao, *Carbohydr. Polym.*, 2021, **270**, 118376.

279 P. Zeng, C. Zhao, C. Liang, P. Li, H. Zhang, R. Wang, Y. Guo, H. Xia and J. Sun, *Sep. Purif. Technol.*, 2023, **306**, 122608.

280 Y. Zheng, J. Wu, L. Zhang, Y. Guo, Z. Xu, Y. Huang, P. Huang, J. Zhang and C. Zhao, *Chem. Eng. J.*, 2022, **450**, 137944.

281 J. Sun, C. Liang, X. Tong, Y. Guo, W. Li, C. Zhao, J. Zhang and P. Lu, *Fuel*, 2019, **239**, 1046–1054.

282 L. Helmlinger, Y. Zhu, J. Gensel, T. Neumeyer, S. Thäter, F. Strube, C. Bauer, B. Rosemann and V. Altstädt, *J. Renewable Mater.*, 2018, **6**, 219.

283 Y. Hu, W. Liu, Y. Peng, Y. Yang, J. Sun, H. Chen, Z. Zhou and M. Xu, *Fuel Process. Technol.*, 2017, **160**, 70–77.

284 J. Sun, W. Liu, Y. Hu, J. Wu, M. Li, X. Yang, W. Wang and M. Xu, *Chem. Eng. J.*, 2016, **285**, 293–303.

285 H.-X. Zhao, J.-C. Li, Y. Wang, Y.-R. Guo, S. Li and Q.-J. Pan, *Sep. Purif. Technol.*, 2023, **307**, 122774.

286 G. Reyes, R. Ajdary, E. Kankuri, J. J. Kaschuk, H. Kosonen and O. J. Rojas, *Carbohydr. Polym.*, 2023, **302**, 120355.

287 M. P. Vocht, P. Tomasic, R. Beyer, A. Müller, U. Zuberbühler, B. Stürmer, F. Hermanutz and M. R. Buchmeiser, *Macromol. Mater. Eng.*, 2022, **307**, 2200093.

288 W. Lu, X. Shi, H. Zhou, W. Luo, L. Wang and H. He, *Chem. Eng. J.*, 2022, **449**, 137885.

289 J. Lin, W. Lu, X. Shi, Q. Lu, L. Wang and H. He, *ACS Sustainable Chem. Eng.*, 2021, **9**, 10184–10195.

290 N. Chouikhi, J. A. Cecilia, E. Vilarrasa-García, L. Serrano-Cantador, S. Besghaier, M. Chlendi, M. Bagane and E. R. Castellón, *Biomass Bioenergy*, 2021, **155**, 106297.

291 Y. Wang, X. He and Q. Lu, *Cellulose*, 2021, **28**, 4241–4251.

292 A. Rehman, G. Nazir, K. Y. Rhee and S.-J. Park, *Chem. Eng. J.*, 2021, **420**, 130421.

293 R. Ahmadi, M. Ardjmand, A. Rashidi and M. Rafizadeh, *Energy Sources, Part A*, 2020, DOI: **10.1080/15567036.2020.1845878**.

294 M. F. A. Hernández, M. F. Rojas, F. Bernard, S. Einloft and L. A. C. Diaz, *Fibers Polym.*, 2020, **21**, 2861–2872.

295 S. Sepahvand, M. Jonoobi, A. Ashori, F. Gauvin, H. J. H. Brouwers, K. Oksman and Q. Yu, *Carbohydr. Polym.*, 2020, **230**, 115571.

296 C. Hou, Y. Wu, T. Wang, X. Wang and X. Gao, *Energy Fuels*, 2018, **33**, 1745–1752.

297 S. Campbell, F. L. Bernard, D. M. Rodrigues, M. F. Rojas, L. Á. Carreño, V. V. Chaban and S. Einloft, *Fuel*, 2019, **239**, 737–746.

298 W. Zhu, M. Ji, Y. Zhang, Z. Wang, W. Chen and Y. Xue, *Polymers*, 2019, **11**, 2021.

299 P. García-Gutiérrez, R. M. Cuéllar-Franca, D. Reed, G. Dowson, P. Styring and A. Azapagic, *Green Chem.*, 2019, **21**, 4100–4114.

300 F. Valdebenito, R. García, K. Cruces, G. Ciudad, G. Chinga-Carrasco and Y. Habibi, *ACS Sustainable Chem. Eng.*, 2018, **6**, 12603–12612.

301 Y. Zhang, X. Gong, X. Chen, L. Yin, J. Zhang and W. Liu, *Fuel*, 2018, **232**, 205–214.

302 M. Gunnarsson, D. Bernin, Å. Östlund and M. Hasani, *Green Chem.*, 2018, **20**, 3279–3286.

303 C. Xu, C. Ruan, Y. Li, J. Lindh and M. Strømme, *Adv. Sustainable Syst.*, 2018, **2**, 1700147.

304 R. S. Dassanayake, C. Gunathilake, A. C. Dassanayake, N. Abidi and M. Jaroniec, *J. Mater. Chem. A*, 2017, **5**, 7462–7473.

305 F. L. Bernard, D. M. Rodrigues, B. B. Polesso, A. J. Donato, M. Seferin, V. V. Chaban, F. Dalla Vecchia and S. Einloft, *Fuel Process. Technol.*, 2016, **149**, 131–138.

306 K. J. Shah and T. Imae, *Biomacromolecules*, 2016, **17**, 1653–1661.

307 N. H. Mohd, N. F. H. Ismail, J. I. Zahari, W. Fathilah, H. Kargarzadeh, S. Ramli, I. Ahmad, M. A. Yarmo and R. Othaman, *J. Nanomater.*, 2016, **2016**, 4804271.

308 T. Y. Han, S. K. Park and J. S. Lee, *Bull. Korean Chem. Soc.*, 2016, **37**, 689–694.

309 Y.-J. Heo and S.-J. Park, *Energy*, 2015, **91**, 142–150.

310 H. Sehaqui, M. E. Gálvez, V. Becatinni, Y. Cheng Ng, A. Steinfeld, T. Zimmermann and P. Tingaut, *Environ. Sci. Technol.*, 2015, **49**, 3167–3174.

311 C. Gebald, J. A. Wurzbacher, A. Borgschulte, T. Zimmermann and A. Steinfeld, *Environ. Sci. Technol.*, 2014, **48**, 2497–2504.

312 C. Gebald, J. A. Wurzbacher, P. Tingaut and A. Steinfeld, *Environ. Sci. Technol.*, 2013, **47**, 10063–10070.

313 X. He, J. A. Lie, E. Sheridan and M.-B. Hägg, *Energy Procedia*, 2009, **1**, 261–268.

314 L. Ansaloni, J. Salas-Gay, S. Ligi and M. G. Baschetti, *J. Membr. Sci.*, 2017, **522**, 216–225.

315 S. Kang, X. Li, J. Fan and J. Chang, *Renewable Sustainable Energy Rev.*, 2013, **27**, 546–558.

316 M. Nasrollahzadeh, M. Ghasemzadeh, H. Gharoubi and Z. Nezafat, *J. Mol. Liq.*, 2021, **342**, 117559.

317 Z. Nezafat, M. M. Karimkhani, M. Nasrollahzadeh, S. Javanshir, A. Jamshidi, Y. Orooji, H. W. Jang and M. Shokouhimehr, *Food Chem. Toxicol.*, 2022, **168**, 113310.

318 M. Nasrollahzadeh, F. Soleimani, Z. Nezafat, Y. Orooji and F. Ahmadpoor, *Biomass Convers. Biorefin.*, 2023, **13**, 12451–12465.

319 Y. Zhu, Z. Li and J. Chen, *Green Energy Environ.*, 2019, **4**, 210–244.

320 B. A. López-Monreal and S. Loera-Serna, *MRS Adv.*, 2022, **7**, 504–507.

321 D. Saha, G. Orkoulas and D. Bates, *Materials*, 2023, **16**, 455.

322 L. Gong and A. Bao, *J. CO_2 Util.*, 2023, **68**, 102374.

323 M. Demir, T. Tessema, A. A. Farghaly, E. Nyankson, S. K. Saraswat, B. Aksoy, T. Islamoglu, M. M. Collinson, H. M. El-Kaderi and R. B. Gupta, *Int. J. Energy Res.*, 2018, **42**, 2686–2700.

324 S. Park, M. S. Choi and H. S. Park, *Carbon Lett.*, 2019, **29**, 289–296.

325 D. Saha, S. E. Van Bramer, G. Orkoulas, H.-C. Ho, J. Chen and D. K. Henley, *Carbon*, 2017, **121**, 257–266.

326 S. Geng, J. Wei, S. Jonasson, J. Hedlund and K. Oksman, *ACS Appl. Mater. Interfaces*, 2020, **12**, 7432–7441.

327 J. Zhao, W. Zhang, D. Shen, H. Zhang and Z. Wang, *J. Energy Inst.*, 2023, **107**, 101179.

328 S. Sani, X. Liu, M. Li, L. Stevens and C. Sun, *Microporous Mesoporous Mater.*, 2023, **347**, 112334.

329 Y. Cui, B. He, Y. Lei, Y. Liang, W. Zhao, J. Sun and X. Liu, *Chin. J. Chem. Eng.*, 2023, **54**, 89–97.

330 M. Li, X. Liu, C. Sun, L. Stevens and H. Liu, *J. Environ. Chem. Eng.*, 2022, **10**, 107471.

331 L. Shao, N. Liu, L. Wang, Y. Sang, P. Zhan, L. Zhang, J. Huang and J. Chen, *Chemosphere*, 2022, **288**, 132499.

332 E. Atta-Obeng, B. Dawson-Andoh, E. Felton and G. Dahle, *Waste Biomass Valorization*, 2019, **10**, 2725–2731.

333 L. Xu, Y. Xiu, F. Liu, Y. Liang and S. Wang, *Molecules*, 2020, **25**, 3653.

334 K. C. Kemp, V. Chandra, M. Saleh and K. S. Kim, *Nanotechnology*, 2013, **24**, 235703.

335 J. Oh, Y.-H. Mo, V.-D. Le, S. Lee, J. Han, G. Park, Y.-H. Kim, S.-E. Park and S. Park, *Carbon*, 2014, **79**, 450–456.

336 C. Chen, D.-W. Park and W.-S. Ahn, *Appl. Surf. Sci.*, 2014, **292**, 63–67.

337 P. Gruene, A. G. Belova, T. M. Yegulalp, R. J. Farrauto and M. J. Castaldi, *Ind. Eng. Chem. Res.*, 2011, **50**, 4042–4049.

338 S. Yang, L. Zhan, X. Xu, Y. Wang, L. Ling and X. Feng, *Adv. Mater.*, 2013, **25**, 2130–2134.

339 M. Zhao, J. Guo, Q. Xin, Y. Zhang, X. Li, X. Ding, L. Zhang, L. Zhao, H. Ye and H. Li, *Sep. Purif. Technol.*, 2023, **324**, 124512.

340 H. Shi, J. Yang, Z. Ahmad, H. Zhang and J. Chen, *Sep. Purif. Technol.*, 2023, **325**, 124608.

341 D. Rodrigues, J. Wolf, B. Polesso, P. Micoud, C. Le Roux, F. Bernard, F. Martin and S. Einloft, *Fuel*, 2023, **346**, 128304.